



SYNTHESIS OF ELECTROCHROMIC OXYGEN-DOPED POLYCYCLIC AROMATIC HYDROCARBONS

MPhil Thesis 2019



Jack Andrew Fletcher-Charles
C1318945

This thesis is being submitted in partial fulfilment of the requirements for the degree of MPhil.

Signed: _____

Date: _____

This work has not been submitted in substance for any other degree or award at this or any other university or place of learning, nor is it being submitted concurrently for any other degree or award (outside of any formal collaboration agreement between the University and a partner organisation).

Signed: _____

Date: _____

I hereby give consent for my thesis, if accepted, to be available in the University's Open Access repository (or, where approved, to be available in the University's library and for inter-library loan), and for the title and summary to be made available to outside organisations, subject to the expiry of a University-approved bar on access if applicable.

Signed: _____

Date: _____

This thesis is the result of my own independent work, except where otherwise stated, and the views expressed are my own. Other sources are acknowledged by explicit references. The thesis has not been edited by a third party beyond what is permitted by Cardiff University's Use of Third Party Editors by Research Degree Students Procedure.

Signed: _____

Date: _____

Word Count: 16,224

(Excluding summary, acknowledgements, declaration, contents pages, appendices, tables, diagrams and figures, references, bibliography, footnotes and endnotes)

Table of Contents

<i>Acknowledgements</i>	iii
<i>List of Abbreviations</i>	iv
<i>Abstract</i>	vi
1. Introduction	7
1.1 Electrochromism and Electrochromic devices (ECDs)	7
1.2 Electrochromic Polymers.....	8
1.3 Electrochromic Polycyclic Aromatic Hydrocarbons	10
1.3.1 Heteroatom Doped PAHs	13
1.3.2 O-doped PAHs.....	16
1.4 Aim of the Project.....	20
2. Results and Discussion	23
2.1 Synthesis.....	23
2.1.1 1,4-cyclised Anthracene Target Molecule (34)	23
2.1.2 1,5-Cyclised Anthracene Target Molecule (43)	28
2.1.3 1,4-cyclised Naphthalene Target Molecule (56).....	32
2.1.5 1,5-Naphthalene Target Molecule (63)	40
2.2 Optoelectronic Characterisation	46
2.2.1 Spectroscopy.....	46
2.2.2 Electrochemical analysis	47
2.2.3 Spectroelectrochemical Analysis	49
2.2.3 Prototype Electrochromic Devices	51
3. Conclusions/Perspectives	54
4. Experimental	55
General Remarks:	55
Materials and Methods:	55
2-bromo-5-(<i>tert</i> -butyl)phenol (38): ⁹⁹	56
1-bromo-4-(<i>tert</i> -butyl)-2-methoxybenzene (39): ¹¹⁷	56
9,10-bis(4-(<i>tert</i> -butyl)-2-methoxyphenyl)-9,10-dihydroanthracene-9,10-diol (40):.....	57
9,10-bis(4-(<i>tert</i> -butyl)-2-methoxyphenyl)anthracene (41):	58
6,6'-(anthracene-9,10-diyl)bis(3-(<i>tert</i> -butyl)phenol) (35):	58
9,10-bis(4-(<i>tert</i> -butyl)-2-methoxyphenyl)-1,5-dichloro-9,10-dihydroanthracene-9,10-diol (46):	59
9,10-bis(4-(<i>tert</i> -butyl)-2-methoxyphenyl)-1,5-dichloroanthracene (45):	60
6,6'-(1,5-dichloroanthracene-9,10-diyl)bis(3-(<i>tert</i> -butyl)phenol) (44):	60
2,10-di- <i>tert</i> -butylbenzo[1,2,3-kl:4,5,6-k'l']dixanthene (43):	61
2,10-di- <i>tert</i> -butyl-4b,12b-epidioxybenzo[1,2,3-kl:4,5,6-k'l']dixanthene (47):	62

(4-(<i>tert</i> -butyl)-2-methoxyphenyl)boronic acid (62):.....	62
1,4-dibromonaphthalene (61): ¹⁰⁶	63
1,4-bis(4-(<i>tert</i> -butyl)-2-methoxyphenyl)naphthalene (58):	63
6,6'-(naphthalene-1,4-diyl)bis(3-(<i>tert</i> -butyl)phenol) (57):.....	64
3,10-di- <i>tert</i> -butylbenzo[3,4]isochromeno[7,8,1-mna]xanthene (56):	65
1-(4-(<i>tert</i> -butyl)-2-methoxyphenyl)naphthalene (67):.....	65
5-(<i>tert</i> -butyl)-2-(naphthalen-1-yl)phenol (66):.....	66
1,5-dimethoxynaphthalene (73): ¹¹⁸	67
1,5-dibromo-4,8-dimethoxynaphthalene (72): ¹⁰⁹	67
1,5-bis(4-(<i>tert</i> -butyl)phenyl)-4,8-dimethoxynaphthalene (71):	68
4,8-bis(4-(<i>tert</i> -butyl)phenyl)naphthalene-1,5-diol (70):	68
1,5-dibromo-3,7-di- <i>tert</i> -butylnaphthalene (77): ¹¹⁰	69
3,7-di- <i>tert</i> -butyl-1,5-bis(4-(<i>tert</i> -butyl)-2-methoxyphenyl)naphthalene (76):.....	70
6,6'-(3,7-di- <i>tert</i> -butylnaphthalene-1,5-diyl)bis(3-(<i>tert</i> -butyl)phenol) (75):.....	71
2,6,9,13-tetra- <i>tert</i> -butylnaphtho[2,1-b:6,5-b']bisbenzofuran (78):.....	72
NMR Spectra of Synthesised Compounds:	73
2,6,9,13-tetra- <i>tert</i> -butylnaphtho[2,1-b:6,5-b']bisbenzofuran (78).....	93
X-Ray Crystallography.....	95
Quantum Yield Calculations	97
Electrochemical Analysis	97
Electrochromic Device Building	98
Fabrication of a liquid electrolyte device:	98
Fabrication of a cured electrolyte device:	98
References.....	100

Acknowledgements

I would like to thank Cardiff University and Professor Davide Bonifazi for the opportunity to perform research within an area of chemistry which I thoroughly enjoy. This experience has only made me more certain that I am progressing towards a career in academic research, a path I am very excited about.

I would also like to extend my thanks to the European Commission and in particular the MCSA-RISE: INFUSION project (Project ID: 734834) for the opportunity to take part in a placement abroad in Portugal, working with our industrial partners Ynvisible. The experience I gained from working in another country as a part of a company which specialises in a different area of chemistry was invaluable and has helped my progress as both a person and a chemist.

To all my colleagues and friends at Ynvisible: thank you from the bottom of my heart. You all made it so easy to adjust to a new country, new area of chemistry, and a new language. I wish you all the best of luck and hope we can continue to collaborate for the foreseeable future. I also wish to thank the Fotoquimica department of FCT-NOVA, in particular: Professor Jorge Parola, Dr. Cesar Laia, Dr. Artur Moro, and Tiago Moreira all of whom were there whenever I needed advice or help with equipment, and who graciously allowed me to use their labs for much of the synthetic section of this thesis. I wish you all the very best, and hope that I see you again soon. Muito Obrigado!

A special thanks to Dr. Antoine Stopin and Dr. Tanja Miletic who were the guiding lights for this thesis. Their synthetic chemistry knowledge, lab tips and tricks, and teaching were of extreme importance, without them both I would not have been able to produce such a piece of work.

Finally, I would like to thank my family and friends who supported me throughout this thesis. Without all your support this work would not have been possible. Thank you for your visits, which kept me sane at the most stressful of times, and for all the patience and love you have shown me; it may not seem like it at times, but I appreciate it whole-heartedly.

List of Abbreviations

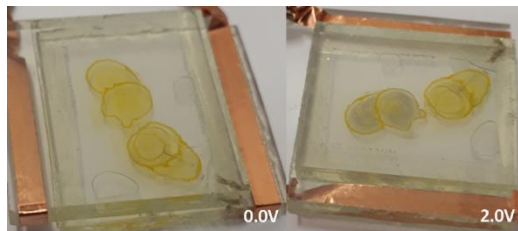
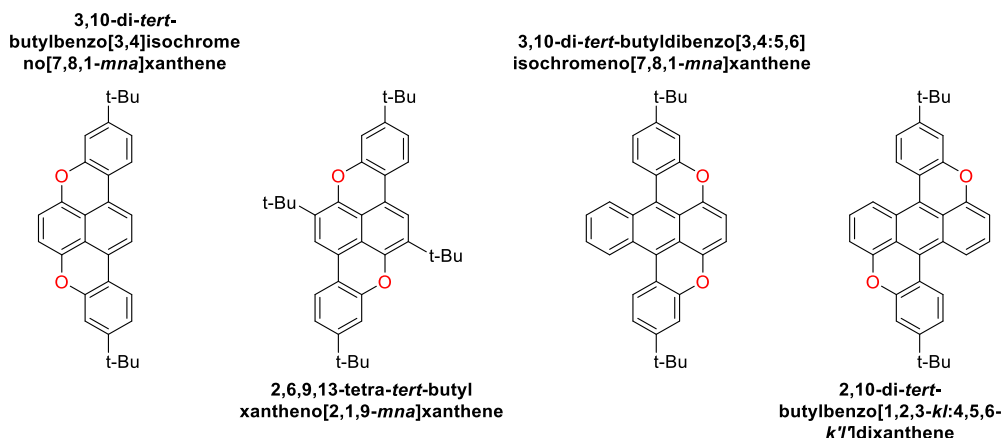
Abs	Absorption
B(OMe) ₃	Trimethyl Borate
Bu ₄ NBF ₄	Tetrabutylammonium Tetrafluoroborate
°C	Degrees Celsius (0 °C = 273.15 K)
calc.	Calculated
conc.	Concentrated
CV	Cyclic Voltammetry
e ⁻	Electron
ECD	Electrochromic Device
EI	Electron Ionisation
EM	Electromagnetic
eq.	Equivalents
ES	Electrospray Ionisation
FTO	Fluorine-doped Indium Tin Oxide
h	Hours
Hex	Hexanes
HOMO	Highest Occupied Molecular Orbital
HR	High Resolution
IR	Infrared
ITO	Indium Tin Oxide
K	Kelvin
LCDs	Liquid Crystal Displays
LR	Low Resolution
LUMO	Lowest Unoccupied Molecular Orbital
M	Molar
M.p.	Melting Point
MeI	Iodomethane
MS	Mass Spectroscopy
NBS	<i>N</i> -bromosuccinimide

<i>n</i> -BuLi	<i>n</i> -Butyllithium
N-Doped	Nitrogen Doped
nm	Nanometres
NMR	Nuclear Magnetic Resonance Spectroscopy
NOESY	Nuclear Overhauser Effect Spectroscopy
O-Doped	Oxygen Doped
P3MT	Poly(3-methythiophene)
PAH	Polycyclic Aromatic Hydrocarbon
PDDTP	Poly(2,3-di(thien-3-yl)-5,7-di(thien-2-yl) thieno[3,4- <i>b</i>]pyrazine)
PEDOP	Poly(3,4-ethylenedioxypyrrole)
PEDOT	Poly(3,4-ethylenedioxothiophene)
Pet Et	Petroleum Ether
PET	Polyethylene terephthalate
PivOH	Pivalic Acid
PPh ₃	Triphenylphosphine
PXX	Peri-xanthenoxanthene
r.t.	Room Temperature
R _f	Retention Factor
t-Bu	<i>tert</i> -Butyl
<i>tert</i> -BuLi	<i>tert</i> -Butyllithium
TLC	Thin Layer Chromatography
UV	Ultra-violet
V	Volts
WO ₃	Tungsten Oxide
ε	Absorption Coefficient
λ	Wavelength
ν	Frequency
Φ	Fluorescence Quantum Yield

Abstract

The synthesis of two O-doped anthracene-based molecules possessing red/pink colour was achieved. These molecules were found to possess high sensitivity to air and, according to literature, react with singlet oxygen.⁹⁶ In addition, an air-stable O-doped naphthalene-based molecule, 3,10-di-tert-butylbenzo[3,4]isochromeno[7,8,1-mna]xanthene, was synthesised using a CuO mediated cyclisation reaction. A short investigation into the selectivity of the reaction using a reference molecule was carried out. This demonstrated that both pyrano and furano product formation was equally favoured. Attempts to synthesise a second naphthalene-based molecule, 2,6,9,13-tetra-tert-butylxantheno[2,1,9-mna]xanthene, led to the isolation of a difurano- molecule in 17 % yield and trace amounts of pyrano-furano- molecule.

The spectroelectrochemical analysis of 3,10-di-tert-butylbenzo[3,4]isochromeno[7,8,1-mna]xanthene was performed, demonstrating a reversible colour change from yellow to blue at a potential of 0.9 V in solution. A drop-cast prototype ECD using and FTO-glass was constructed and gave rise to a device which exhibited the colour change described above at a potential of 2.0 V.



1. Introduction

1.1 Electrochromism and Electrochromic devices (ECDs)

Electrochromism is the ability of a material to reversibly change its optical properties through redox processes.^{1,2} Over the past 30 years, this area of chemistry has experienced increased interest, especially with respect to organic electronics. Electrochromic devices (ECDs) have become greatly sought after in recent years, and have led to their inclusion in the manufacture of devices such as; smart windows, displays, motorbike helmet visors, and in particular: anti-glare rear view mirrors.^{1,3–5} The increase in popularity of ECDs can be attributed to their low operating potentials, the ability to retain colour after removal of the applied potential, their non-emissive nature, the greater viewing angle when compared to liquid crystal devices (LCDs), and the possibility to tune the colour using the potential applied.^{6,7} A typical ECD (Figure 1) is made up of seven layers and works through application of a bias between two electrodes which causes oxidation or reduction of the electrochromic layer; thus leading to optical changes.^{3,8} The change in optical properties of a device arises from the different absorptions associated with the accessed oxidised or reduced state of the deposited electrochrome. The first material which was shown to exhibit this phenomenon was tungsten oxide, when Deb et al. demonstrated that a thin film of WO_3 deposited on a gold electrode adopted a deep blue colour when a potential of 2 V was applied.⁹

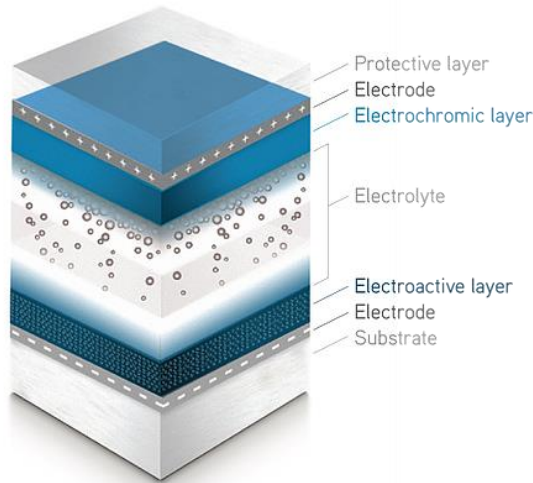


Figure 1: Simple schematic of a typical multicomponent electrochromic window produced by our collaborators, Ynvisible.¹⁰

Since this discovery, tungsten oxide has become one of the most prominent materials applied to the fabrication of ECDs and study of electrochromism.^{11–19} More modern research has exploited other transition metal oxides such as: Nickel,^{20–25} Vanadium,^{26,27} Molybdenum,^{28,29} as well as mixed metal oxides,³⁰ to produce a wide array of devices.

More recently, organic substrates have experienced increased interest and have been found to provide many advantages over their inorganic counterparts. Some of these advantages are as follows: i) organic substrates can be deposited onto flexible materials allowing for manufacture of flexible devices,² ii) the properties of the electrochromic substrate can be tuned through introduction of heteroatoms or other synthetic methods, iii) production of organic electronics is said to be more cost-effective than analogous inorganic electronics as they do not require energy intense methods of purification (e.g. the refining of silicon to electronic grade silicon) and often the materials are more easily processed for manufacture.³¹

1.2 Electrochromic Polymers

Much of the research utilising organic substrates exploiting polymers for the fabrication of ECDs has been based on polythiophenes. This is because they offer materials which possess fast switching times, good colouration efficiency, and easier processing for device fabrication when compared to the equivalent metal oxides.³² As well as these advantages, polythiophenes can be easily synthesized and possess good chemical stability.^{2,4}

There are numerous examples in the literature of different colour transitions demonstrated by polythiophene derivatives. Unsubstituted polythiophene appears red in its neutral state and blue in its oxidised state when a potential of + 0.3 V or greater is applied.^{2,31,33} Tuning the monomer unit by addition of different R groups at the 3- and 4- positions has led to an extensive range of coloured materials becoming available, for example, the polymer poly(3,4-ethylenedioxythiophene) (PEDOT) (**1**) possesses a blue neutral state and a lighter blue oxidised state when a potential of -0.25 V is applied.^{2,34} A simpler polythiophene example which demonstrates the tailoring of colour by variation of R groups at the 3- position is the polythiophene derivative poly(3-methylthiophene) (P3MT). This derivative possesses an orange-red neutral state, similar to that of unsubstituted polythiophene, however at 0.72 V the oxidised state is transparent light blue.^{31,35}

Further expansion of this work led to the synthesis of an orange polythiophene, poly(3,4-bis(ethylhexyloxy)thiophene), and expansion of the range of colours accessed by this category of electrochromic materials through tailoring of the auxiliary R groups.³⁶ The synthesised polymer was found to transition from its neutral orange state to a transmissive oxidised state at + 0.57 V. Kumar and Reynolds observed another colour transition demonstrated by a polythiophene derivative when, in 1996, they synthesized PEDOT-C₁₄H₂₉ (**2**) – a combination of tailoring properties using the extension of R groups and the addition of the ethylene dioxy moiety; a potential of +0.3 V was used to reversibly oxidise the polymer, leading to a transition of the material from the deep purple of its neutral state to a transparent light green of the oxidised state.³⁷ More recently, work completed by Sonmez et al. synthesized and applied a new green polythiophene: poly(2,3-di(thien-3-yl)-5,7-di(thien-2-yl) thieno[3,4-*b*]pyrazine) (PDDTP) (**3**), to the

fabrication of an ECD. It was combined with two other polymers discussed earlier: PEDOT and P3MT (**4**) and used to produce a device which gave intense colours: red from P3MT, the green PDDTP, and the blue of PEDOT in their neutral states. Upon oxidation at +0.58 V the device moved towards transparency (Figure 2).³²

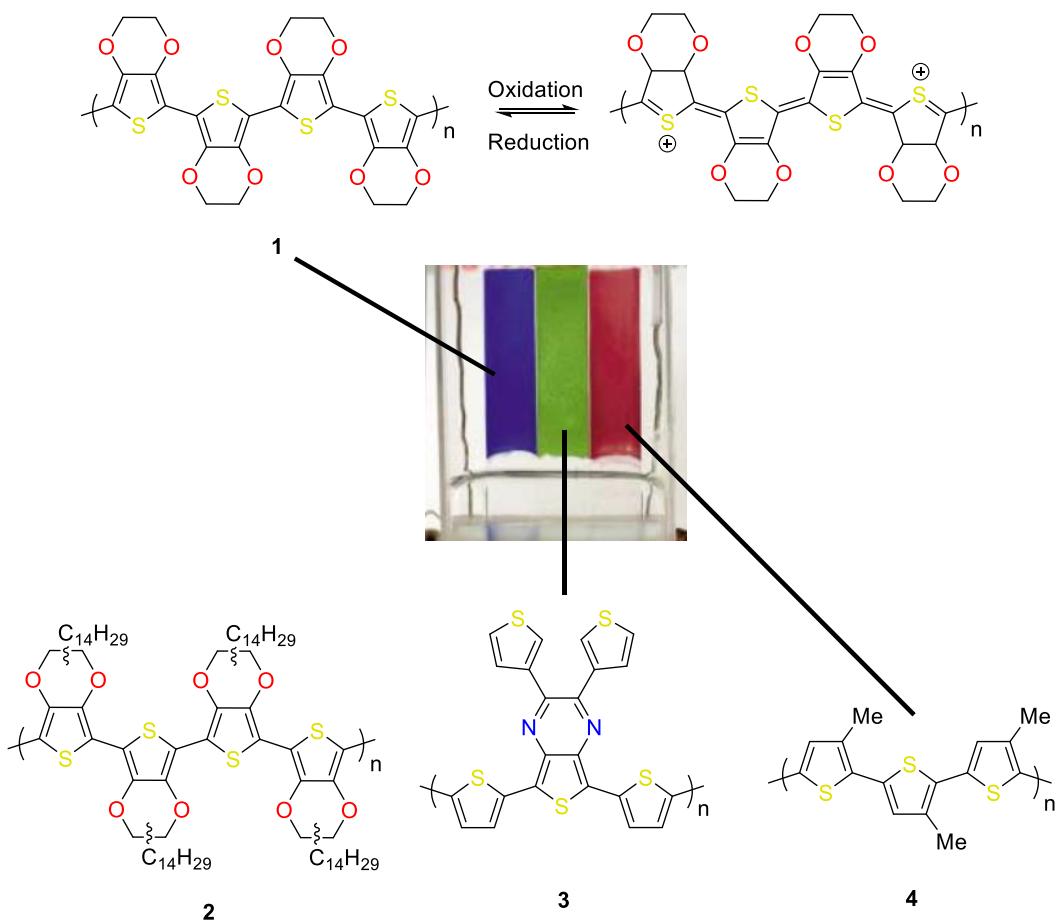


Figure 2: PEDOT (1) along with the structure of its oxidised state,³⁸ along with the structures of other examples discussed in the text: PEDOT-C₁₄H₂₉ (2), poly(2,3-di(thien-3-yl)-5,7-di(thien-2-yl) thieno[3,4-b]pyrazine) (PDDTP) (3), and P3MT (4).

As mentioned earlier, polythiophenes dominate the electrochromic field of research; however, they are not the only polymers shown to exhibit electrochromism. Another class of polymers which have been applied to the fabrication of electrochromic devices are polypyrroles. Poly(3,4-ethylenedioxyppyrrole) (PEDOP) (**10**) was found to exhibit similar electrochromic properties to PEDOT, its thiophene analogue;³⁴ the polymer appears red in its neutral state and upon oxidation at -0.5 V transitions to a blue-gray colour. PEDOP was also shown to be more readily oxidised (-0.25 V for PEDOT); this thought to be due to the more electron-rich nature of the polymer backbone when compared to PEDOT.^{34,39} The trivalent nature of the nitrogen atom within the polypyrrole backbone has allowed a different method for tailoring colour to be explored when compared to the polythiophene analogues: modification of R groups bound to the

nitrogen. An example of this method for tailoring colour can be seen in the work of Diaz *et al.*, who synthesised a series of N-substituted polypyrroles (Figure 3).⁴⁰

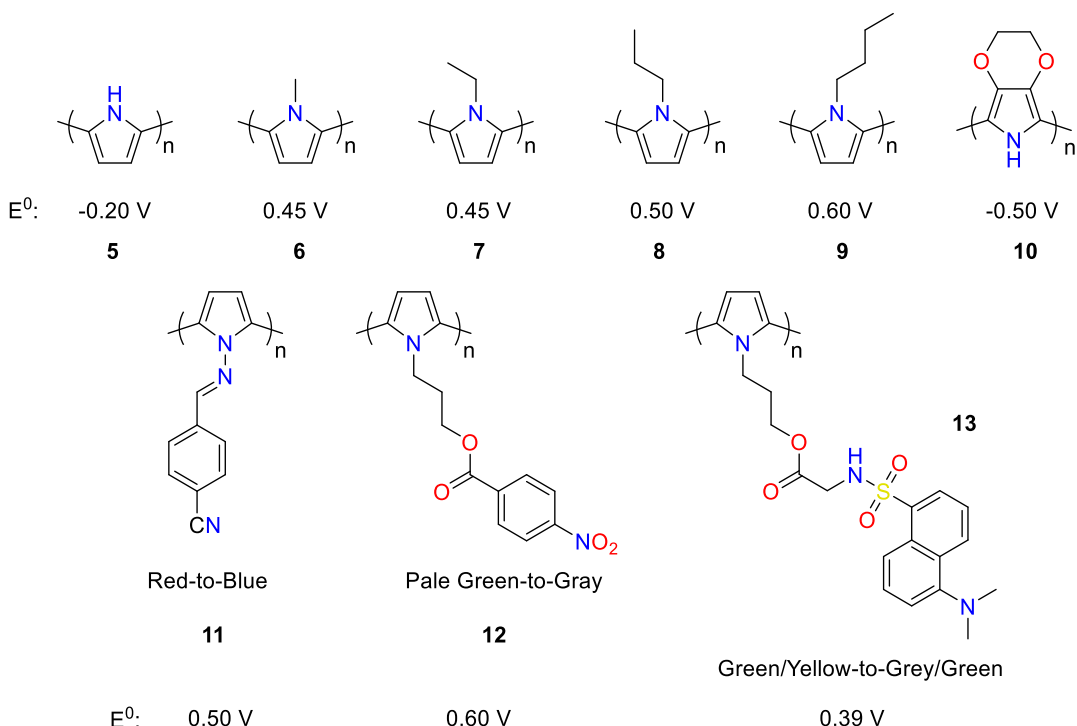


Figure 3: Polypyrroles synthesised by Diaz *et al.* and their oxidation potentials (**5-9**); The structure of PEDOP with its oxidation potential (**10**); Other polypyrroles synthesised in literature along with their oxidation potentials and the reported colour changes (**11-13**).

This showed that substitution at this position also had a significant effect on the oxidation potential of the polymer; +0.45 V for poly-N-methylpyrrole compared to -0.2 V of unsubstituted polypyrrole. Further research by various groups has led to more complex polymers encompassing many different types of substituents such as methyl, ethyl, butyl, and phenyl bound to the nitrogen atom (Figure 3). This has given access to a large selection of colours and devices possible, from the red-to-blue transition of **11**, to the yellow-to-brown of unsubstituted polypyrrole.⁴¹⁻⁴⁴

This is not an exhaustive review of polymeric electrochromic materials, for examples such as polycarbazoles,⁴⁵⁻⁵⁰ polyfurans,^{51,52} polyanilines,⁵³⁻⁵⁷ extensive reviews may be found in the literature.

Though electrochromic polymers have greatly furthered the study of electrochromism and development of electrochromic devices; recently a new strategy which utilises the synthesis and tailoring of small molecules to obtain electrochromic properties has come to the fore.

1.3 Electrochromic Polycyclic Aromatic Hydrocarbons

The use of small molecule electrochromic materials has become a viable strategy to fabricate ECDs. Polycyclic aromatic hydrocarbons (PAHs) electrochromes can give access to an extensive range of

colours,⁵⁸ and selective doping of heteroatoms during their synthesis can allow for precise tailoring of colour: this is a topic which will be covered in more depth later (Section 1.3.1). In some cases, PAHs with electrochromic properties occur naturally, thus removing the need for complex synthesis as is the case for some polymers. The solubility issues polymers often experience can be avoided as many PAHs are readily soluble in common organic solvents; this allows for more straightforward processing and building of devices using techniques such as spray-coating.^{59,60} For these reasons PAHs have been brought to the fore of organic electronics in recent years.

Multilayer graphenes are one of the largest PAHs to have been applied to the fabrication of ECDs, as seen in the work by Polat *et al.*⁶¹ The authors were able to produce several devices that possessed a grey-to-transparent colour transition at a potential of 5 V. Work from Ji *et al.* built upon this as the authors fabricated an ECD using functionalised nanographenes (Figure 4), moving towards smaller molecules, with the chemical formula of C₁₃₂H₃₆(COOH)₂ adsorbed on the surface of the electrode layer.⁶² This gave a device which showed colour change from orange to brown (see figure 4) on application of a much lower potential (+1.27 V) when compared to the multi-layered graphene device of Polat *et al.*⁶²

Fullerenes can also exhibit some electrochromic behaviour; in 1993, Cordoba de Torresi *et al.* demonstrated this by applying a current to a film of C₆₀ fullerene, using lithium ions as the charge carriers. They observed a change in absorption spectrum in the near-infrared which they attributed to the formation of the C₆₀¹⁻ species.⁶³ Other work from 1994 confirmed these findings and was able to produce a visible colour change: from light brown to dark brown.⁶⁴ Although this early work demonstrated the electrochromic nature of C₆₀ fullerenes, more recent research has been focussed on the incorporation of fullerenes into devices which utilise other electrochromic materials to enhance properties such as colouration efficiency and switching time.^{65,66}

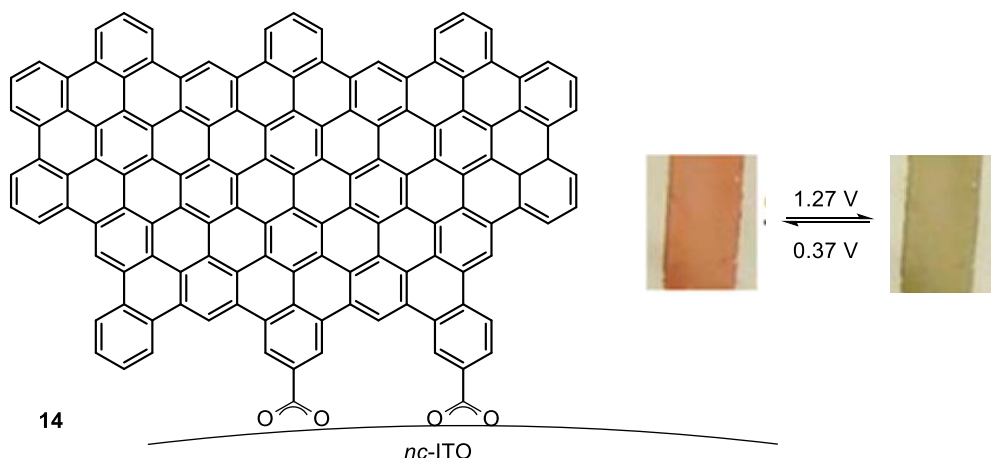


Figure 4: Electrochromic graphene molecule discussed on page 5 (**14**), adsorbed to nano-crystalline ITO and the device fabricated using this molecule.

Fabrication of an ECD using small molecule PAHs can be found in the work of Stec *et al.* whose research produced an almost transparent device using perylene which could be turned royal blue (- 3.5 V) to olive (+ 4.0 V) on application of a potential (Figure 5a).⁵⁸ The colour change arose from the insertion or removal of an electron from the HOMO or LUMO respectively. This device requires an unusually high potential for an ECD due to the formation of plasmonic states causing the colourless-to-blue and colourless-to-olive colour changes.⁵⁸ Another example of electrochromic properties demonstrated by a PAH can be found in the work of Ishigaki *et al.*⁶⁷ The authors designed a highly strained phenanthrene derivative (Figure 5c) which underwent bond-breakage upon application of a potential (+0.95 V), leading to a highly coloured red dication state. The initial strained phenanthrene derivative could then be regenerated by application of a negative potential, leading to C-C bond formation and obtaining of the original colourless material once again.⁶⁷ In recent work by Corrente *et al.* a number of electrochromic molecules based on dibenzofulvene were produced (Figure 5b).⁶⁸ These molecules covered a range of different colours: colourless, pale pink, pale orange, orange-red, etc. The authors used modification of substituents at the exocyclic fulvene bond to tune the absorption and band gap of the synthesized molecules. Through their work, they were able to fabricate several ECDs which possess transitions from a coloured or colourless state to a black state with good cyclability (>10,000 cycles).⁶⁸ These various examples demonstrate the great range of colours and devices which can be accessed by PAHs so far, research is still ongoing and acts to expand the list of known electrochromic materials.

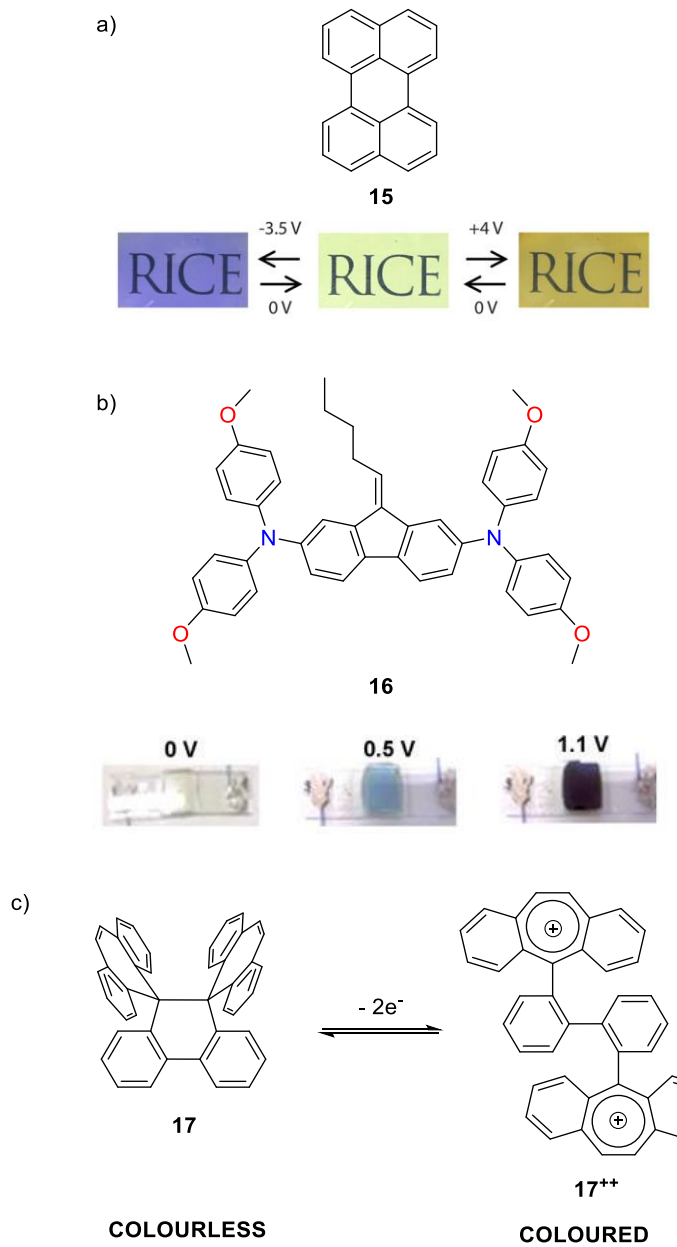


Figure 5: a) The device fabricated by Stec. *et al.* with the colour changes at -3.5 V and $+4.0\text{ V}$ demonstrated; b) One of the dibenzofulvene derivatives synthesised by Corrente *et al.* and its associated ECD; c) The structure of a phenanthrene derivative from Ishigaki *et al* and the proposed structure of its coloured dication.

1.3.1 Heteroatom Doped PAHs

Much of the synthesis of heteroatom doped PAHs has been used to engineer molecules which possess reversible oxidation or reduction processes, a crucial property for electrochromic materials. One class of heteroatom-doped PAH which has been investigated thoroughly are viologens.⁵ These compounds consist of two pyridinium moieties often bound to one-another at the 4-position. Groups bound to the nitrogen atoms as well as the counter anions associated with the pyridinium can be tailored to allow access to different colours through modification of the HOMO-LUMO gap.⁵ The dication form of these molecules can be reversibly reduced upon application of a potential; often starting at a colourless state, transitioning

to a highly coloured radical cation often a shade purple hence the name ‘viologen’. The radical cation can then be further reduced to an uncharged state following a second electron transfer, the structure of these three oxidation states can be seen in figure 6.^{5,69}

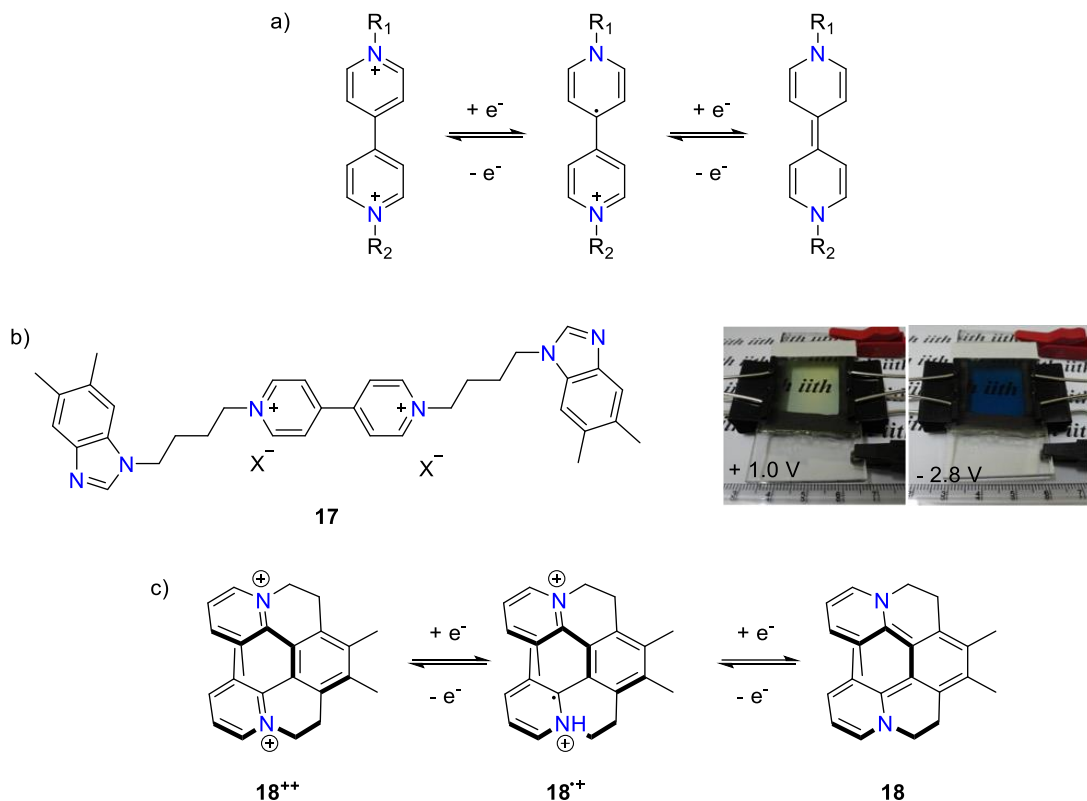


Figure 6: a) The common redox stages of an example viologen; b) A prototype electrochromic device in the bleached and coloured states fabricated using the viologen **17**;⁶² c) The structure of the helical viologen synthesised by Zhnag *et al.* discussed in section 1.3.1.⁷⁰

A specific example of an ECD fabricated using viologens can be found in work done by Zhang *et al.* who synthesised a helical viologen (**18⁺⁺**) with the pyridinium moieties provided by a quinoline.⁷⁰ Viologens have also been utilized as polymers to avoid solubilisation of the electrochrome and diffusion of colour throughout the supporting electrolyte in ECDs, a common problem when using small molecule electrochromic materials.⁵

Another example of electrochromic N-doped PAHs can be found in the work of Takase *et al.* In 2007 the authors synthesised a hexaazacoronene derivative (**19**) which was also found to possess several reversible oxidation states.⁷¹ By performing cyclic voltammetry, the authors were able to demonstrate that the synthesised molecule had four reversible oxidation states at 0.355 V, 0.520 V, 1.52 V, and 1.88 V. Upon oxidation of the neutral species to its monocation, the material transitioned from an orange to a green, further oxidation to the dication state gave access to a dark-green material.⁷¹

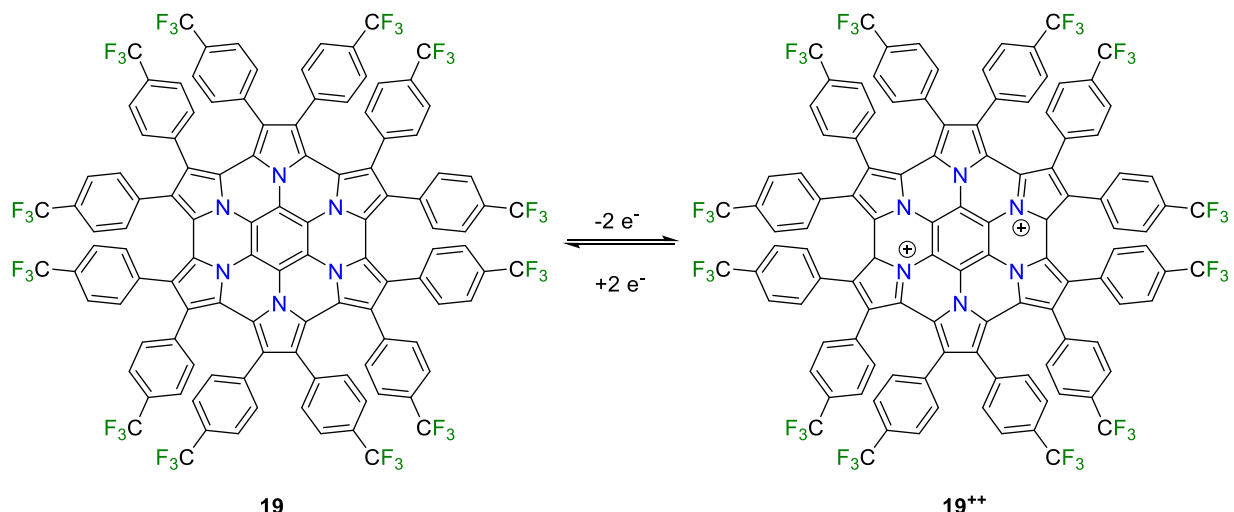


Figure 7: The hexaazacoronene example discussed in section 1.3.1 along with a proposed resonance structure of its dication state.

Phosphorous is another heteroatom which has been exploited by researchers to engineer electrochromic PAHs. Examples such as the large phosphorous containing molecules synthesized by Romero-Nieto *et al.* in 2011;⁷² in this work they describe dendritic molecules which were the first P-doped molecules shown to exhibit electrochromism (Figure 8a). Further developments by Baumgartner *et al.* incorporated a phosphorous atom in viologen-type molecules.^{73,74} In this work, the authors were able to demonstrate reversible reductions at low operating potentials (+0.1 V), and applied the synthesised molecules (Figure 8b) to the fabrication of prototype ECDs; achieving colourless to blue and colourless to green devices.

Other heteroatoms such as sulphur,⁷⁵ selenium,⁷⁶ and tellurium^{77,78} have also been used to great effect to synthesise PAHs possessing electrochromic properties; particular focus will now be payed to the O-doped examples.

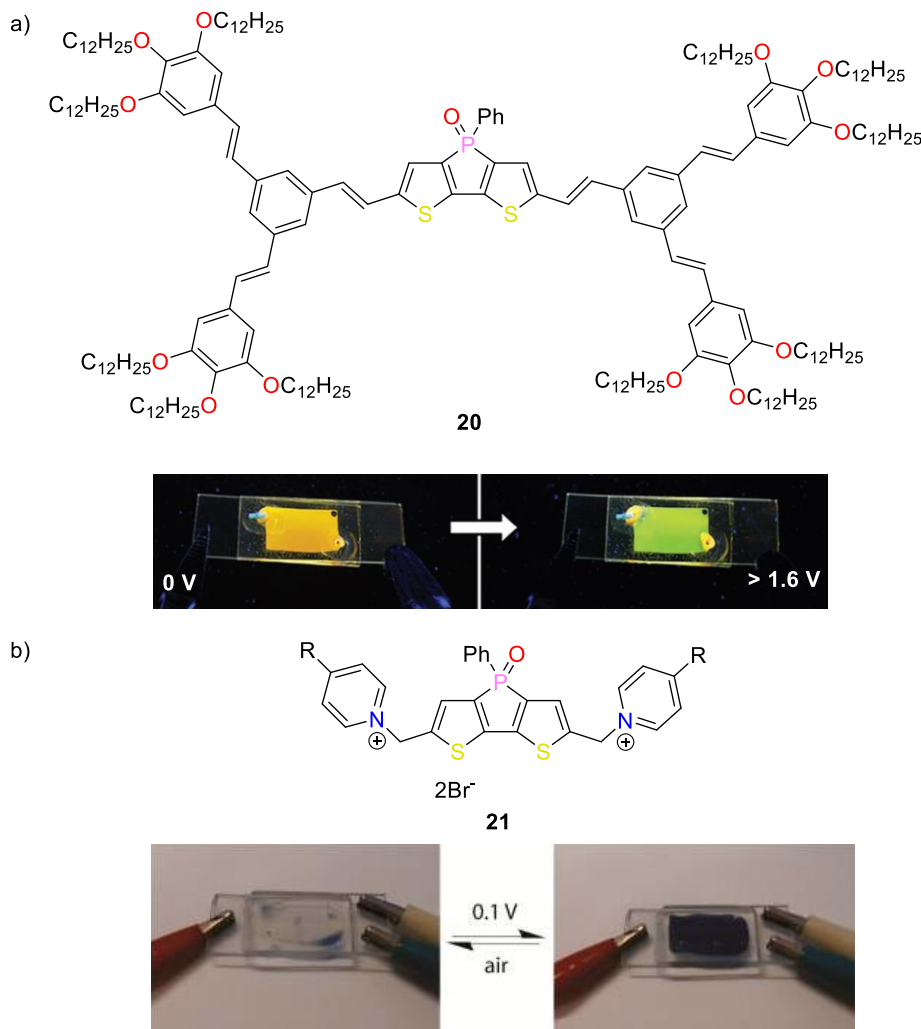


Figure 8:a) Dendritic molecule synthesised by Romero-Nieto *et al* and the associated device which shows a colour transition of orange-to-green at potentials $>+1.6$ V; b) An example of a phosphorous containing viologen-type molecule synthesised by Baumgartner *et al* and the associated ECD demonstrating a colourless-to-blue transition.

1.3.2 O-doped PAHs

The insertion of oxygen atoms, similarly to doping of other heteroatoms, can lead to a tailoring of the HOMO-LUMO gap, and thus the colour of the material. In particular, O-doping has been used to great effect in the area of organic electronics to produce materials devices such as organic light emitting diodes and field effect transistors.^{79,80}

Well-known examples of electrochromic O-doped PAHs can be found in quinones. Quinones, as well as other O-doped PAHs, have been known for their wide range of colours and use in dyes for many years.^{81,82} Some of the earliest research investigating the electrochromic properties of these materials was performed by Destine-Monvemay *et al.* in 1989.⁸³ This work found that a variety of different quinones, including tetrachloro-1,2-benzoquinone (**22**), possessed reversible reduction peaks which gave rise to different absorption spectra when compared to the neutral species.⁸³ A range of quinones, from simple molecules to

more complex ones, such as the extended anthraquinone derivative (**24**) synthesised by Yao *et al.*,⁸⁴ have been investigated with respect to their electrochromic properties.

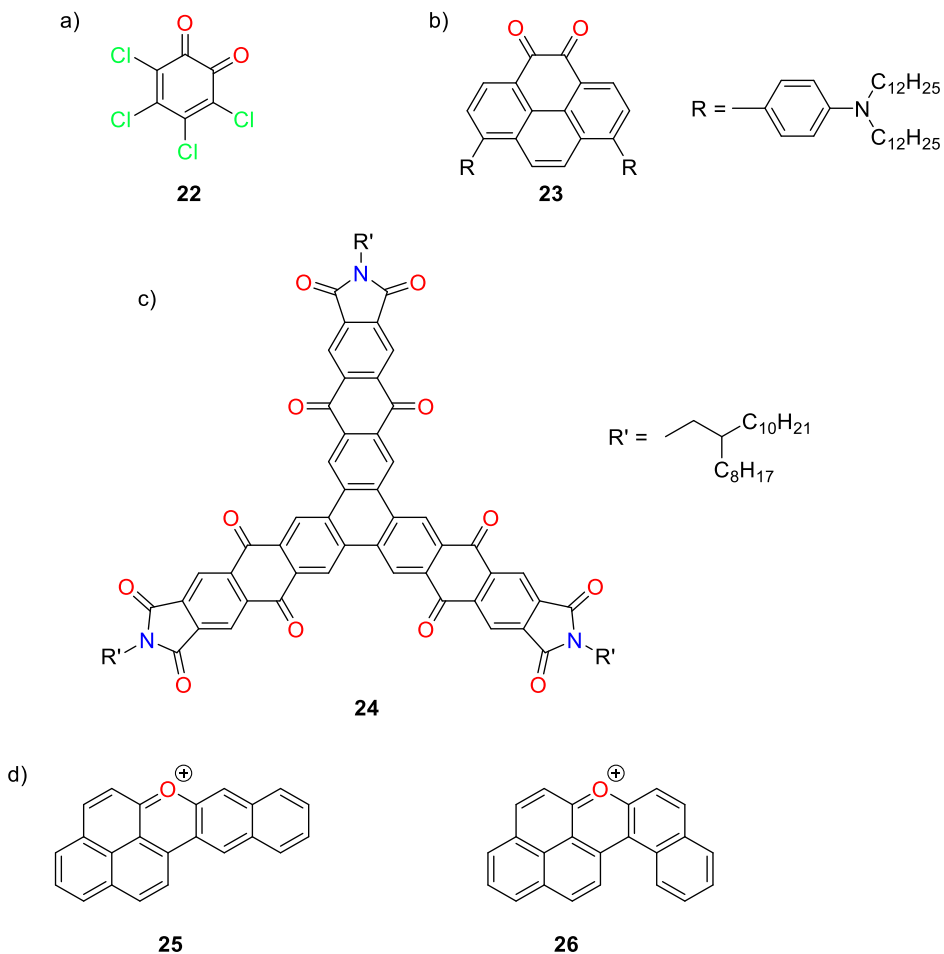
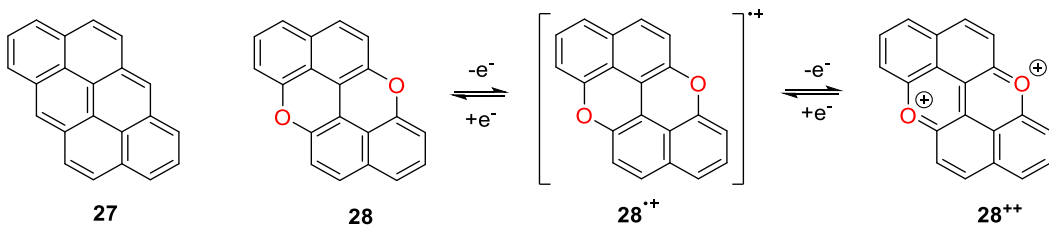


Figure 9: a) The structure tetrachloro-1,2-benzoquinone investigated by Destine-Monvemay *et al* with respect to its electrochromical properties; b) The pyrenedione functionalised in the 4,5- positions synthesised during the work of Keller *et al*; c) The extended anthraquinone derivative (**24**) synthesised by Yao *et al* and discussed in section 1.3.2; d) Two pyrilium containing molecules (**25** and **26**) synthesised by Anamimoghadam *et al*.

All of the quinone species investigated take part in a reversible reduction to form a radical anion species as well as dianions in some cases such as naphthalene-1,4,5,8-tetrone and pentacene-5,7,12,14-tetraone.⁸⁵⁻⁸⁷ Similar systems to the quinones discussed; pyrene di-ketones, were investigated by Keller *et al.* in 2013 for their possible application to electrochromic devices.⁸⁸ The authors demonstrated that the colour of the molecules could be tailored by the positioning of electron-withdrawing groups within the molecule. Electron withdrawing groups at the 2,7- gave rise to a deep-blue colour, 4,5- led to a yellow material (**23**), and the 1,8- derivative was purple. The synthesised molecules all possessed electrochromic properties, with both reduction and oxidation peaks observed. The observed oxidation peaks were attributed to the loss of an electron from the HOMO of the molecules which appeared to be localised to the nitrogen-containing

electron-withdrawing groups. The reduction peaks arose from a low-lying LUMO which was localised around the pyrene-dione component of the molecules.⁸⁸

Researchers have begun adopting the approach of incorporating the oxygen atoms within six membered rings of the PAHs, substituting them for a carbon atom within a fully aromatic system. Several recent articles have synthesised pyrylium containing PAHs which have exhibited reversible reduction peaks caused by the reduction of the cation present.^{89,90} Molecules synthesised by Anamimoghadam *et al* (**25** and **26**) were reduced at -0.43 V and -0.59 V respectively. These molecules also demonstrated a second reduction peak at more negative potentials, however these oxidation states appear to be unstable under aerobic conditions.⁹⁰



Scheme 1: Scheme demonstrating the transition from anti-aromatic to the aromatic system on oxidation of PXX, its carbon-only analogue can be seen for comparison.

While stable pyrylium containing PAHs have been a recent development, electrochromic materials possessing pyrano moieties have been investigated for many years. In 1988 Dettling *et. al.* synthesized a derivative of peri-xanthenoxanthene (PXX) which was found to be reversibly oxidised by application of a potential (Scheme 1).⁹¹ Frenking *et al.* demonstrated the same process with the unsubstituted PXX and described the colour change seen: yellow to blue to violet.⁹² In its neutral state PXX (**28**) possesses a 24π -electron anti-aromatic system, while its carbon-only analogue (**27**) possesses an aromatic system. The disruption of the electron cloud leads a molecule which has localised aromaticity in its neutral state, and an entirely aromatic structure upon oxidation, this gives a greatly red-shifted absorption spectrum upon oxidation.⁹² This antiaromatic-to-aromatic transition has also been observed by Đorđević *et al.* who, in 2017, synthesized PAHs with more extended aromatic systems containing pyrano moieties.⁹³ The authors synthesized molecules **28**, **29**, and **30** by performing Suzuki cross coupling with 1,6-dibromopyrene, 1,8-diiodopyrene, and 1,3-dibromopyrene respectively.

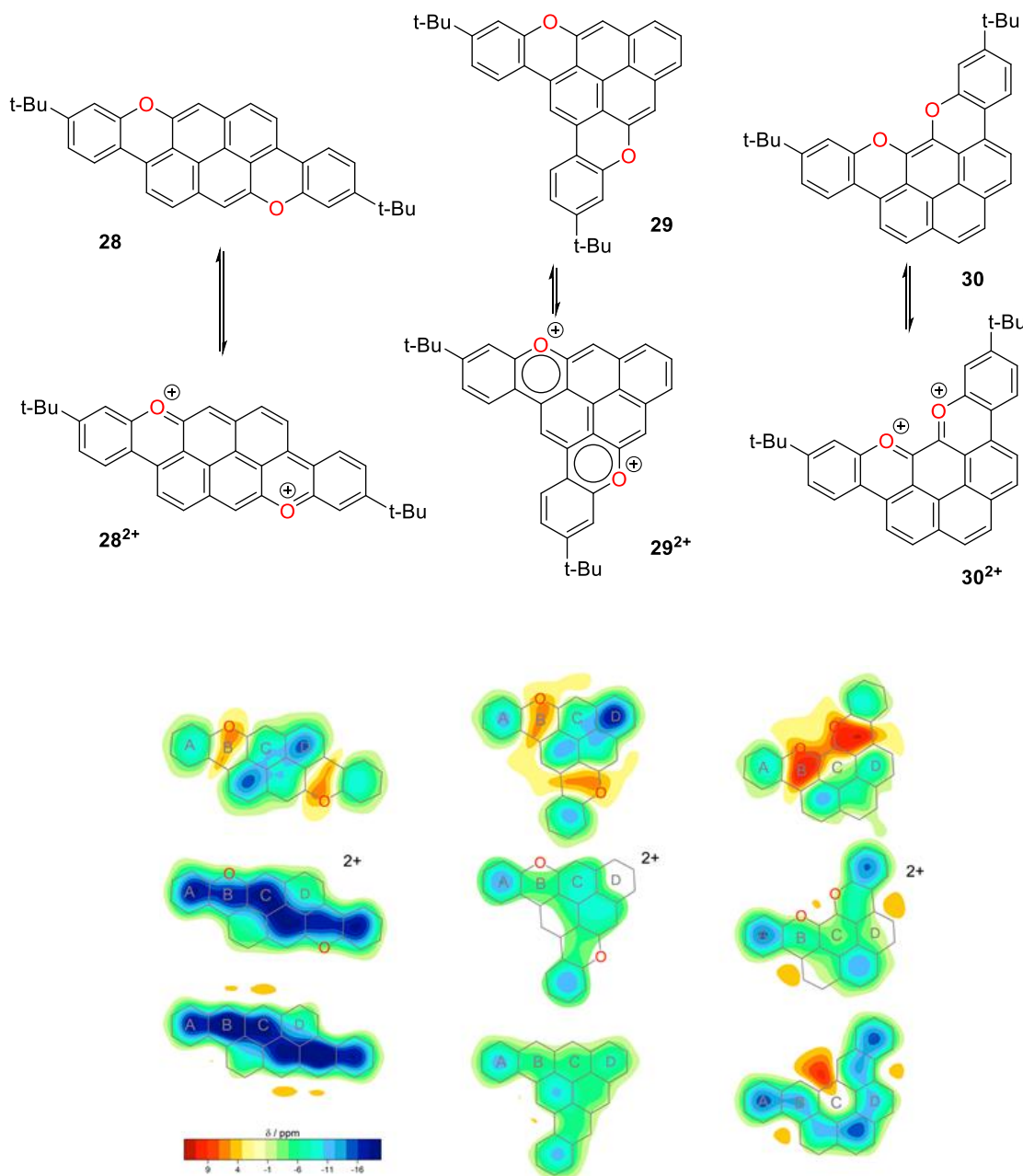


Figure 10: O-doped PAHs synthesized by Đorđević et al. with the NICS of their neutral, and oxidised state demonstrating the effect oxidation has on the aromaticity of the molecule. NICS of carbon analogues can also be seen for comparison.⁹³

The intermediates then underwent an oxidative ring-closure to give the final products. These molecules were all shown to experience a significant red-shift of their absorption spectra when oxidised to their +2 states, similar to the PXX examples discussed earlier. It was reasoned that this was due to the “*local antiaromatic perturbation*”⁹³ caused by the pyrano rings present as demonstrated by NICS studies.

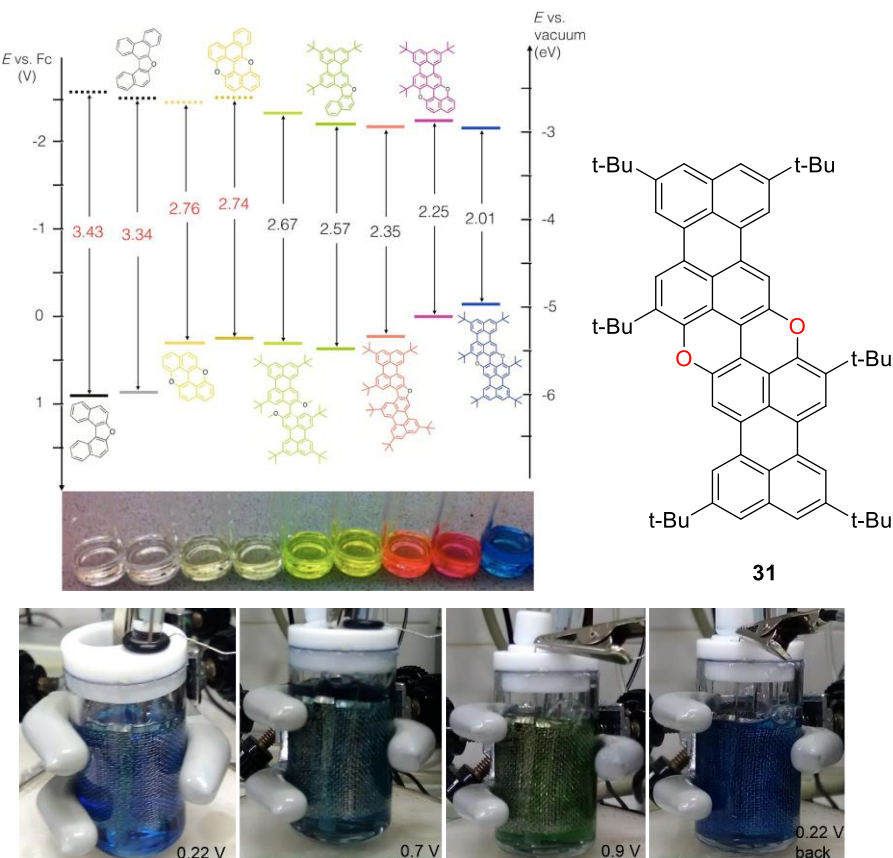


Figure 11: a) The structures of molecules synthesized by Miletic et al. demonstrating the ability to tailor colour through adjustment of conjugation; b) Results of preliminary electrolysis experiments, demonstrating the electrochromic properties **31** possesses.^{94,95}

A series of PXX-derived molecules with colours tailored by extension of the conjugation were synthesised by our group in 2017 (Figure 11).⁹⁴ This work demonstrated that extension of conjugation within a molecule is an invaluable means for tailoring the colour of the material.⁹⁴ It demonstrated that through modification of conjugation and number of pyrano or furano moieties present, a molecule's colour can be greatly affected and can lead to a large range of different colours.

Recently, this work has been expanded upon again by Dr. Tanja Miletic from our group through evaluation of the potential application of **31** to the fabrication of ECDs. Preliminary cyclic voltammetry tests found that in solution, the molecule appeared blue and on reduction changed to green reversibly (Figure 11).⁹⁵ Though several pyrano containing molecules have been synthesised, few have been applied to the area of electrochromism. The ability of O-doping to tune both colours and electrochemical properties of a molecule makes it of extreme importance to the area of small molecule electrochromic materials.

1.4 Aim of the Project

The work of this MPhil aims to synthesise an electrochromic small molecule which possesses a transparent-to-red transition. In doing this the library of O-doped PAHs which may be applied to the fabrication of

ECDs will be expanded greatly. The colourless to red transition is an extremely desirable one because, not only has it not been reported in the literature, but it may also lead to the manufacture of ‘electrochromic pixels’ and thus the application of the technology to low-energy displays. By producing a device using three electrochromic materials which possess transitions from transparent to red, green, and blue respectively it is possible to produce colour which covers the entire visible part of the EM spectrum. The colours obtained can then be tuned by careful control of the potential applied to the device, similar to the current technology used in LCDs.

In order to achieve the colourless/transparent to red transition, the molecule must initially absorb in either the ultraviolet (UV) or infrared (IR) parts of the EM spectrum and upon oxidation experience a shift of their absorption into the visible region.

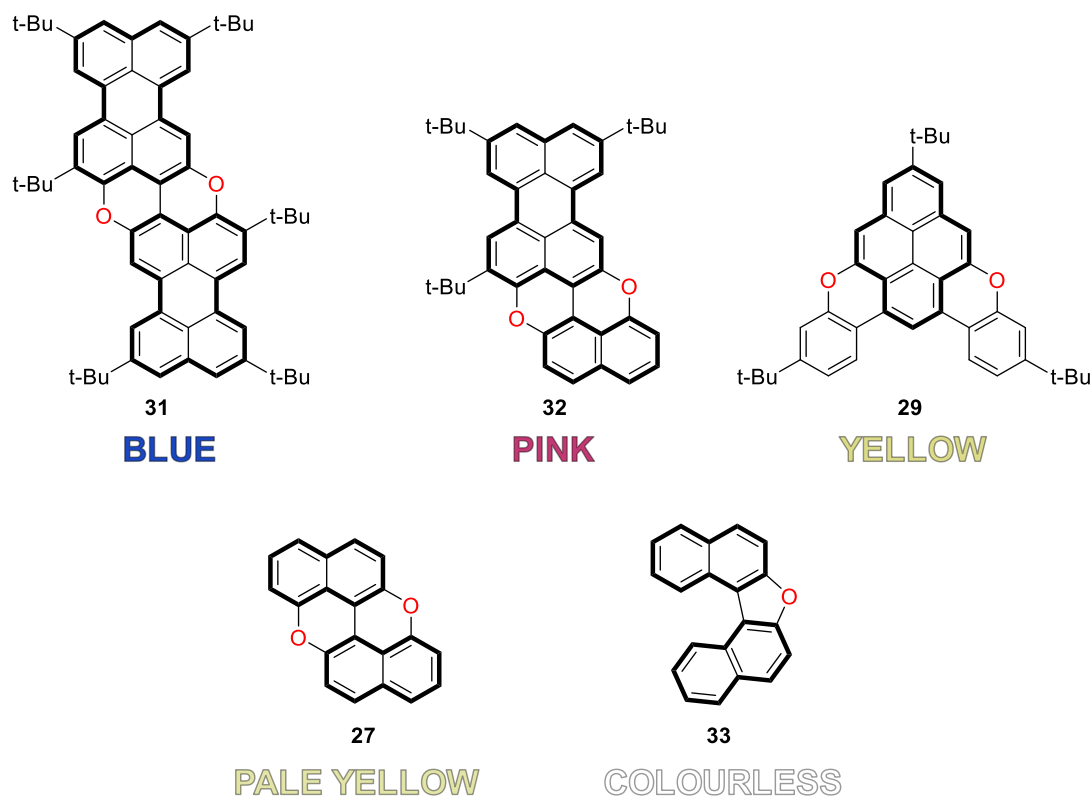


Figure 12: O-doped PAHs which demonstrate the progression of colour with the restriction of conjugation within the molecule.

As discussed in section 1.3.2, restricting the extent of conjugation of a molecule leads to an increase in HOMO-LUMO gap and thus a hypsochromic shift of the absorption spectrum. Figure 12 demonstrates that progressively using smaller ‘hydrocarbon cores’ within O-doped PAHs leads to a shift towards uncoloured materials; travelling from the vivid blue of the perylene based molecules (**31**), to the yellow of the pyrene-based molecules (**29**), and through to the uncoloured naphthalene compound (**33**).

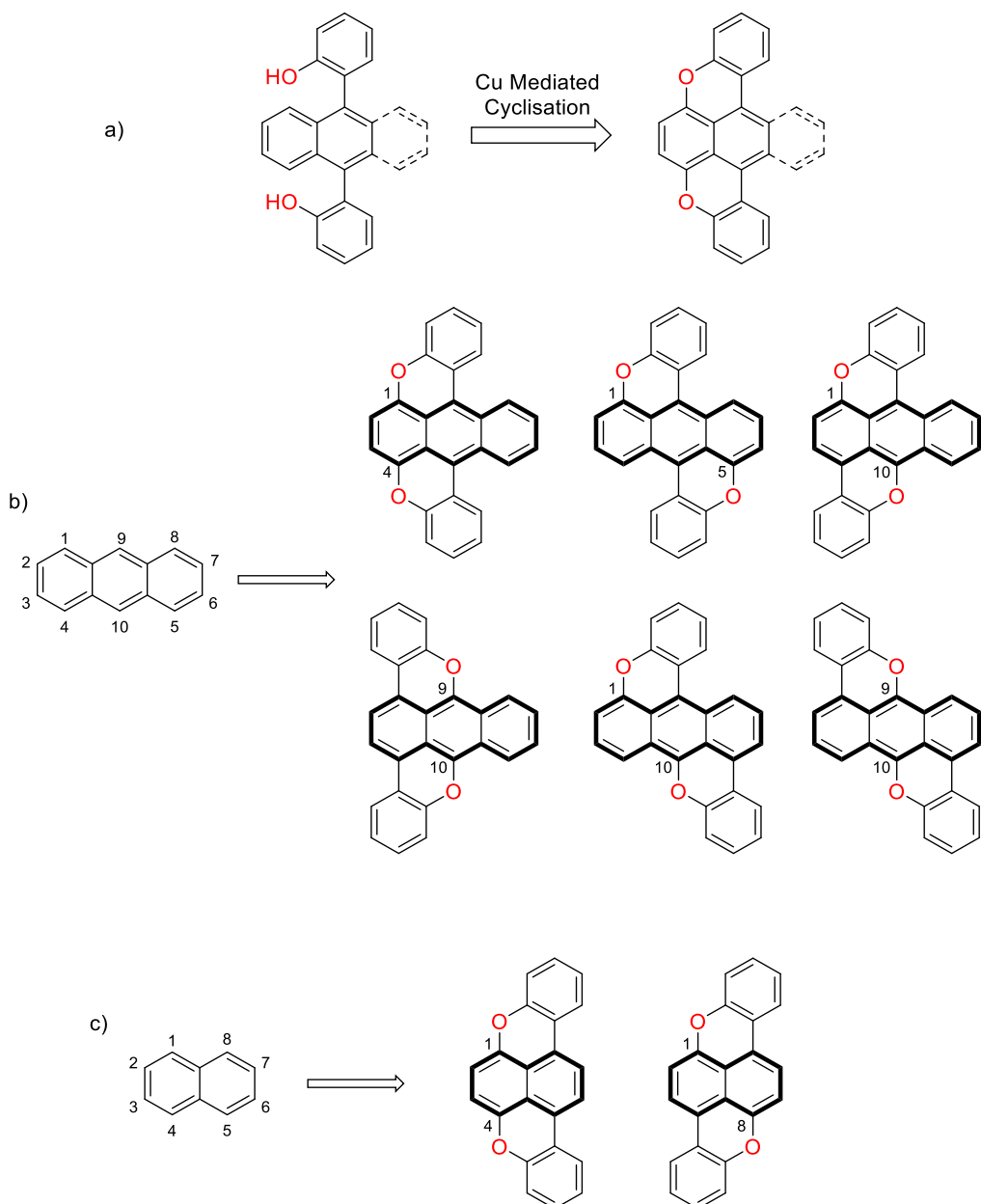


Figure 13: a) The general synthetic strategy for achieving the desired molecules with restricted conjugation; b) Six proposed molecules based on an ‘anthracene core’; c) Two proposed ‘naphthalene-based’ molecules for synthesis; the numbers indicate the positions at which the intramolecular etherification will take place, from this the nomenclature used throughout this thesis is derived.

Eight new O-doped PAHs have been proposed; two of these molecules are based on naphthalene cores, and the remaining six on anthracene cores. Synthesis of these compounds will be achieved by use of the copper mediated intramolecular etherification reaction developed by our group and applied to the work of Dr Miletic,⁹⁴ as well as many other various synthetic methodologies. It is believed that the proposed molecules will absorb in the UV region and thus possess an uncoloured neutral state. Upon oxidation the molecules should experience a red shift into the visible light portion, as has been demonstrated by other O-doped PAHs discussed in section 1.3.2. It was also speculated that the aromatic components of these molecules

would give high absorption coefficients and thus good coloration efficiency on application to the fabrication of a device. Upon successful synthesis of the proposed O-doped PAHs their spectroelectrochemical properties will be investigated fully, after which they will be used to fabricate an ECD using the drop-cast method. The final aim of this project is to then build a working ECD prototype using the spray-coating technique, followed by the full characterisation of the device; investigation of its cyclability, colour efficiency, and switching time.

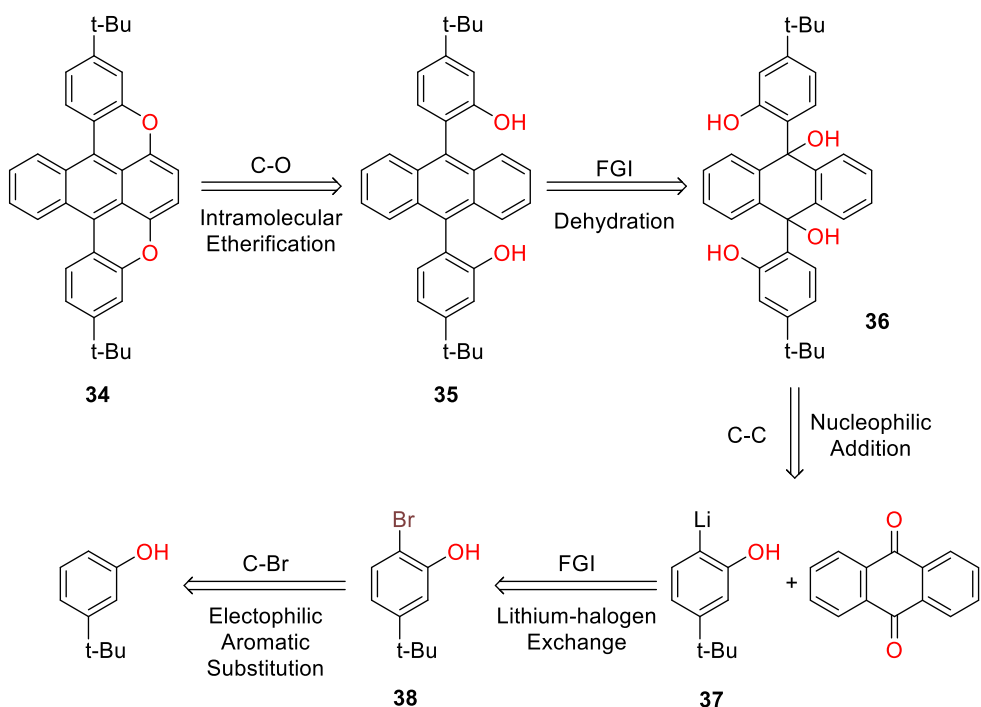
Herein the attempted synthesis of several of these target molecules (Figure 13) is described, as well as their electrochemical characterisation and application to the fabrication of prototype ECDs.

2. Results and Discussion

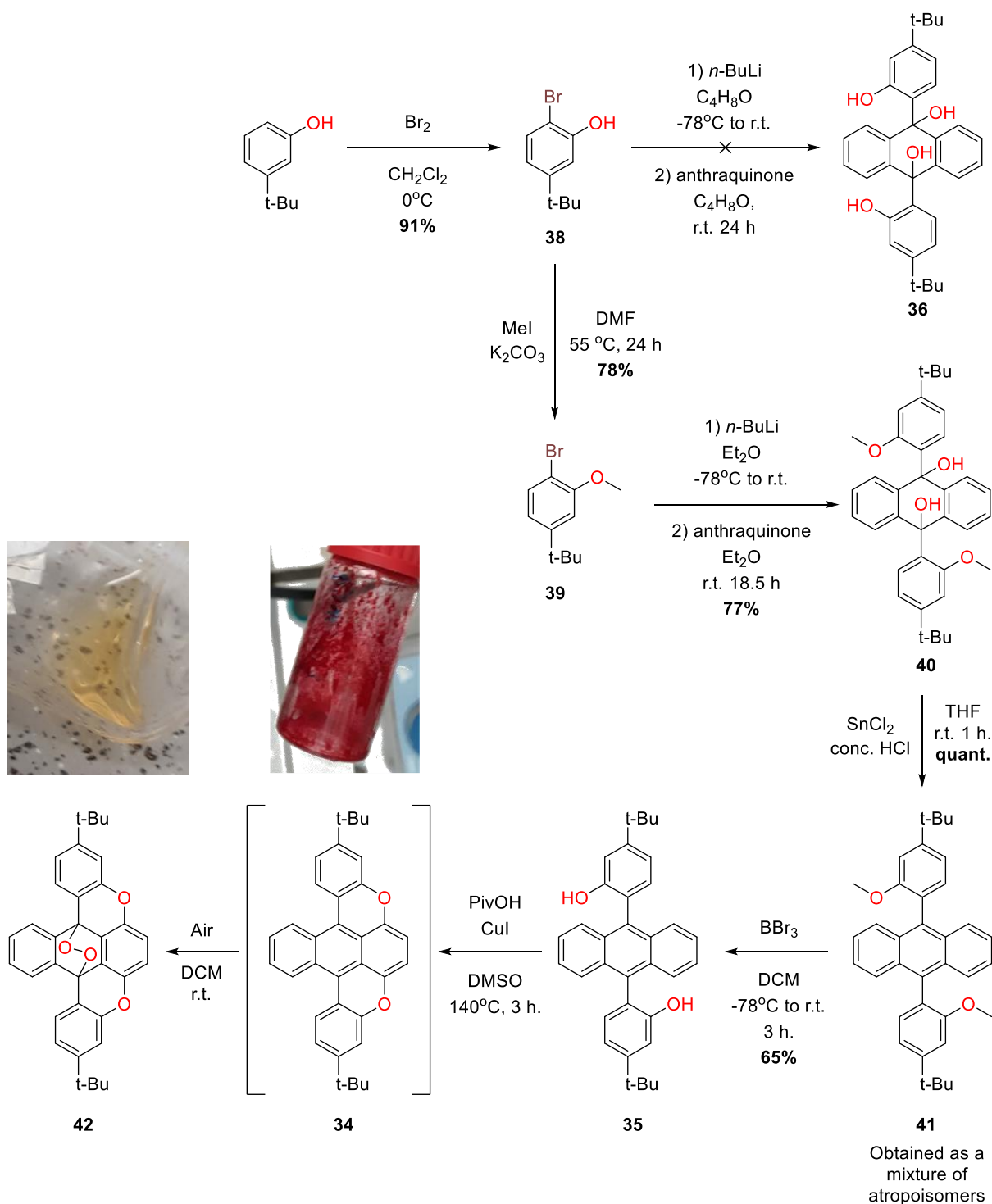
2.1 Synthesis

2.1.1 1,4-cyclised Anthracene Target Molecule (**34**)

The first target molecule to be synthesized was the proposed 1,4-cyclised anthracene isomer (**34**), the synthetic strategy adopted can be seen in Figure 14. Examples of both this anthracene target molecule (**34**) and the 1,5-cyclised anthracene target molecule (see section 2.1.2) were found in the literature.⁹⁶ However, neither had been synthesised using the new intramolecular etherification strategy nor had the investigation of their possible electrochromic properties been reported. It was envisioned that these molecules would lead to a red electrochromic material. To obtain **34** an intramolecular etherification reaction developed by Zhao *et. al.*⁹⁷ and refined by Stassen *et. al.*⁹⁸ could be performed using **35**. To obtain the precursor molecule **35**, the dehydration of anthracene-diol **36** may be carried out. It was thought that the synthesis of **36** would be possible by nucleophilic addition of **37** to commercially available 9,10-anthraquinone. Molecule **37** may be synthesized from **38** using a halogen exchange reaction with an organolithium species such as *n*-BuLi or *tert*-BuLi. To obtain **38** the bromination reaction of commercially available 3-(tertbutyl)phenol was envisaged.

Figure 14: Retrosynthetic analysis for the target molecule **34**.

The synthesis of **38** was achieved using modified conditions based on those developed by Shu *et. al.*⁹⁹ Br₂ was added to a solution of *tert*-butyl-phenol in DCM at 0 °C, followed by instantly quenching the reaction with saturated Na₂S₂O₃ aqueous solution. This gave the desired product in 91% yield. The initial attempts at the nucleophilic addition reaction to form **36**, following a procedure found in literature,¹⁰⁰ were unsuccessful. This reaction was attempted using the addition of 2 eq. of *n*-BuLi to a solution of the bromophenol (**38**) at -78 °C. After warming to room temperature for 0.5 h a suspension of anthraquinone in C₄H₈O was added slowly and the reaction was left to stir overnight. This reaction did not yield the desired product and it was believed that deprotonation of the hydroxyl group on addition of *n*-BuLi to **38** hindered the formation of the desired organolithium which was required for the reaction to proceed. The reaction was repeated using 3.2 eq. of *n*-BuLi, again the desired product was not obtained. To solve this issue, the hydroxyl moiety was protected using a methyl group. This was done by deprotonation of the bromophenol species (**38**) with K₂CO₃ followed by reaction with MeI under anhydrous conditions.¹⁰¹ This gave the methoxybenzene derivative (**39**) in 78% yield, which then successfully took part in the nucleophilic addition reaction to form the desired anthracene-diol (**40**). This reaction was performed in accordance with conditions found in literature;¹⁰⁰ and led to the formation of **40** in 77% yield.



Scheme 2: Attempted synthesis of target molecule **34**. Yield for the formation of **34** is not stated as the molecule degrades rapidly so could not be isolated in a pure state. Endoperoxide yield not stated as the product was lost during purification attempts.

The synthesised anthracene-diol was then reduced following a modified procedure of one found in literature.¹⁰² The experiment was performed by dissolving the anthracene-9,10-diol **40** in THF followed by slow addition of a saturated solution of SnCl₂ in concentrated HCl. The reaction was monitored by TLC and after 3 hours complete conversion of the starting material into two new spots with similar R_f was

observed. NMR of the crude reaction mixture after work up suggested that these spots were atropoisomers of the desired product. This was confirmed by variable temperature NMR; the spectrum measured at room temperature demonstrates a singlet at around 3.55 ppm, this can be assigned to the methoxy group of the desired molecule. However, NMR spectrum measured at 50 °C (Figure 15) demonstrated splitting of the singlet peak associated with the methoxy group, suggesting that conversion between two atropoisomers occurs at higher temperatures but at a relatively slow rate. Upon cooling of the sample, the methoxy peak returns to its original singlet which suggests that one of the atropoisomeric configurations is favoured at room temperature.

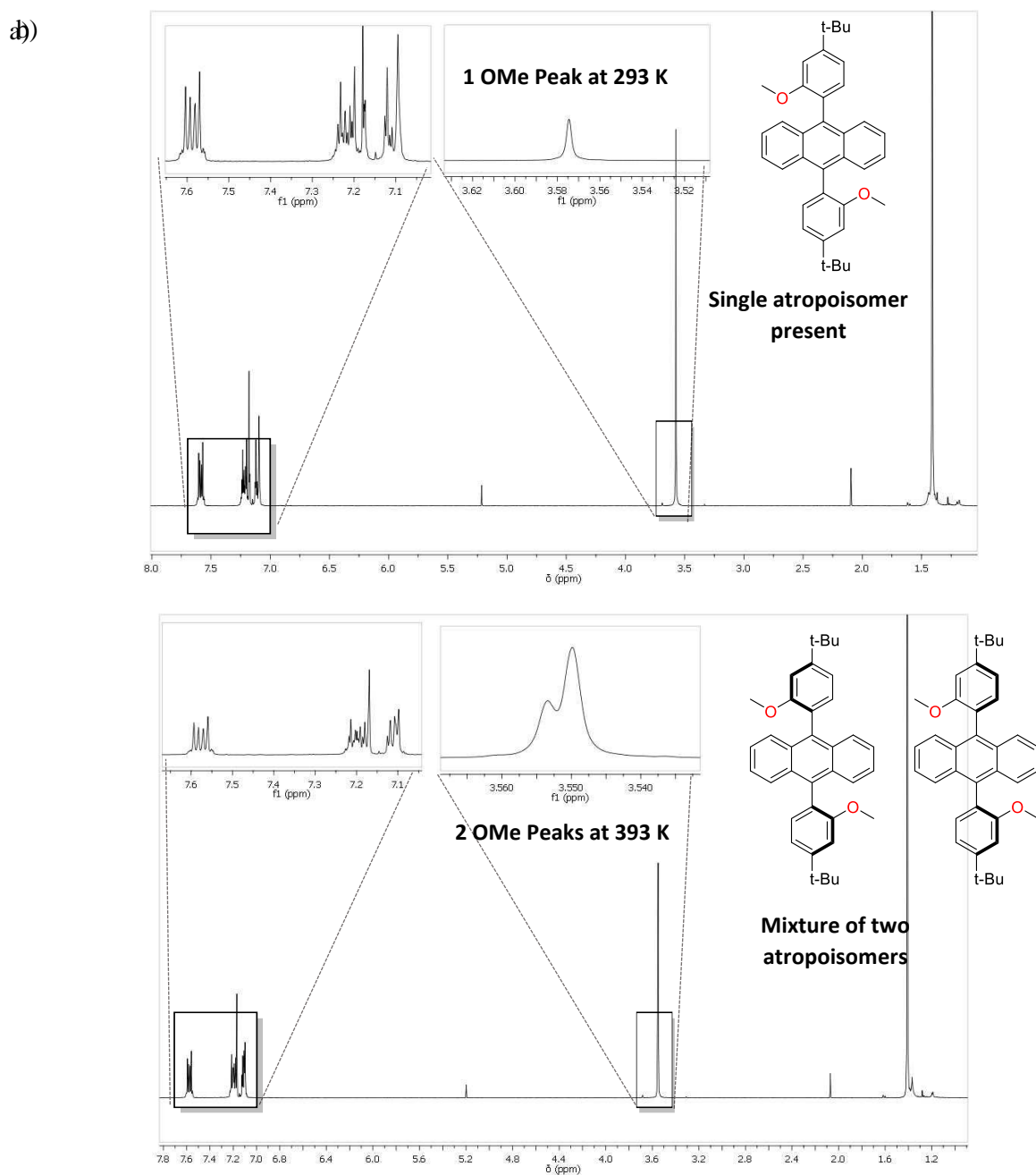


Figure 15: ^1H NMR spectra of 9,10-bis(4-(*tert*-butyl)-2-methoxyphenyl)anthracene (**41**) in CDCl_3 measured at a) 293 K and b) 323 K.

Deprotection of the methoxy groups was performed using a method found in literature.¹⁰³ The anthracene derivative **41** was dissolved in DCM under an inert atmosphere. After covering the round bottom flask with aluminium foil and cooling to -78 °C BBr_3 was added slowly. Following this, the flask was warmed to room temperature and stirred overnight. This gave 65% yield of product **35** (Scheme 2) and allowed access to the final step of this strategy.

This was performed according to a literature procedure,^{97,98} **35**, CuI, and PivOH were dissolved in DMSO and heated to 140 °C for 3h. The reaction resulted in a vivid red solution which, with time and exposure to air, lost its colour. Upon heating a solution of **34** to 100 °C the original colour returned, suggesting that any possible degradation was reversible. Similar molecules synthesised by Yi *et al.* have demonstrated sensitivity to $^1\text{O}_2$.¹⁰⁴ The research by Yi *et al.* proposed that the central electron-rich aromatic ring took part in a reversible Diels-Alder-type reaction with a singlet oxygen molecule. It was believed **34** behaved in the same manner, as evidenced by its reversible colour change, due to its similar structure. Efforts to isolate the endoperoxide derived from **34** product by column chromatography were unsuccessful.

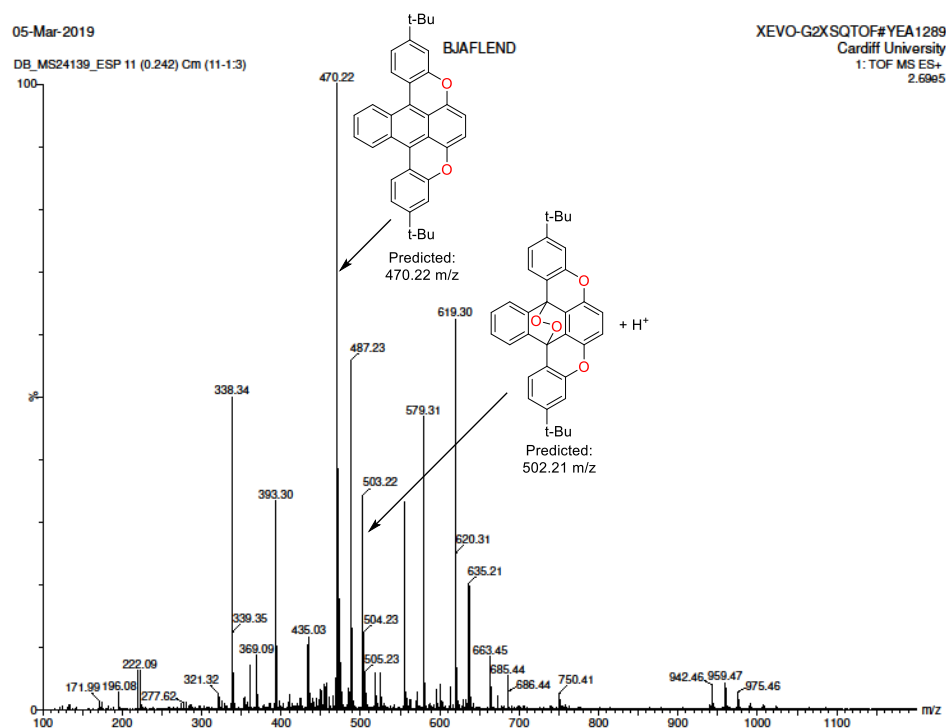


Figure 16: LRMS of the crude obtained from the cyclisation reaction of **35**.

2.1.2 1,5-Cyclised Anthracene Target Molecule (43)

In parallel to the synthesis of **34**, work was undertaken to selectively synthesize anthracene-based target molecule **43** following a strategy similar to the one applied to the synthesis of the 1,4-cyclised anthracene product. To achieve the desired 1,5-anthracene molecule, it was proposed that the intramolecular etherification step could be replaced by an intramolecular nucleophilic aromatic substitution using the dichloroanthracene derivative **44**. To obtain this precursor a deprotection of the bisphenyl anthracene **45** would need to be performed, a reaction which had been used to good effect during the synthetic pathway of target molecule **34**. It was proposed that molecule **45** could be synthesized from the dichloroanthracenediol **46** using a dehydration reaction in a similar manner to the method discussed in section 2.1.1 (Scheme 2, Page 25). The synthesis of **46** was thought to be possible from commercially available 1,5-dichloroanthraquinone and the methoxybenzene derivative (**39**) used during the synthesis of **34** (Scheme 2) as discussed previously.

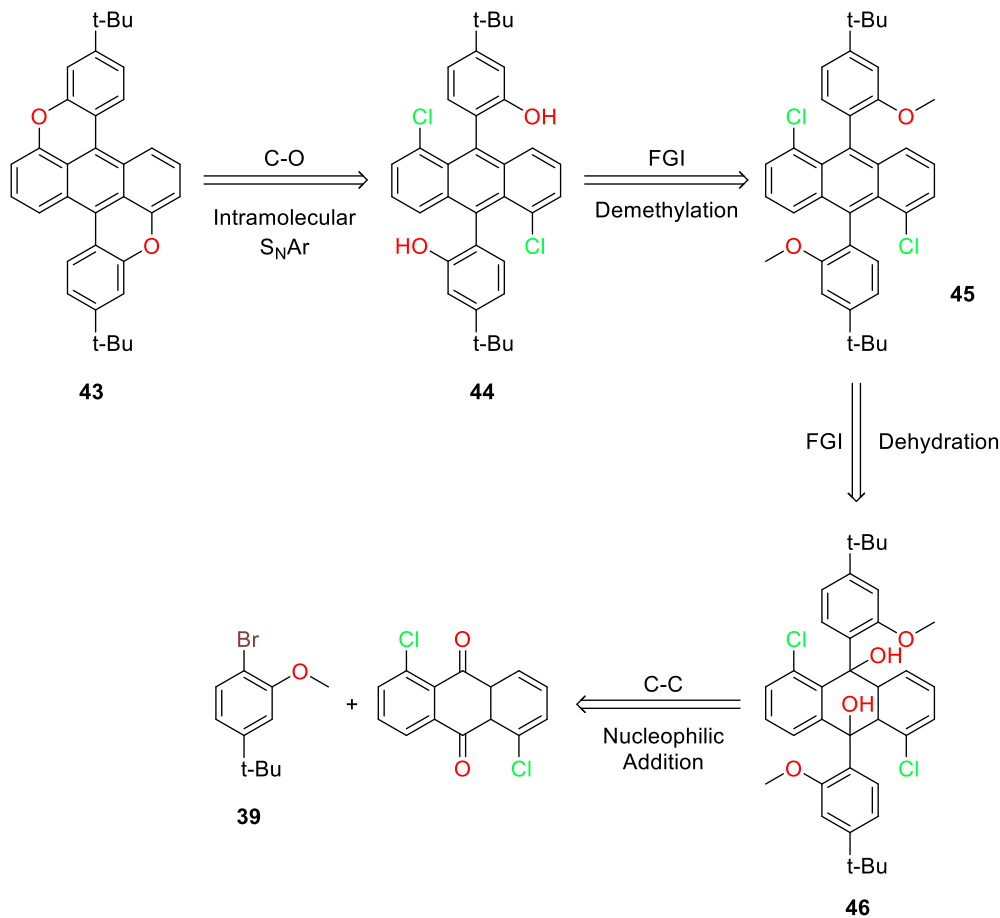
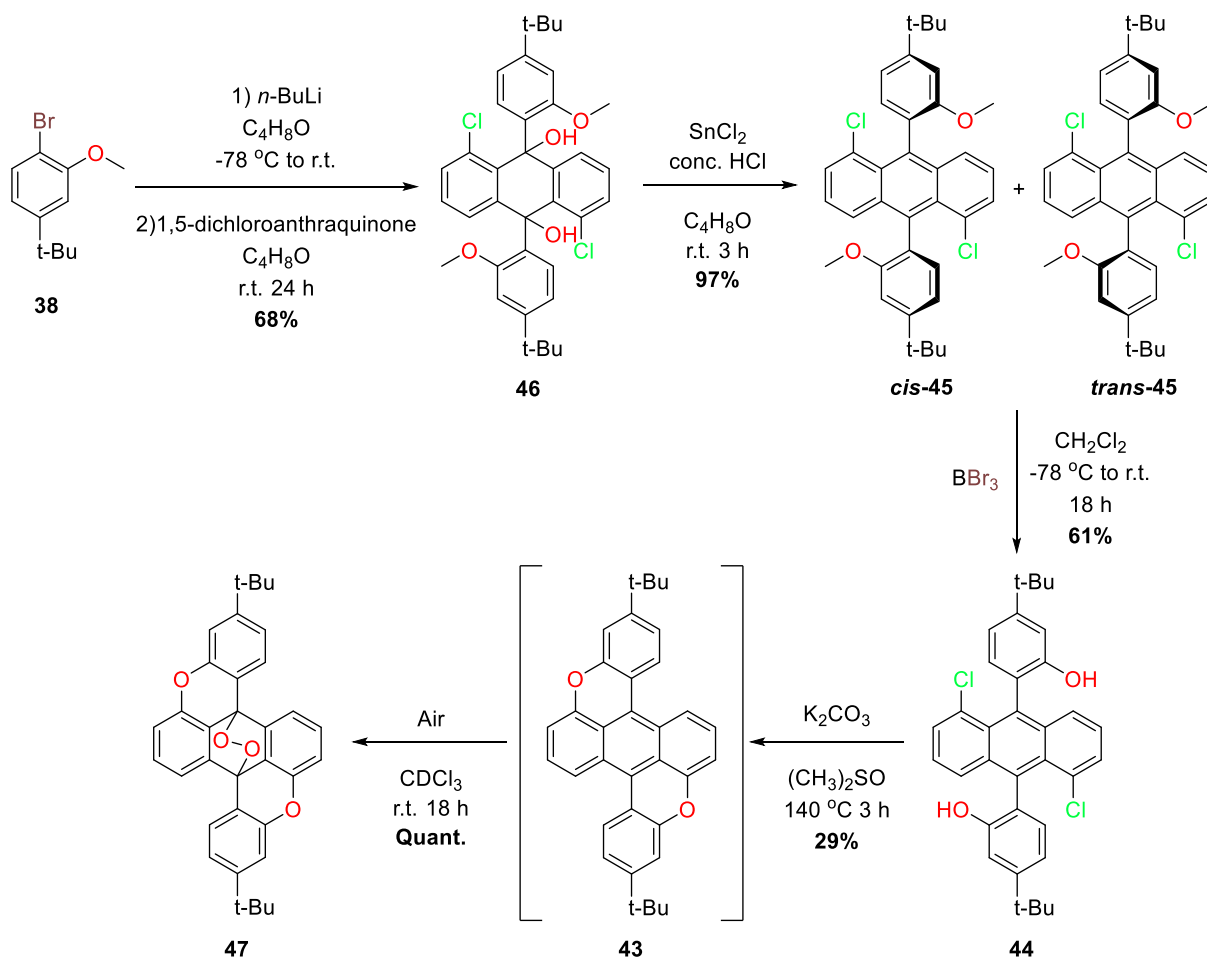


Figure 17: Retrosynthetic analysis of the 1,5-cyclised anthracene target molecule 43.

The synthesis began with the nucleophilic addition of the methoxy benzene species **38** to the 9- and 10-positions of 1,5-dichloroanthraquinone (Scheme 3, page 29). This was done by the addition of 1.1 eq. of *n*-BuLi to a solution of methoxybenzene derivative **38** at -78 °C to form the required organolithium species.

After allowing the reaction mixture to stir at r.t. for 0.5 h a solution of 1,5-dichloroanthraquinone in C₄H₈O was added slowly. The reaction was left to stir at r.t. overnight which led to the formation of **46** in 68% yield.

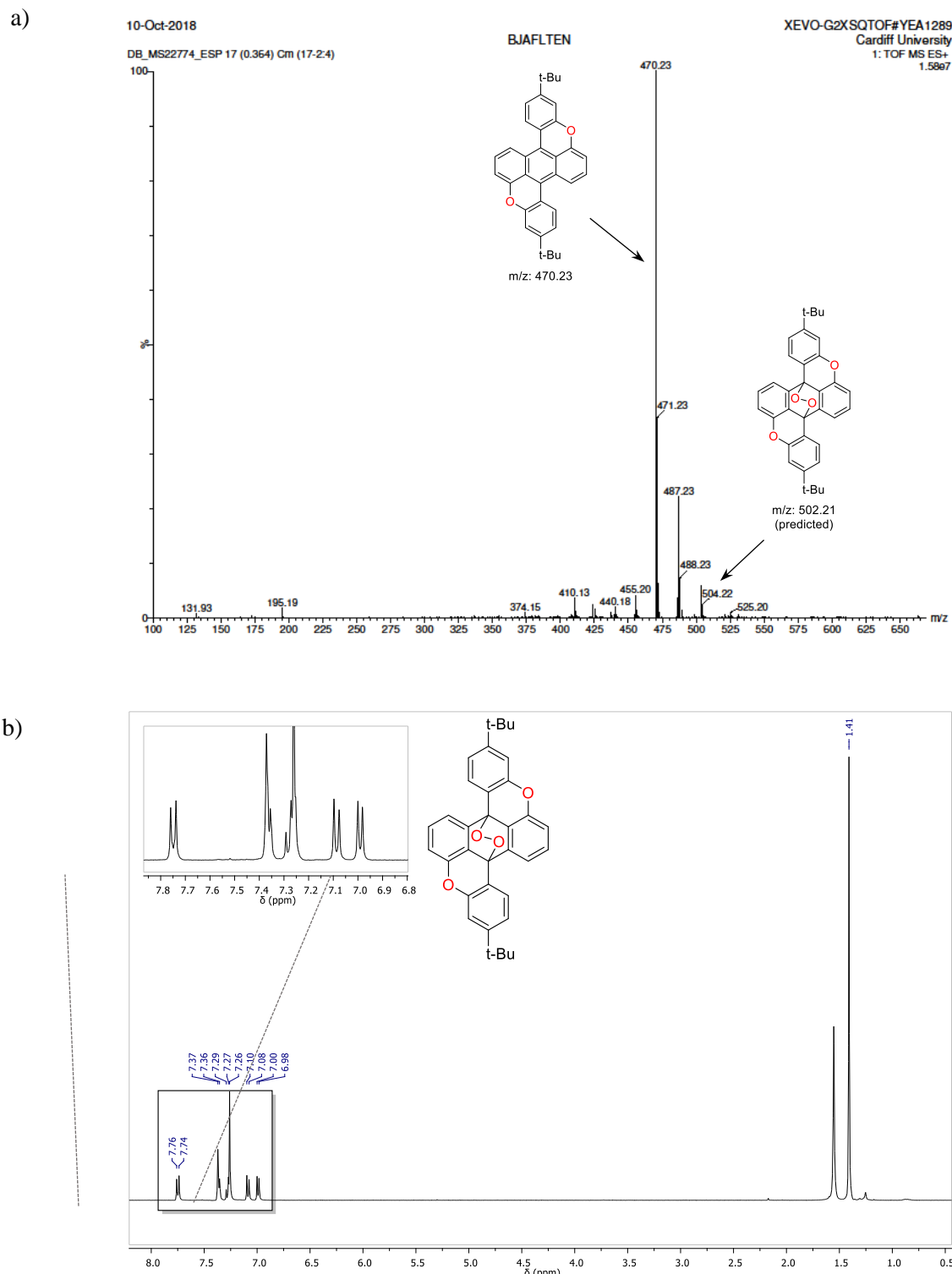


Scheme 3: Synthetic pathway of 1,5-cyclised anthracene target molecule **43**.

The next step was the dehydration reaction using the same conditions as those employed during in section 2.1.1 (Scheme 2, page 25). This method again gave quantitative yields of the desired product (**45**) as an isotropic mixture, similar to the anthracene derivative **41** discussed in section 2.1.1. It is believed that the restricted rotation of the phenyl moieties is caused by the steric demands placed on the molecule by the methoxy groups being in close proximity to the chlorine atoms.

The deprotection of methoxy groups was again performed using BBr₃. This was done by addition of 1 M BBr₃ in DCM to a solution of **45** at -78 °C in the absence of light, followed by warming the mixture to room temperature and allowing it to stir overnight. Purification by column chromatography generated product **44** in 61% yield.

To achieve the synthesis of molecule **43**, an intramolecular S_NAr reaction using **44** as the starting material was employed. This was performed by deprotonation of the hydroxyl groups of **44** using K₂CO₃ under inert atmosphere. The mixture was then heated to 140 °C for 3 h giving a vivid red solution. Attempts to purify the product by column were unsuccessful as it appeared to degrade in contact with SiO₂ and air, in a similar manner to **34**. However, purification by precipitation from DCM/Hex was proven to be possible.



leaving the solution in the NMR tube under air overnight, a good spectrum showing only the endoperoxide was present (Figure 18a).

2.1.3 1,4-cyclised Naphthalene Target Molecule (**56**)

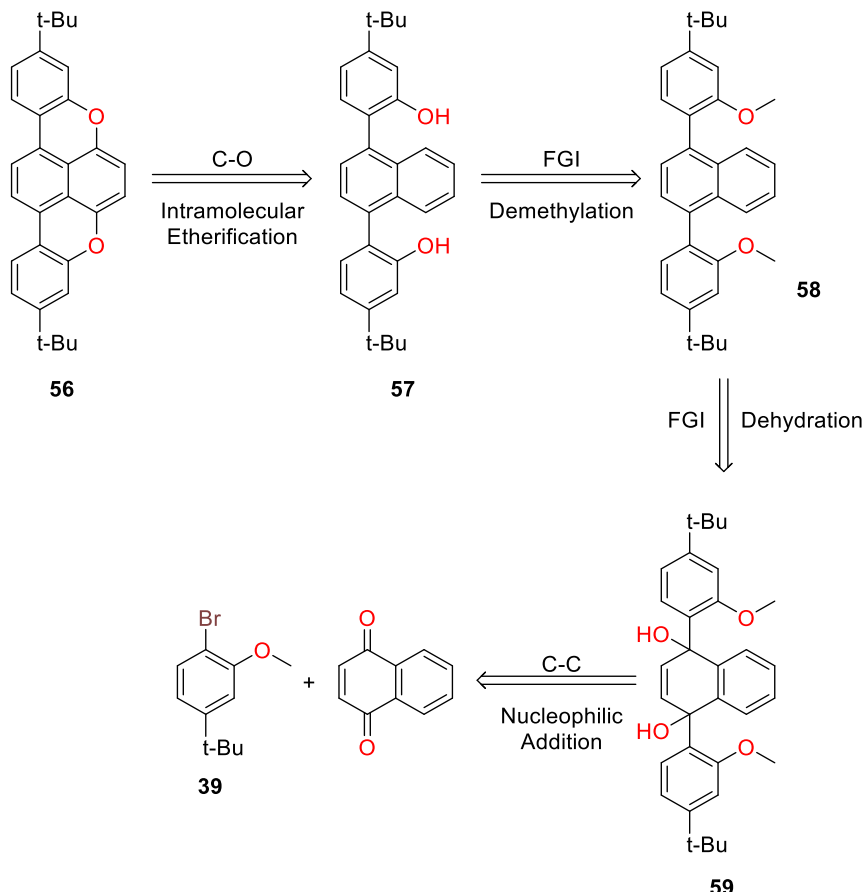
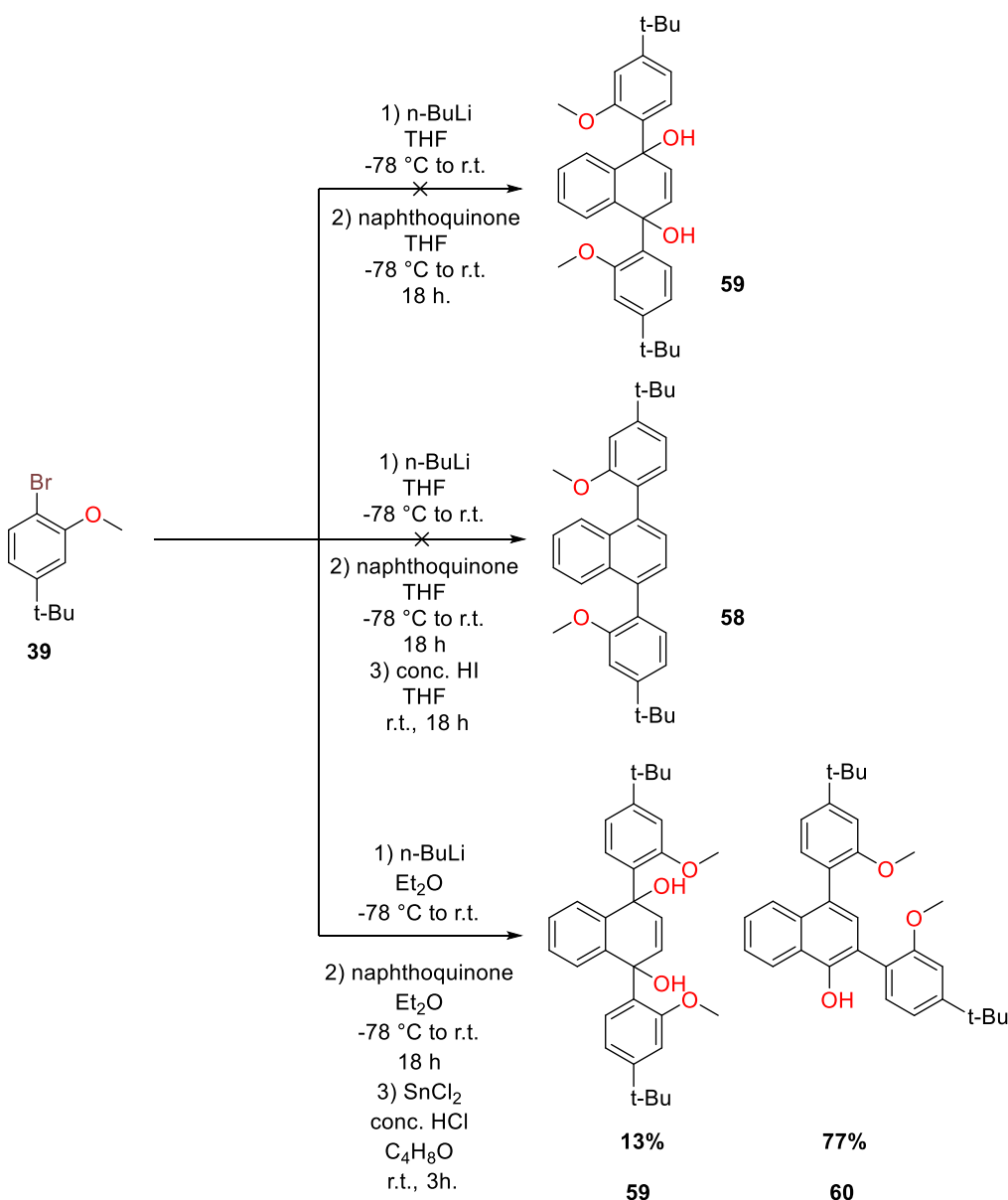


Figure 19: Initial retrosynthetic analysis of 1,4-cyclised naphthalene target molecule **48**.

As both the 1,4- and 1,5- cyclised anthracene-based target molecules synthesized thus far appear to be sensitive to air, work was also started on a 1,4-cyclised naphthalene target molecule (**56**). It was believed that the absence of the third aromatic ring of the molecule’s “core” would lead to increased stability in air. It was theorised that the molecule would lack an aromatic moiety electron-rich enough to readily react with a singlet oxygen molecule. Decreasing the conjugation in the molecule would also lead to blue shifted absorption spectrum when compared to **34** and **43**. It was thought that synthesis of this molecule would give us access to a material which is initially transparent but appears coloured upon oxidation. Through retrosynthetic analysis of the target molecule (Figure 19), a similar approach adopted for the synthesis of **34** was chosen (see section 2.1.1).



Scheme 4: Attempts to synthesize **59** and **58** as part of the initial synthetic pathway for the 1,4-cyclised naphthalene product.

The target molecule can be obtained through intramolecular etherification of bisphenol-naphthalene derivative **57**. Molecule **57** can be synthesized from molecule **58** by a deprotection method as used in the synthesis of **35** (Scheme 2). The same dehydration technique discussed earlier using SnCl₂ could be applied to the synthesis of **58** from the intermediate naphthalene-diol **59**. The nucleophilic addition reaction used for the synthesis of **46** (Scheme 3) and **40** (Scheme 2) would be used to synthesize **59** from commercially available 1,4-naphthoquinone and a methoxybenzene derivative (**39**).

Initial attempt to synthesize **59** following the same procedure used during sections 2.1.1 and 2.1.2 was unsuccessful. This method used 2.9 eq. of *n*-BuLi added to a solution with 3 eq. of methoxybenzene derivative **39** at -78 °C. After stirring at room temperature for 0.5 h the solution was cooled again to -78 °C

and a suspension of naphthoquinone in THF was added. The reaction led to isolation of only starting material.

Similar naphthalene-diol molecules were found in literature, they were synthesised in by Dodge and Chamberlin in 1988 and appeared to be sensitive to air.¹⁰⁵ It was believed that this may have been the reason for the failure of the initial synthesis attempt.

To avoid problems with degradation of **59**, it was decided that a one-pot nucleophilic addition reaction followed by dehydration to achieve naphthalene derivative **58** would be the best course of action. The nucleophilic addition reaction was performed in the same manner as before: addition of *n*-BuLi to the methoxybenzene derivative **39** at -78 °C, warming to r.t. for 0.5 h then cooling again for the addition of naphthoquinone, warming to r.t. and allowing the reaction to stir at this temperature overnight. Upon completion of this part of the reaction, the flask was covered with aluminium foil and concentrated HI was added as a reducing agent. The reaction was left overnight again then worked up and purified. This also did not yield any of the desired product, instead unreacted **39** was recovered. Unreacted naphthoquinone was also found along with trace amounts of **59**.

It was then decided to repeat the experiment changing the method of reduction. As reduction of diols by SnCl₂ in conc. HCl had been used to good effect when synthesising the other target molecules, it was decided that it should be applied to this synthesis. This reduction method did not lead to the formation of the desired molecule being. However, it did produce naphthalene diol **59** (13% yield) along with by-product **60** (77% yield). The formation of **60** is said to be produced by loss of one molecule of water from **59** followed by a migration of the phenyl group and loss of a proton.¹⁰⁵ Another explanation for the formation of this product may be the nucleophilic addition to the 3- position of the naphthoquinone instead of the 1-position, similar to a nucleophilic addition to an enone. However, detailed investigation and discussion of this mechanism is beyond the scope of this project. Therefore, at this point the synthetic strategy was re-evaluated and adjusted.

The formation of the target molecule was still to be accessed by an intramolecular etherification reaction, as well as **57** being obtained through a demethylation reaction performed in the same manner as before. However, to by-pass the naphthalene diol stage of the pathway, a cross coupling reaction could be used to synthesize **58** from commercially available 1,4-dibromonaphthalene and **39**.

1,4-dibromonaphthalene (**61**) was synthesised according to a procedure found in literature;¹⁰⁶ a solution of naphthalene was cooled to -35 °C, Br₂ was added and the reaction left to stir in the cooling bath overnight. This gave good yield of **61** which then gave access to **58**.

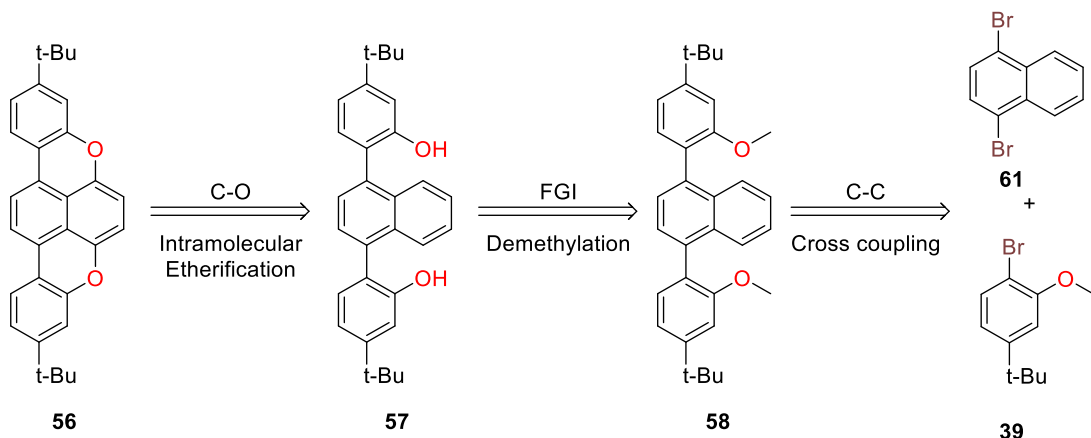
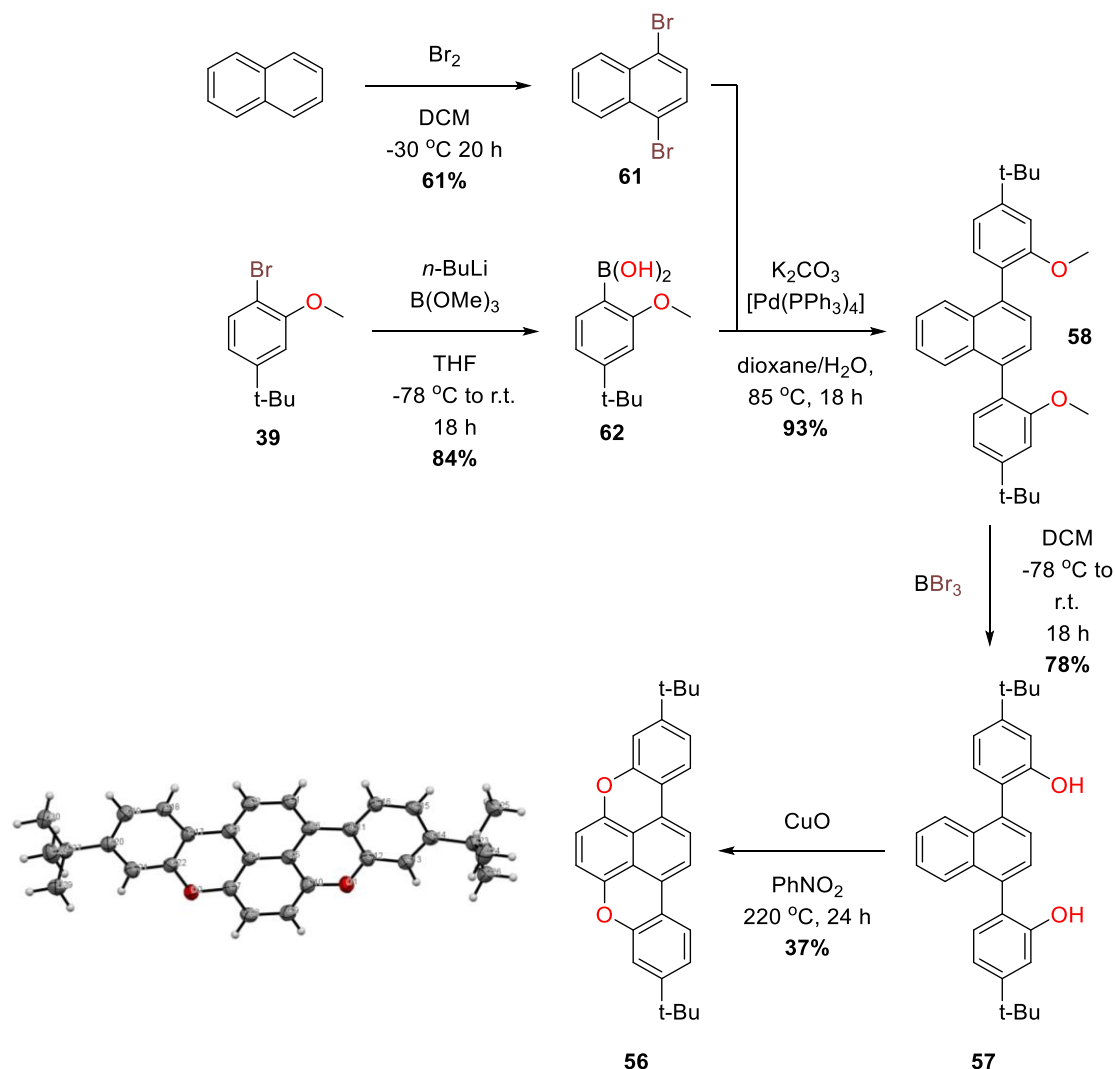


Figure 20: Adjusted retrosynthetic analysis of target molecule **56**.

While **61** was being synthesized, the second species needed for the cross-coupling reaction (**62**) was synthesised in parallel. This was done using a borylation method developed by Dordevic *et. al.*:⁹³ *n*-BuLi was added to a solution of **39** at -78 °C, this was followed by the slow addition of B(OMe)₃ and warming of the mixture to r.t. overnight.

Once synthesis of both **62** and **61** was achieved they were applied to a Suzuki reaction using modified conditions based on those developed by Suzuki *et. al.* The initial attempt used 3 eq. of **62** to 1 eq. of 1,4-dibromonaphthalene (**61**), 4 eq. of K₂CO₃, and 7 mol% of [Pd(PPh₃)₄], in a 5:1 toluene/H₂O solvent mixture, following literature protocols.¹⁰⁷ The reaction yielded 37% of the desired product with a large amount of mono-substituted product (60%). Following this the solvent mixture was changed to 5:1 dioxane/H₂O, all other conditions were kept constant. This led to a reaction which gave product **58** in 37% yield along with some starting material. The dioxane/water mixture appeared to give greater conversion to the desired product, so was chosen as the solvent system for the scale-up. Upon adjusting the solvent mixture to 4:1 C₂H₈O₂/H₂O it was found that the yield markedly improved: 93% of the bis-substituted product was obtained. Following this reaction, a demethylation reaction was done using the same procedure as described earlier. This yielded bis-phenol species **57** in 78% yield, which was then subjected to the final step of the synthetic pathway.

Initial attempts to obtain **56** were unsuccessful, following the procedure used to obtain **34** led to little conversion of the starting material with no desired product present. A second procedure utilising another copper source was found in literature.¹⁰⁸ A CuCl catalyst was used in place of the CuI/pivalic acid system and the reaction was heated to 120 °C.



Scheme 5: Synthetic pathway used to achieve the synthesis of the 1,4-cyclised naphthalene target molecule (**56**) along with the ORTEP representation of the molecule obtained from preliminary X-ray diffraction experiments. Diffraction experiments performed by D. Romito.

This method led only to degradation of the starting material. The next approach used CuO in PhNO₂ heated to 220 °C for 24 h under air.⁹³ This reaction yielded the desired product as an orange powder which was highly fluorescent in solution (for the electrochemical properties and application of this molecule to prototype ECDs, see section 2.2). X-ray crystallography confirmed the formation of the di-pyrano product. TLC of the reaction crude also suggested the presence of a mixture of products with the same R_f as the desired product, though these were not isolated. One of the new spots seen may be due to the 6,7-cyclised di-furano product (**63**). As the di-pyrano product was obtained from this reaction it was envisioned that the reaction could occur in two ways: a stepwise mechanism, or a simultaneous ring closure mechanism.

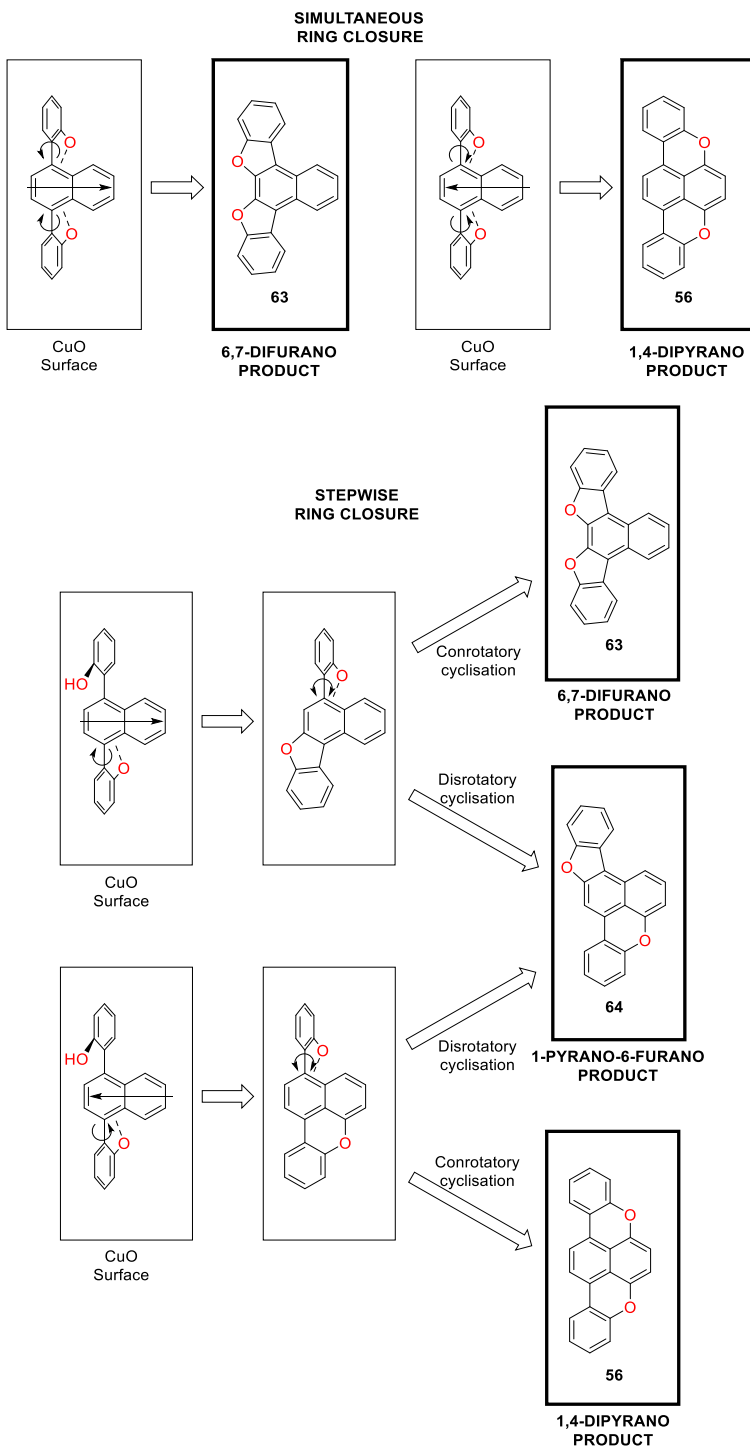


Figure 21: Schematic demonstration explaining the possible mechanism for ring closure of the 1,4-cyclised naphthalene product. The rotation of the rings and translation of the naphthalene core lead to the formation of the di-pyrano, di-furano, and furano-pyrano possible products. Solubilising groups omitted for clarity.

The simultaneous ring closure mechanism proceeds through the adsorption of both hydroxy groups on to the CuO surface, the system then undergoes planarization with the rings effectively ‘snapping’ shut simultaneously. It was thought that this mechanism would give rise to only two products: the desired di-pyrano **56**, and the di-furano molecule **63**. This selectivity is thought to be due to the translation of the

naphthalene core across the CuO surface as the molecule becomes planar (Figure 21). This should lead to both cyclisations happening on the same side of the naphthalene core, either the 1,4- side or the 6,7- side depending on the direction of translation, thus leading to the di-furano and di-pyrano products.

The stepwise mechanism was thought to proceed by initial adsorption of one of the hydroxy moieties on to the CuO surface, this then undergoes cyclisation at the 1- or 7- position depending on the direction of the translation of the naphthalene core. Following this, the second hydroxy group adsorbs to the CuO surface and takes part in the same cyclisation, which is again dependent on the translation of the naphthalene core. This means that the second cyclisation occur at the 4- or 6- position, thus leading to the possibility of an additional product: the furano-pyrano molecule **64**.

To investigate this reaction further and prove any selectivity for the pryan product of the cyclisation reaction, the synthesis of a molecule possessing a single pryan moiety (**65**) was proposed. A retrosynthetic analysis of the desired molecule **65** proposed that it could be synthesised using a similar strategy to that of 1,4-cyclised naphthalene product **56** (Scheme 5). The final molecule can be obtained by an intramolecular etherification reaction of **66** following the same procedure as for the 1,5-cyclised naphthalene product discussed earlier in this section.

This precursor may be synthesised using a demethylation reaction of **67** similar that discussed in section 2.1.1. The synthesis of this molecule can be achieved using a Suzuki cross-coupling reaction of commercially available 1-bromonaphthalene and the boronic acid **62** formed during the synthetic pathway of **56**.

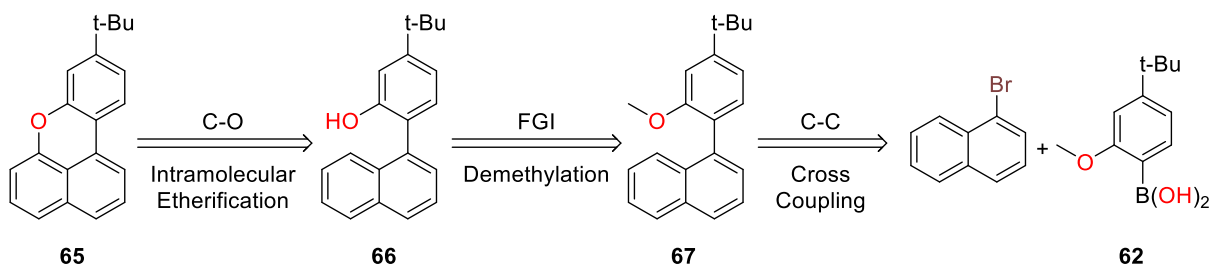
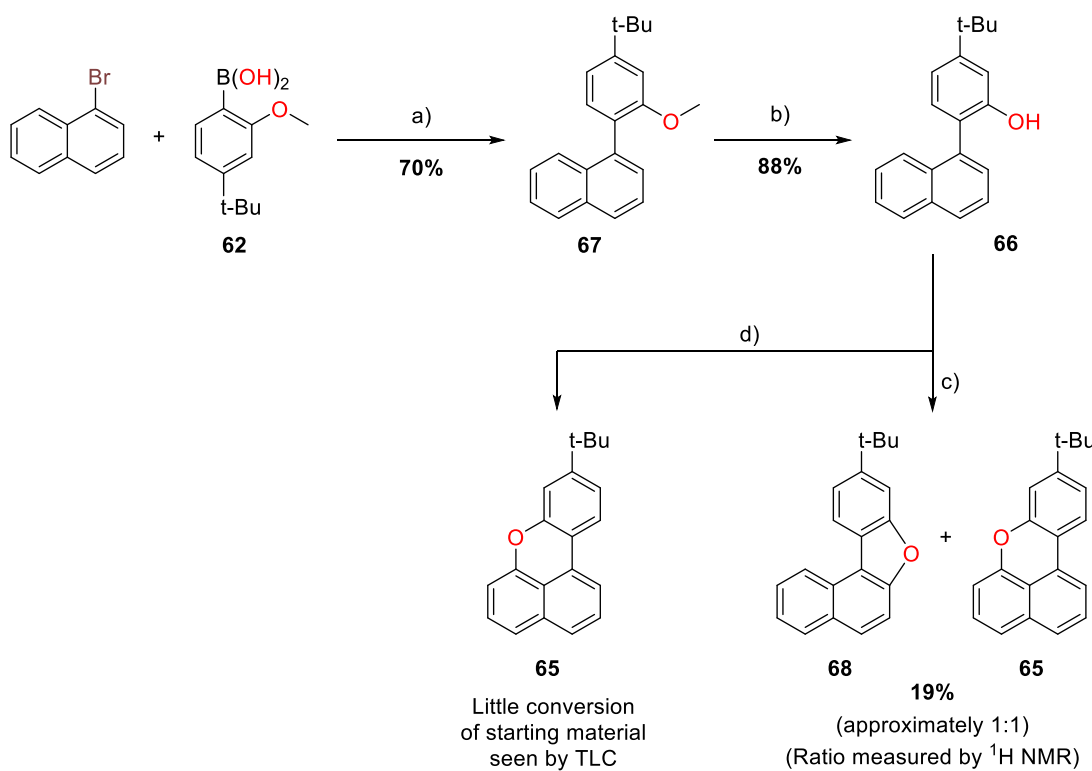


Figure 22: Retrosynthetic analysis of 1-naphthalene target molecule.

Precursor **67** was synthesised using a Suzuki reaction of commercially available 1-bromonaphthalene and boronic acid **62**. This reaction followed the same procedure discussed in section 2.1.3: 1-bromonaphthalene, boronic acid **62**, and K_2CO_3 were dissolved in a degassed mixture of dioxane/H₂O under an inert atmosphere, $[Pd(PPh_3)_4]$ was then added and the flask heated to 85 °C overnight. Upon purification of the crude reaction mixture by column chromatography, the desired product was obtained in 70% yield.

Demethylation of this precursor using BBr_3 following the same method as previously discussed (section 2.1.1), led to the synthesis of **66** in 88% yield which was then used to access target molecule **65**. An initial attempt to synthesise this target molecule was performed using the same conditions as those used during the synthesis of **56**. NMR suggested that this led to a product which contained a mixture of the desired pyrano containing molecule, and the furano containing by-product **68**. It was found that these isomers could not be separated by column chromatography as they possess the same retention factor by TLC. Attempts to purify by crystallization and precipitation were unsuccessful. Gel permeation chromatography was also attempted and gave a mixture of products with a ratio of 1:0.6. Complete separation of the isomers could not be achieved.



Scheme 6: Synthetic pathway used during the synthesis of target molecule **65**; a) K_2CO_3 , $[\text{Pd}(\text{PPh}_3)_4]$, dioxane/ H_2O , $85\text{ }^\circ\text{C}$, 18h; b) BBr_3 , DCM, $-78\text{ }^\circ\text{C}$ to r.t., 18 h; c) CuO , PhNO_2 $220\text{ }^\circ\text{C}$, 24 h; d) CuI , PivOH , DMSO, $160\text{ }^\circ\text{C}$ 16 h.

The cyclisation experiment was repeated using the conditions used for the synthesis of the anthracene core molecules discussed earlier (section 2.1.1 and 2.1.2). This was to investigate possible selectivity of the CuI pathway for the pyrano product. Following the reaction conditions established in section 2.1.1, led to very little conversion of the starting material. It is believed that more energy is required to activate the C-H bond of the naphthalene moiety compared to the anthracene molecules discussed in section 2.1.1 and 2.1.2, thus at lower temperatures the reaction does not take place. As the CuO -based reaction investigated earlier utilises harsher conditions, this leads to greater yield of cyclisation products. However, the higher temperatures appear to cause the loss of any selectivity for the desired pyrano product.

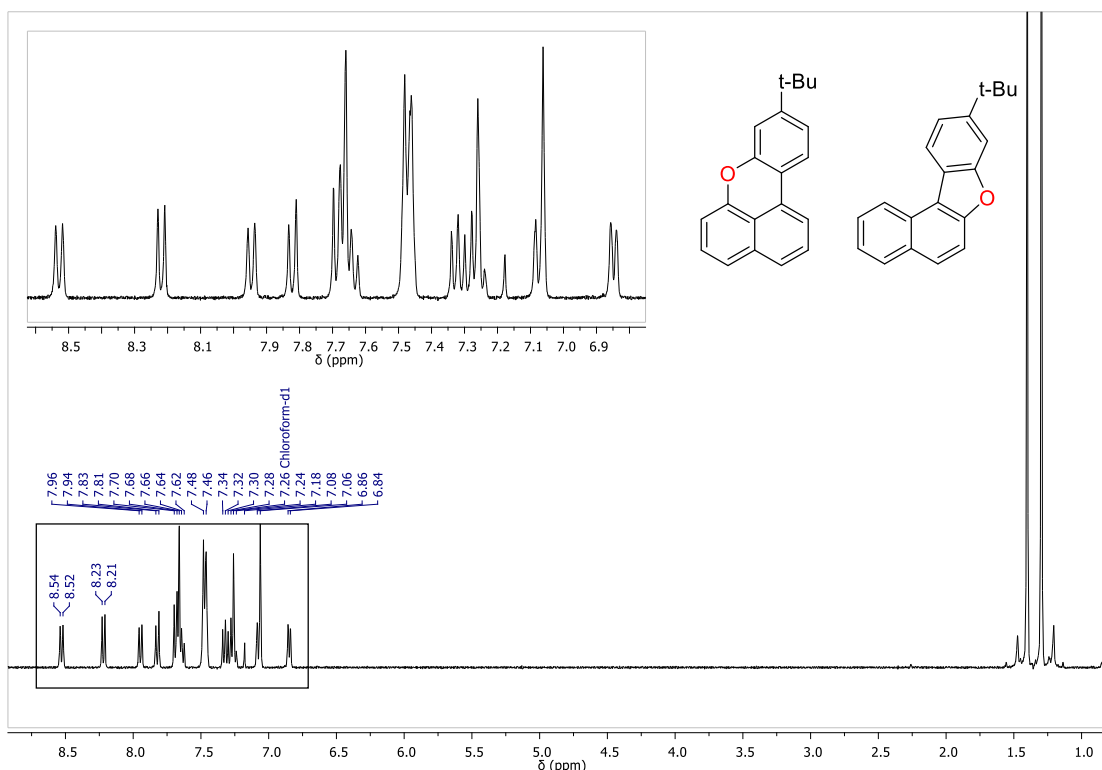


Figure 23: ¹H NMR in CDCl₃ spectrum of the 1:1 mixture of products formed during the CuO mediated cyclization of **65**.

2.1.5 1,5-Naphthalene Target Molecule (63)

Following this, work moved on to the synthesis of the second naphthalene target molecule **69** (Figure 24). The retrosynthetic analysis suggests that the final molecule can be obtained by intramolecular etherification reaction of naphthalene-diol **70**. This precursor may be produced by demethylation of **71** following similar methods discussed earlier in this section. To obtain the intermediate **71**, a cross-coupling reaction was envisioned using the commercially available 4-(*tert*-butyl)phenylboronic acid and dibromonaphthalene derivative **72**. The molecule **72** may be produced from 1,5-dimethoxynaphthalene **73** via a bromination reaction. This precursor can be reached from commercially available 1,5-dihydroxynaphthalene by performing a methylation reaction similar to the one discussed in section 2.1.1(Scheme 2).

1,5-dimethoxynaphthalene was successfully synthesised in 78% yield following the methylation procedure discussed earlier in this thesis; 1,5-dihydroxynaphthalene and K₂CO₃ were dissolved in DMF under inert atmosphere, MeI was added and the reaction was heated to 55 °C for 20 h. Following the synthesis of **73**, 1,5-dibromo-5,8-dimethoxynaphthalene **72** was synthesised.

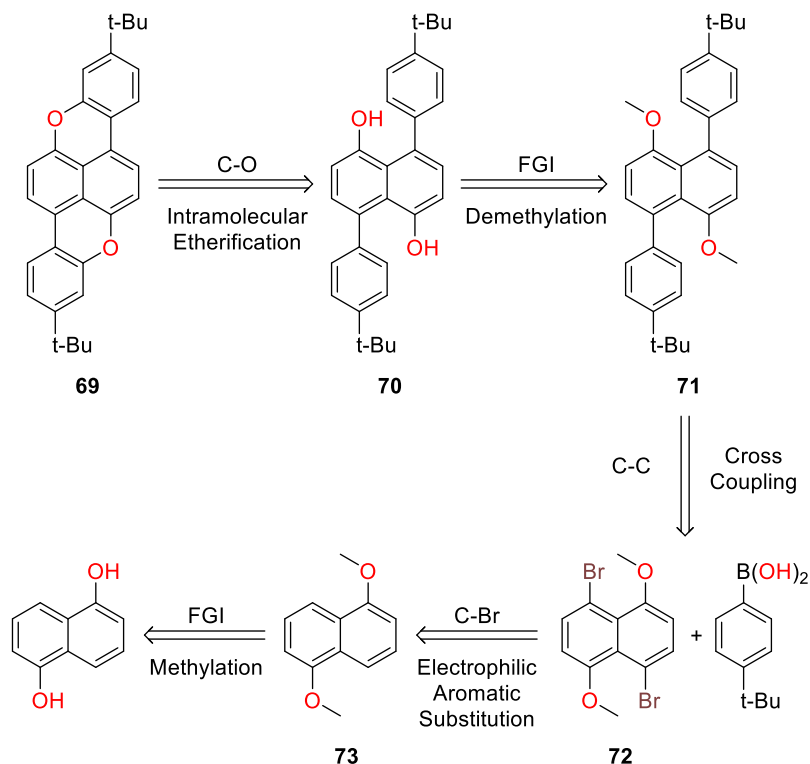
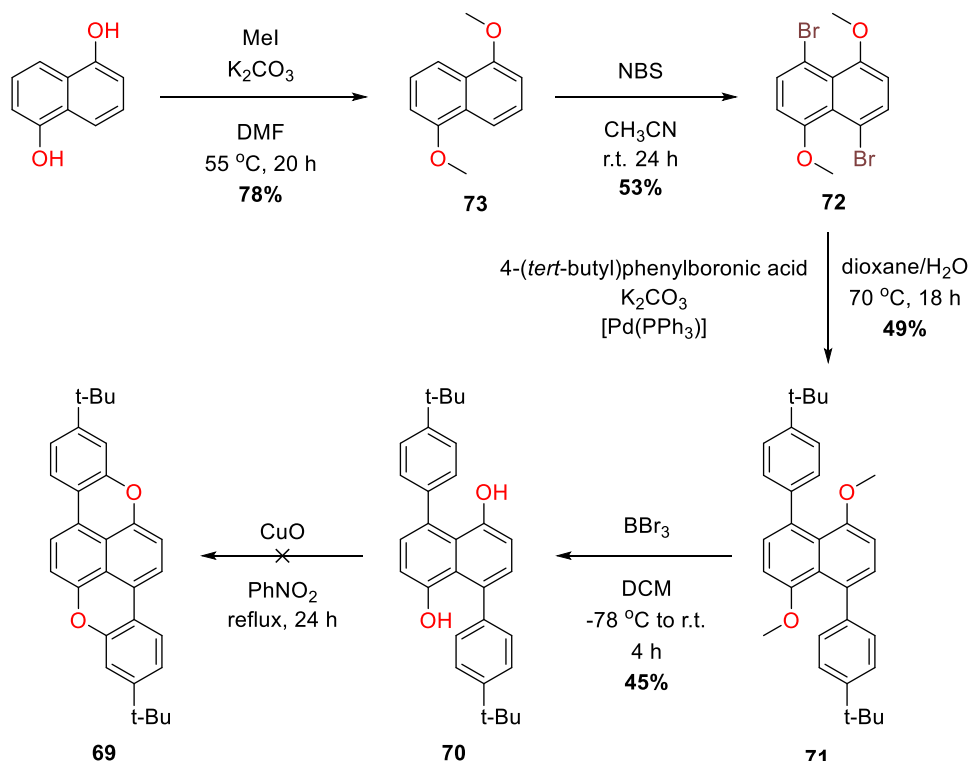


Figure 24: Retrosynthetic analysis of the proposed 1,5-cyclised naphthalene product.

This was done using a bromination reaction using conditions found from literature;¹⁰⁹ **73** along with N-bromosuccinimide (NBS) was dissolved in CH_3CN under an inert atmosphere and the reaction was stirred at room temperature for 24 h. This gave the desired product **72** in 53 % yield. An initial attempt to obtain the cross-coupled product (**71**) following the same procedure established in section 2.1.3 was unsuccessful; very little conversion was seen when monitoring the reaction with TLC, and 77% of **72** was recovered. It was believed that insolubility of the starting material **72** led to poor conversion as the starting material never appeared to go fully into solution. After adjusting the solvent mixture to a ratio of 8:1 dioxane/ H_2O , the reaction was performed once again; the presence of the desired product was proven by mass spectroscopy, with 25 % yield obtained after purification. However, when performing the reaction with a solvent mixture of C_4H_8O/H_2O (4:1), it was found that the yield could be further improved. The demethylation of **71** was performed using the same conditions as discussed in section 2.1.1; BBr_3 was added to a solution of **71** at -78 °C under an inert atmosphere and in the dark, the reaction was then stirred at room temperature for 4 hours. Purification by trituration with petroleum ether gave the desired product (**70**) in 45% yield.



Scheme 7: Initial synthetic pathway applied to the synthesis of target molecule **69**.

An initial intramolecular etherification test reaction using **70** was conducted. Low conversion of the starting material was observed and the stability of precursor **70** was called into question, as on standing in air the white crystals slowly turned black. As such, a second synthetic strategy was proposed to achieve the synthesis of **69** (Figure 25).

This new strategy proposed that the final molecule (**74**) could be obtained following the same intramolecular etherification reaction discussed previously (section 2.1.4), the precursor for which (**75**) may be obtained by the demethylation of **76**. It was proposed that this bis-substituted naphthalene intermediate could be synthesised using a Suzuki cross-coupling reaction between the boronic acid (**62**) seen in section 2.1.3 and the 1,5-dibromonaphthalene derivative **76**. The synthesis of this molecule may be achieved by bromination of the commercially available 2,6-di-*tert*-butyl-naphthalene.

Synthesis of **77** was performed using literature conditions developed by Harvey *et al.*:¹¹⁰ 2,6-di-*tert*-butyl-naphthalene and 1 mol% AlCl₃ were dissolved in DCM. To this mixture a solution of bromine was added, and the reaction was left to stir at room temperature for 24 h. This gave the desired product in good yield without the need for purification. The synthesis of intermediate **76** was achieved by Suzuki cross-coupling reaction following the procedure established in section 2.1.3.

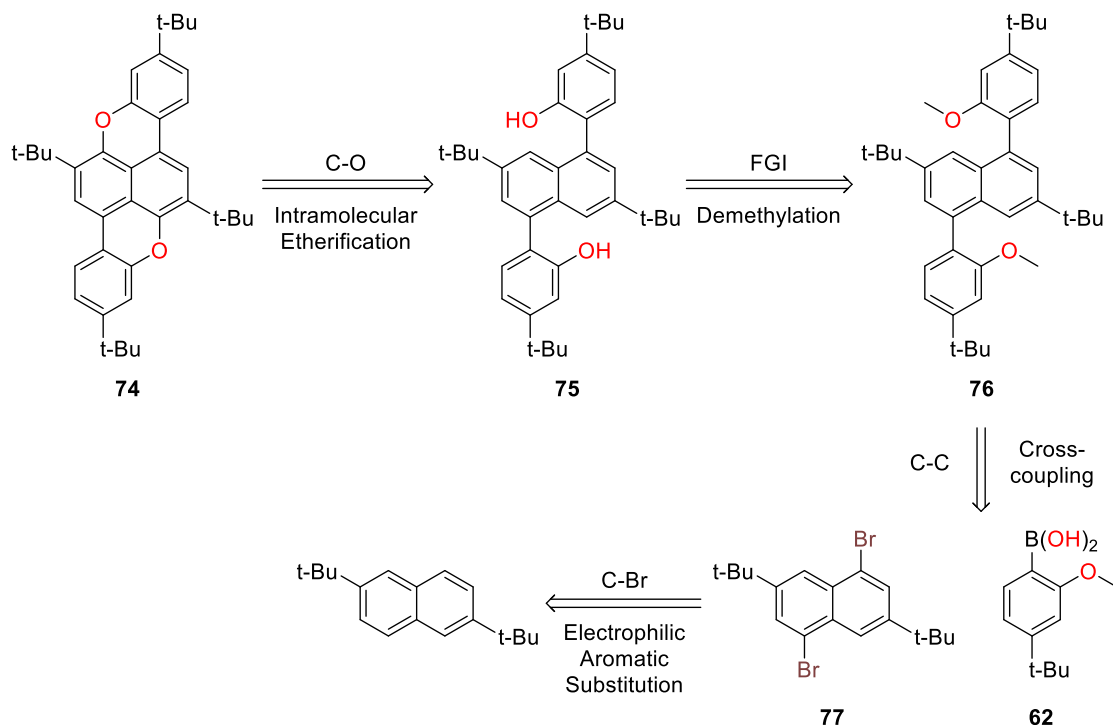


Figure 25: The retrosynthetic analysis of the target molecule **74** demonstrating the new synthetic strategy.

Dibromonaphthalene **77**, boronic acid **62**, and K_2CO_3 were dissolved in a degassed mixture of dioxane/ H_2O under inert atmosphere, $[\text{Pd}(\text{PPh}_3)_4]$ was added, and the reaction heated to 85°C for 20 h. The reaction produced product **76** in 56% yield. Further optimisation of the conditions is needed to achieve greater yields of the bis- substituted product.

The demethylation of **76** was performed following the procedure discussed throughout this thesis; BBr_3 was added to a solution of **76** at -78°C before being warmed to room temperature for 4 h. This gave the desired product in 48% yield, giving access to the final step of the synthetic strategy. The intramolecular etherification reaction was performed using a CuO mediated pathway, similar to that seen in section 2.1.4. Heating a suspension of **75** and CuO in PhNO_2 to reflux for 24 h led to complete conversion of the starting material and the formation of three new products, as seen by TLC (figure 26). Purification by column was attempted but unsuccessful as it appeared some of the products degraded on silica. Instead purification by precipitation from $\text{C}_2\text{H}_5\text{COOCH}_3/\text{CH}_3\text{OH}$ gave a bright yellow powder. NOESY NMR (Figure 38, see appendices) suggests that this is the desired pyrano

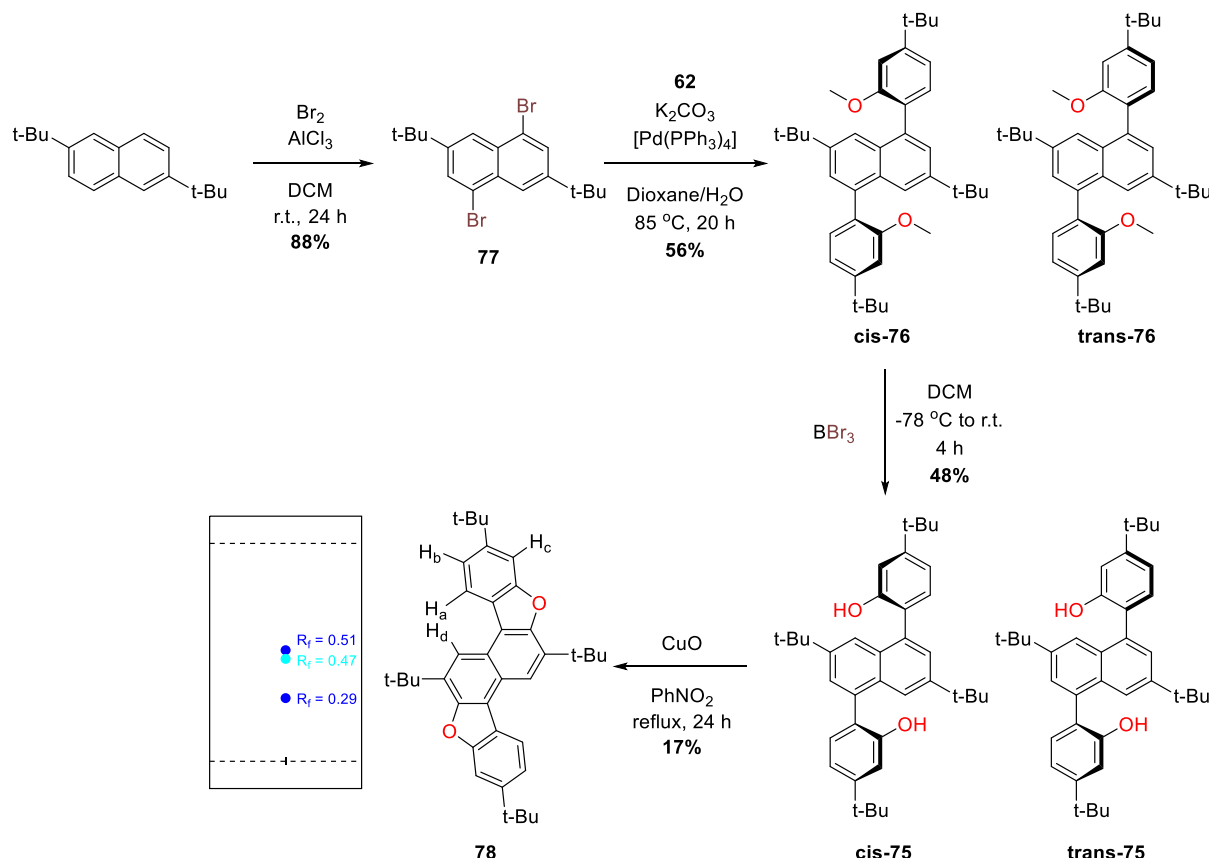


Figure 26: Synthetic pathway applied to the synthesis of the 1,5-cyclised naphthalene product, along with the isolated product **78**. Sketch of TLC from the reaction crude demonstrating the formation of three new products, all of which fluoresce blue under 256 nm light.

product as the spectra shows very little interaction between the H_a and H_d protons (Figure 26). A small interaction between these peaks was expected for the desired pyrano product and a large interaction for the furano product due to the proximity of the protons to each other in space. However, X-ray diffraction experiments proved that this was not the desired product, instead the di-furano product **78** had been isolated (figure 27).

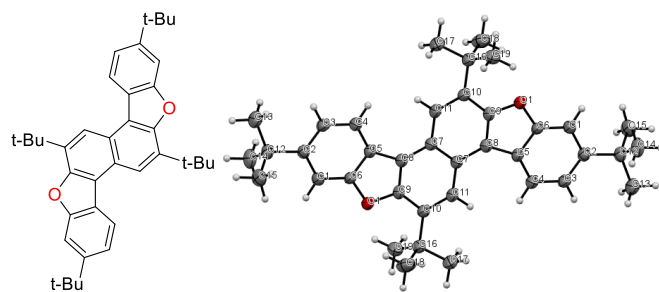


Figure 27: The di-furano product **78** along with ORTEP representation of the crystal structure found from X-ray diffraction experiments. Diffraction experiments performed by D. Romito.

The furano-pyrano product was also isolated in trace amounts by precipitation from C₄H₈O/CH₃OH, as seen by NMR. The formation of the 3,7-difurano product as well as the 1-pyrano-3-furano product suggests

that the reaction may travel through a stepwise mechanism, as discussed in section 2.1.4. If the reaction were to proceed through a simultaneous ring-closure dependent on the translation of the naphthalene core, then only the 1-pyrano-3-furano product would be expected (Figure 28). The isolation of the di-furano product suggests that the mechanism instead goes through a stepwise process.

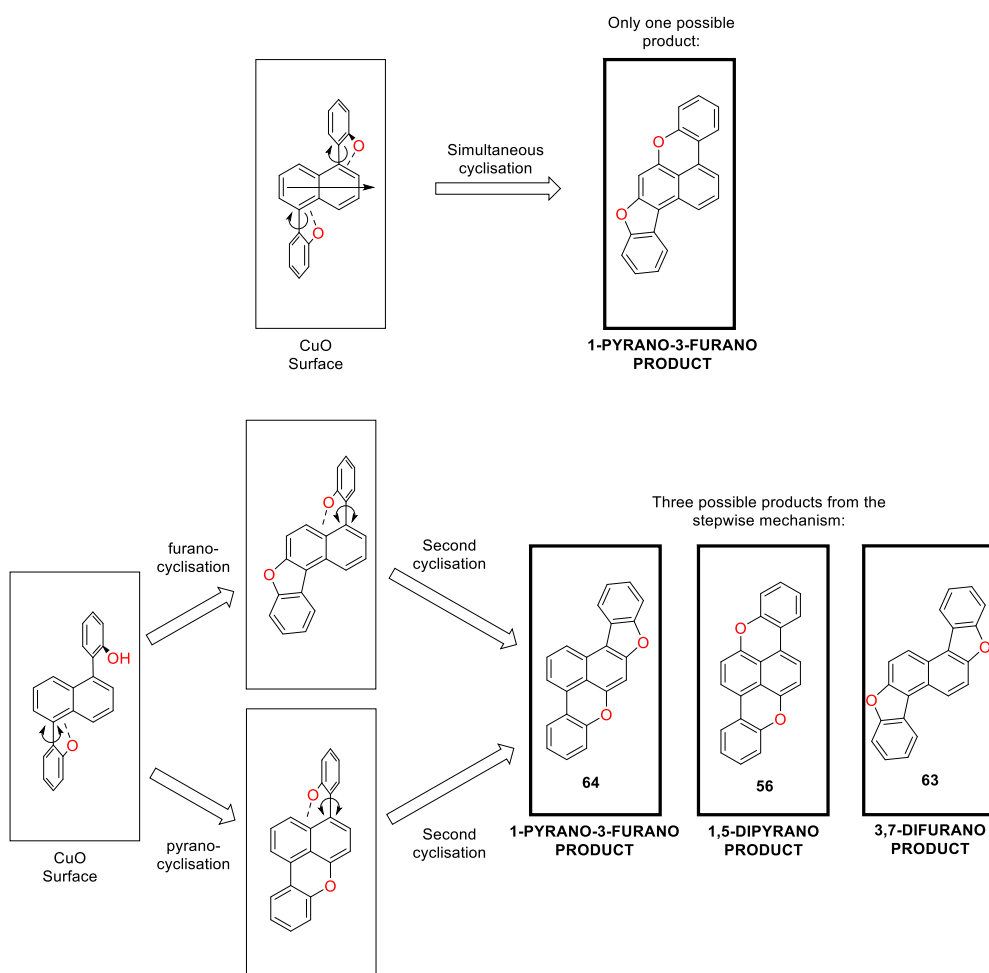


Figure 28: Diagram demonstrating the selectivity of the simultaneous mechanism compared to that of the stepwise mechanism. Solubilising groups omitted for clarity.

Separation of the cyclisation crude by GPC was attempted, this was unsuccessful so HPLC was performed. Separation using a recycling HPLC with hexane as the eluent was found to be possible (figure 29); small quantities of **78** and the pyrano-furano product (**79**) were isolated. The presence of each was confirmed by ^1H NMR of the pure collected fractions. The desired molecule was not isolated using this method and investigations into isolating **74** are ongoing.

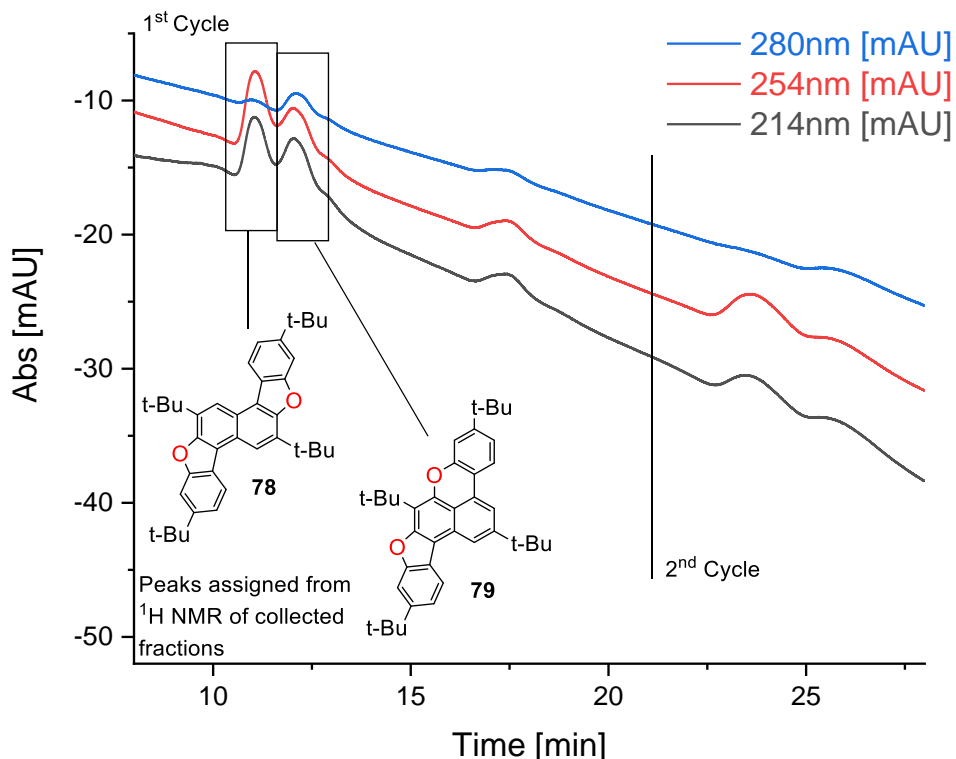
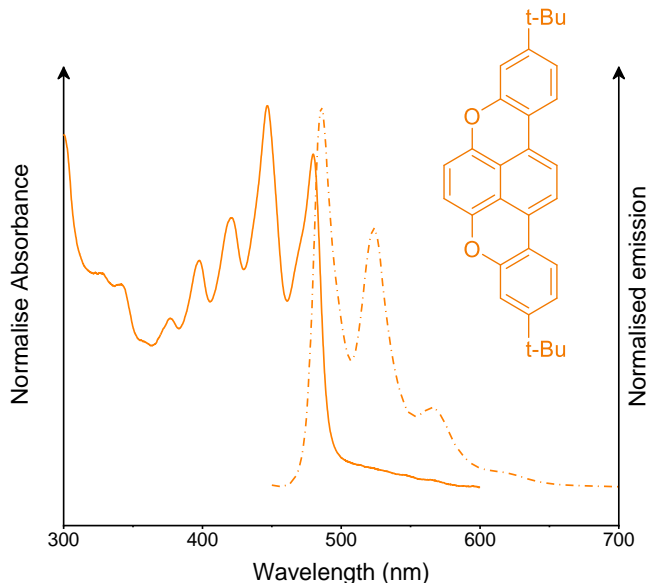


Figure 29: Chromatogram obtained during the HPLC purification of the 1,5-cyclisation crude. Purification was performed using a NEXT recycling preparative HPLC equipped with a UV-vis 4Ch NEXT PDA detector, an eluent of Hexane, and a flow rate of 10 ml/min.

2.2 Optoelectronic Characterisation

2.2.1 Spectroscopy



Upon achieving the synthesis of the 1,4-cyclised naphthalene product (**56**) its absorption and emissive properties were investigated. The molecule was found to possess a strong absorption bands in the visible

region ($\epsilon = 39\ 100\ \text{dm}^3\ \text{mol}^{-1}\ \text{cm}^{-1}$ in DCM), from 350 to 500 nm. The molecule possesses a fluorescent bright yellow colour in solution, as demonstrated by its high absorption coefficient, similar to other electrochromic materials such as PXX ($\epsilon = 22\ 400\ \text{dm}^3\ \text{mol}^{-1}\ \text{cm}^{-1}$ in its 2+ state)⁹². Quantum yield calculations also found the molecule to possess very high emission quantum efficiencies ($\Phi = 0.98$).

2.2.2 Electrochemical analysis

An investigation of the electrochemical properties possessed by the 1,4-cyclised naphthalene product (**56**) was then conducted. Measurement of the CV in solution was carried out using an electrolyte solution in which the neutral state was soluble: 0.1 M Bu₄NBF₄ in DCM. The 1,4-cyclised naphthalene product was dissolved in the electrolyte and nitrogen was bubbled through the solution for the duration of the experiment. The sample underwent five scans, from -1.5 V to 1.5 V and back, at a scan rate of 100 mV/s (Figure 31a). This was then repeated at scan rates of 50 mV/s, and 200 mV/s. The experiment demonstrates that the product possesses two oxidation peaks the first of which appears to be completely reversible. Variation of intensity of the second oxidation peak with increasing scan rates suggests that this oxidation is not completely reversible.

The reversibility of the first oxidation can be proven by plotting the square root of the scan rate against the current (Figure 31b). A linear trend proves the reversible nature of the oxidation; although a good linear fit has been achieved, a greater number of scan rates are needed to obtain a more reliable trend. Work on performing CV at a greater number of scan rates is underway.

The behaviour of the second oxidation state and appearance of a shoulder at approximately 1.1 V could possibly be explained by the stabilisation of the oxidised states through mixed valence complexes. Molecules synthesised and investigated by Christensen et. al. also demonstrated the development of a broad shoulder during CV analysis.¹¹¹ The authors found that this was due to the association of uncharged species and radical cations formed upon oxidation. To confirm if this is the case with the 1,4-cyclised naphthalene, electrocrystallisation followed by XRD of the crystals could be attempted. Another means to confirm the presence of mixed valence compounds could be EPR spectroelectrochemical studies.

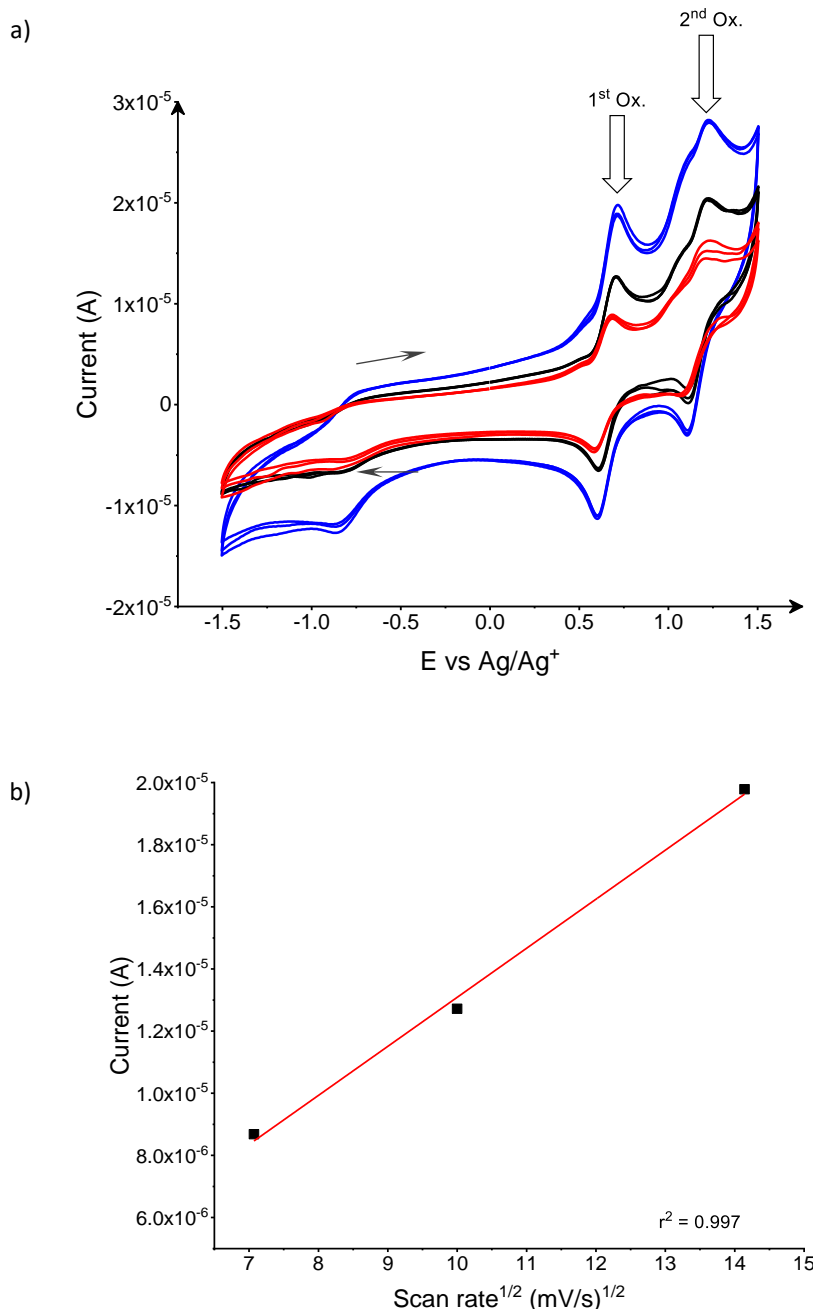


Figure 31: a) CV of 1,4-cyclised naphthalene product at 50 mV/s (red), 100 mV/s (black), and 200 mV/s (blue) performed in 0.1 M Bu₄NBF₄ solution; b) linear trend of the square root of the scan rate vs. the cathodic current demonstrating the reversibility of the 1st oxidation of the 1,4-cyclised naphthalene product.

Following CV in solution, an electrolysis experiment was performed as a method of demonstrating the colour of the two oxidation states of **56**. The experiment was performed under nitrogen using a platinum grid as the working electrode, a platinum wire counter electrode, no reference electrode was required as the current was not measured during the experiment. The product appears to transition from its yellow neutral state to a green as its first oxidation state and then on to a green-blue for the second oxidised state.



Figure 32 Pictures from the electrolysis experiment demonstrating the colour changes caused by oxidation.

Thin film cyclic voltammetry of **56** was then attempted by depositing **56** on a piece of indium tin oxide coated polyethylene terephthalate (PET/ITO) then submerging the film in an electrolyte in which **56** was insoluble (Figure 33). The electrochemical cell also contained a platinum wire as a counter electrode and a reference electrode. The final aim of this work is to apply the synthesized molecules to solid state ECDs, therefore knowledge of its behaviour as a thin film is necessary.

This was then submerged in an electrolyte of 0.1 M LiClO₄ in acetonitrile and it underwent a potential scan from 0 V to 1.5 V to -1.5 V. It appeared that although the neutral state of the molecule was insoluble, the charged state diffused throughout the electrolyte (Figure 33). This caused a rapid loss of intensity for the peaks on the CV as the contact with the electrochrome was lost, and therefore electrochemical processes would no longer occur for the material which was not adhered to the PET/ITO.

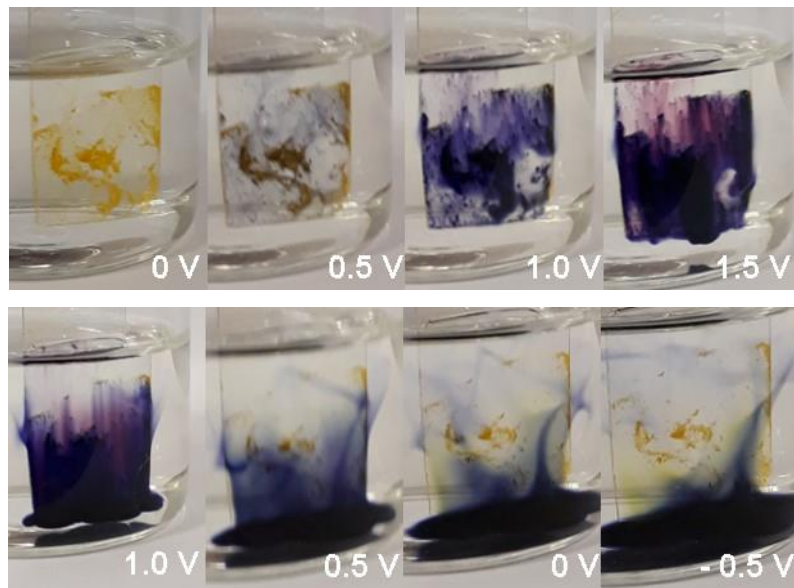


Figure 33: Pictures of the thin film CV attempt using **56**. Cycle starts at 0 V; colour change is seen from 0.5 V onward with a very vivid blue colour observed. The original colour of the substrate is seen once again as the potential returns to 0 V

2.2.3 Spectroelectrochemical Analysis

The measurement of change in absorption spectra for each of the oxidation species (Figure 34) was performed using a 0.02 mM solution of **56** in 0.1 M TBABF₄ using a specially designed thin film cuvette

in which an ‘optically transparent’ platinum grid was placed as the working electrode, along with a platinum wire as a counter electrode, and a reference cell. Upon application of +0.9 V, new bands appear in the absorption spectrum from 500 nm to 750 nm, as well as a new peak at 250 nm (Figure 34a). The peaks attributed to the neutral species are also shown to reduce in intensity. This clearly demonstrates the conversion of the neutral species into its first oxidised state. However, it appears that there was not complete conversion during the timeframe of this experiment. The appearance of new bands which fall between 500–750 nm explains the green colour observed during the electrolysis experiment.

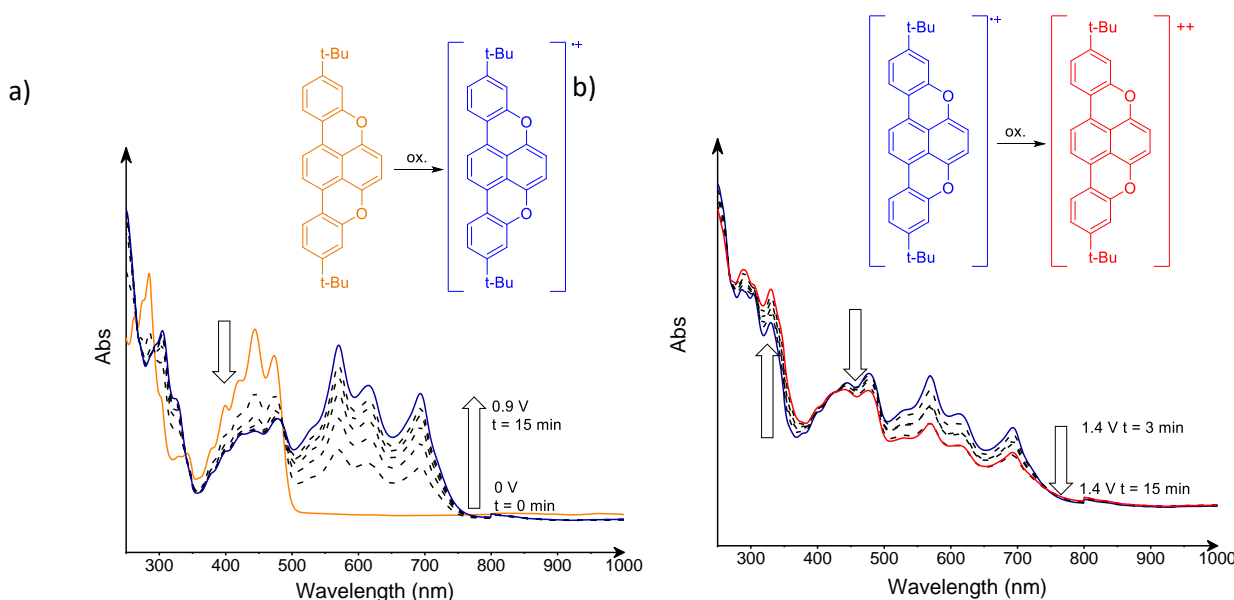


Figure 34: a) Absorption spectra of the 1,4-cyclised naphthalene product and its first oxidised species upon application of +0.9 V for 15 minutes; b) The change in absorption spectra of the first oxidation state to the second upon application of 1.4 V. This demonstrates a drop in intensity of the band at 500 – 750 nm after the application of the potential for 3 minutes. Experiments were performed in 0.1M Bu₄NBF₄ solution

Upon application of 1.4 V, the material experiences a second change in absorption (Figure 34b). The absorption spectrum demonstrates an initial increase of the peaks from 500-750 nm, likely due to the formation of the first oxidised state. The peaks associated with the first oxidised state begin to decrease after three minutes at 1.4 V, and a peak at approximately 360 nm greatly increases in intensity. After 20 minutes at 1.4 V, the potential was returned to 0 V. This caused an increase in intensity of peaks from 380-450 nm along with the decrease of peaks at 500-700 nm and 300-350 nm, suggesting that the molecule slowly returned to its neutral state.

The inherent instability of both anthracene cyclised products (**34** and **43**) meant that it was not possible to evaluate their oxidation and reduction potentials by CV in solution using the same method that was applied to **56**. When an attempt was made to perform a CV experiment on **43** in solution, using the discussed conditions, no oxidation peaks were seen.

2.2.3 Prototype Electrochromic Devices

Following the spectroelectrochemical study of the 1,4-cyclised naphthalene product, this compound was chosen to fabricate the first prototype ECD. In order to analyse the electrochromic transition of the compound in such a device, the drop-cast method was chosen. This was chosen because the technique allows for a fast checking of the colour change in the device while possessing the advantage of requiring very small quantities of material. The device is made by deposition of the electrochromic material onto a substrate which is coated with an electroactive layer, the electrolyte which is provided by our collaborators (Ynvisible) as a liquid or a solid is incorporated, and the device closed (Figure 35). The exact composition of the electrolyte contained within the device is unknown as the recipe is currently under patent.

Initially, a device utilising the electrolyte in the liquid phase was constructed. Upon the application of a potential of 1.5 V to the device, no colour change was observed. It is thought that this issue was caused by partial or complete solubility of the deposited 1,4-cyclised naphthalene (**56**) in Ynvisible's electrolyte. By pressing on the device, it was shown that the drop-cast spots moved freely and over time their colour diffused throughout the entire electrolyte. A solubility test using propylene carbonate, the major component of the electrolyte, confirmed that **56** was soluble in this electrolyte mixture.

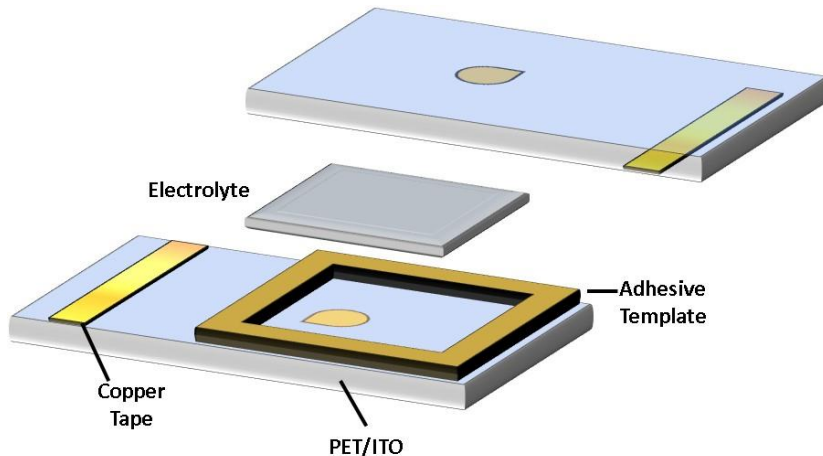


Figure 35: Cross section of the drop-cast prototype ECD fabricated using PET/ITO and Ynvisible's electrolyte.

A second device which utilised Ynvisible's electrolyte as a solid electrolyte was then fabricated (Figure 35). This was done to determine whether the molecule remain deposited on the electroactive substrate once the electrolyte had undergone a polymerisation reaction. Prior to device fabrication, the electrolyte was deposited on to PET/ITO within an adhesive template and spread until it filled this template, it was then cured under UV light for 5 minutes. The device was then built using the construction seen in Figure 36. Applying a potential of 1.5 V to the device did not result in an observable colour change. Upon increase of the potential to 2.0 V a partial colour change of the deposited sample was seen. Further testing of the device at 3.0 V led to the destruction of the PET/ITO substrate.

An alternative electrolyte developed by A. Stopin was adopted for the fabrication of a third drop-cast device.¹¹³ The 0.1 M LiClO₄ in ethylene glycol electrolyte has been applied, with great success, to the assembly of prototype ECDs containing PXX derivatives as well as polythiophenes. Solubility tests conducted on the 1,4-cyclised naphthalene product in ethylene glycol found that it had little to no solubility. This eliminated the possibility of device failure due to diffusion of the electrochromic material.

The device utilising 0.1 M LiClO₄ in ethylene glycol as an electrolyte (Figure 36b) possessed the same behaviour as that observed for the cured-electrolyte device; partial colour change of the deposited electrochrome at low potentials and device failure at 3.0 V. Therefore, a device which could access higher operating potentials was envisaged so that the second oxidation state may be reached.

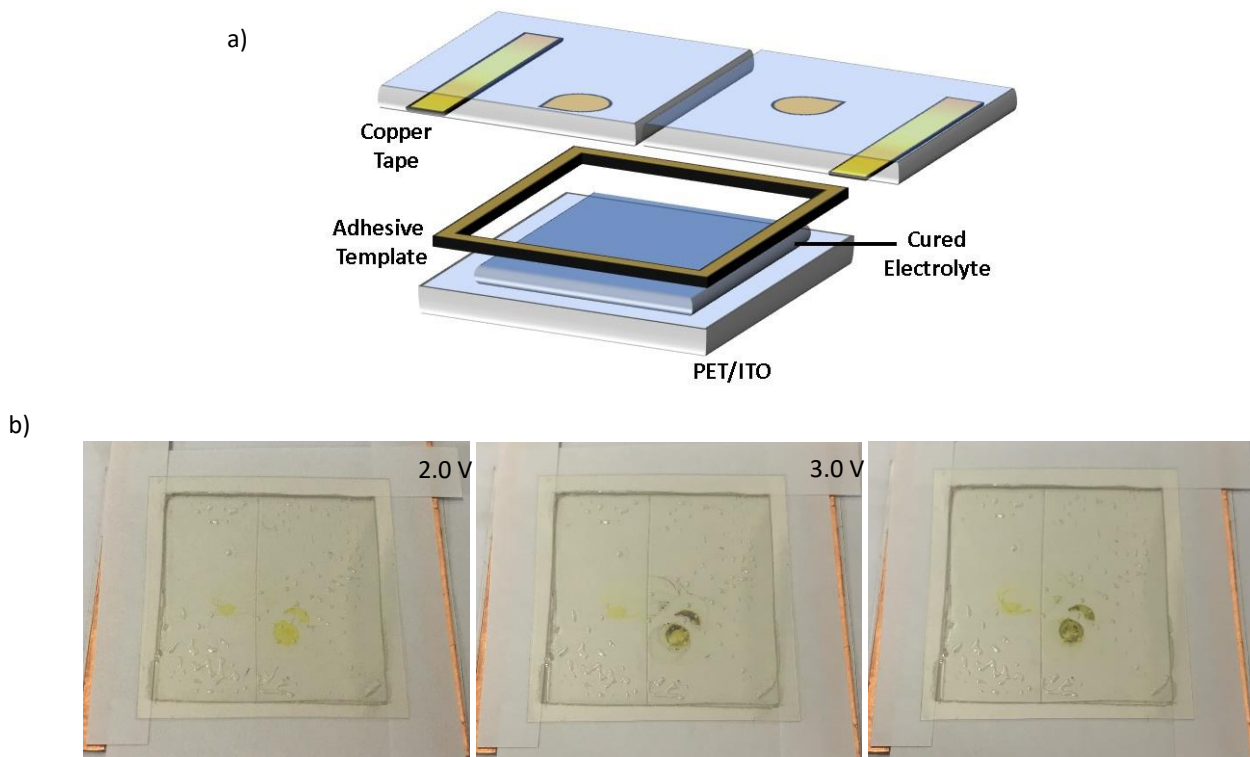


Figure 36: a) Cross section of the cured electrolyte prototype ECD discussed b) and the observed colour change of the deposited electrochrome.

A glass/FTO (fluorine-doped indium-tin oxide) support was proposed as a replacement for PET/ITO. This support was chosen as the electroactive component, FTO, has demonstrated the ability to operate at potentials higher than ITO.¹¹⁴ A potential of 2.0 V was applied to the device. This produced a yellow-to-blue transition of the deposited electrochrome, with areas of the spot retaining its original colour (Figure 37). An increase in potential to 3.0 V led to a more intense blue colour and a darkening of the remaining yellow colour. Further increase of the potential to 4.0 V did not produce a second colour change as was suggested by the spectroelectrochemical study. Prolonged application of this potential produced small bubbles within the electrolyte, causing device failure.

An explanation for the formation of bubbles may be the electrolysis of water present within the electrolyte as electrolysis occurs at lower potentials (+ 1.23 V in an ideal system). Another possible explanation may be reaction of FTO has also been shown to take part in electrolysis potentials below that of the applied potential.¹¹⁴ Oxidation of ethylene glycol has been observed at potentials lower than 4.0 V and thus may be the cause of the production of gas within the device.^{115,116} Further device optimization and fabrication of spray-coated device are currently ongoing.

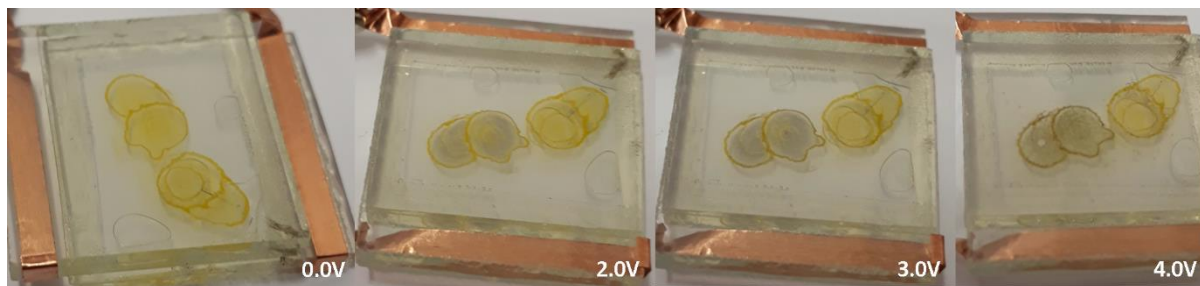


Figure 37: Prototype ECD fabricated using naphthalene target molecule **56**, based on a Glass/FTO substrate.

3. Conclusions/Perspectives

In conclusion, synthesis of two O-doped anthracene-based molecules possessing red/pink colour was achieved. These molecules were found to possess high sensitivity to air and, according to literature, react with singlet oxygen.⁹⁶ Following on from this, an air-stable O-doped naphthalene-based molecule (**56**) was synthesised using a copper mediated intramolecular etherification. The reaction led to the formation of two new highly fluorescent spots on TLC, one which was isolated and confirmed to be the desired dipyrano- product, and one which was reasoned to be the difurano- product. It is believed that the selectivity for only two products from this reaction arises from the rotation of the naphthalene core. This means that ring closure must always occur on only one side of the naphthalene. Investigation of the selectivity of this reaction then took place using **65** as a reference. This showed that the reaction utilising CuO showed no preference to form the desired pyrano moiety over the competing furano moiety. Attempts to synthesise a second naphthalene-based molecule led to the isolation of a difurano- molecule (**78**) in 17 % yield and trace amounts of pyranofurano- molecule (**79**). It was believed that this was due to the lack of an axis for the naphthalene core to rotate around, meaning that the cyclisation could occur on either side.

The spectroelectrochemical analysis of **56** was performed and has demonstrated that the molecule possesses a reversible colour change from yellow to blue at a potential of 0.9 V in solution. A drop-cast prototype ECD using **56** and FTO-glass was constructed utilising an ethylene glycol electrolyte. This gave rise to a device which exhibited the colour change described above at a potential of 2.0 V.

Further work could include the application of **56** to the fabrication of a spray-coated prototype ECD. This spray-coated device will allow properties such as cyclability, colouration efficiency, and switching time of the material to be established.

The synthesis of an electroactive polymer utilising the 1,4-cyclised naphthalene molecule as a chromophore may also be investigated. It is believed that a polymer utilising this molecule will give rise to: a material with lower operating potentials – allowing for the use of PET/ITO flexible substrates without fear of device destruction, a higher absorption coefficient, and higher insolubility in less polar electrolyte systems – allowing for the fabrication of working ECDs which utilise our collaborator's patented electrolyte.

4. Experimental

General Remarks:

Thin layer chromatography (TLC) was performed using pre-coated aluminium sheets using 0.20 mm silica gel 60 with fluorescent indicator F254 manufactured by Merck.

Column chromatography was carried out using silica gel 60 (particle size 40-60 µm) from Applichem or using neutral Al₂O₃ supplied by Carlo Erba Reagents. **Melting Points (mp):** were measured, uncorrected, on a Stuart SMP1 analogue melting point apparatus. **Nuclear Magnetic Resonance (NMR)** spectra were recorded using a Bruker Fourier 300 MHz spectrometer equipped with a dual (13C, 1H) probe or Bruker Fourier 400 MHz equipped with a broadband multinuclear (BBO) probe. ¹H spectra were obtained at 400 MHz or 300MHz and ¹³C at 100 MHz or 75 MHz with complete decoupling for proton. All spectra were obtained at room temperature unless otherwise specified. Chemical shifts were reported in ppm according to the standard of tetramethylsilane (TMS). The splitting of peaks is described as s (singlet), d (doublet), t (triplet), dd (doublet of doublets), and m (multiplet).

Infrared spectra (IR) were recorded using a Shimadzu IR Affinity 1S FTIR spectrometer.

Mass Spectrometry (MS): High resolution ESI mass spectra (HRMS) were performed on a Waters LCT HR TOF mass spectrometer in the positive or negative ion mode all analyses were carried out at Cardiff University. **UV-Vis Absorption spectroscopy:** were measured using Varian CARY 100 Bio UV-Vis spectrophotometer using quartz cell (path length of 1 cm).

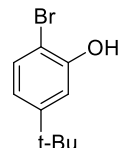
Spectra measured during spectroelectrochemical experiments were measured using a Varian CARY 5000 UV-Vis-NIR spectrometer. **Ultraviolet-Visible emission spectroscopy:** emission spectra were recorded on an Agilent Cary Eclipse fluorescence spectrofluorimeter. Fluorimetric measurements were performed at 25 °C.

Materials and Methods:

Degassing of solutions/solvent mixtures was done by bubbling of nitrogen through the solution with sonication followed by sealing the system under an inert atmosphere. Anhydrous conditions were achieved through heating of round bottom flasks to 100 °C in the oven overnight, and allowing to cool under vacuum, followed by purging with nitrogen. Anhydrous solvents were dried over activated molecular sieves for at least 24 hours prior to use. Low temperatures were achieved using low temperature baths: -84 °C with ethyl acetate/liquid nitrogen, 0 °C with ice/H₂O. Inert atmosphere was maintained using nitrogen-filled balloons equipped with a syringe and needle which was used to pierce the silicon stoppers used to seal the flask's necks. Chemicals were purchased from Sigma Aldrich, TCI,

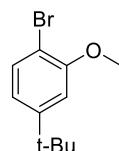
Alfa Aesar, or Flurochem and used as supplied except naphthoquinone which was purified by recrystallization from hexane prior to use.

2-bromo-5-(*tert*-butyl)phenol (38):⁹⁹



Commercially available 3-*tert*-buyl phenol (5.00 g, 33.4 mmol) was weighed into an oven-dried flask. The system was purged with nitrogen and dry DCM (20 ml) was added. After stirring for 0.5 h at r.t., the flask was cooled to 0 °C and a solution of Br₂ (1.7 ml, 33.2 mmol) in DCM (5 ml) was added dropwise. The reaction was quenched with saturated Na₂S₂O₃ solution and the organic layer was then separated from the aqueous layer, washed with water (3 x 50 ml), dried over Na₂SO₄, and concentrated *in vacuo*. The desired product was purified by chromatography column (SiO₂; eluent: Hex to Hex/DCM 8:2). This gave 6.999 g (30.6 mmol, 91%) of the desired product as a colourless oil. ¹H NMR (400 MHz, CDCl₃) δ 7.38 (d, *J* = 8.5 Hz, 1H), 7.09 (d, *J* = 2.2 Hz, 1H), 6.86 (dd, *J* = 8.5, 2.2 Hz, 1H), 5.52 (s, 1H), 1.31 (s, 9H); ¹³C NMR (101 MHz, CDCl₃) δ 153.2, 151.8, 131.4, 119.2, 113.5, 106.9, 34.7, 31.2; MS (EI, m/z) found: 228.01, required 228.02; characterisation in accordance with literature.⁹⁹

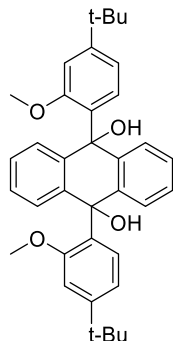
1-bromo-4-(*tert*-butyl)-2-methoxybenzene (39):¹¹⁷



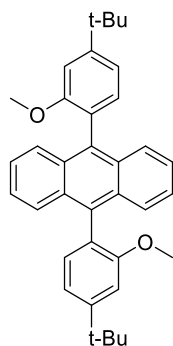
2-bromo-5-(*tert*-butyl)phenol (1.45 g, 6.3 mmol) along with oven-dried K₂CO₃ (2.72 g, 19.7 mmol) were weighed into a round bottom flask. The flask was flushed with nitrogen and dry DMF (8 ml) was added, followed by MeI (1.87 g, 13.2 mmol). The flask was heated to 55 °C for 42 h, after which the reaction was cooled to r.t. and any excess MeI was quenched with 1 M aq. NaOH. The mixture was diluted with water and the crude extracted with EtOAc (3 x 40 ml). After this the organic layers were combined and washed with 1 M NaOH, water, and brine; the product was dried over MgSO₄ and concentrated *in vacuo*. This yielded 1.20 g (4.9 mmol, 78%) of pale-yellow crystalline material which required no further purification. **M.p.:** 38 - 40 °C; ¹H NMR (400 MHz, CDCl₃) δ 7.44 (d, *J* = 8.3 Hz, 1H), 6.93 (d, *J* = 1.8 Hz, 1H), 6.87 (dd, *J* = 8.3, 1.9 Hz, 1H), 3.91 (s, 3H), 1.32 (s, 9H); ¹³C NMR (101 MHz,

CDCl_3) δ 155.5, 152.3, 132.6, 119.1, 109.7, 108.5, 56.1, 34.9, 31.3; **MS** (EI m/z): found 242.03, required 242.03; characterisation in accordance with literature.¹¹⁷

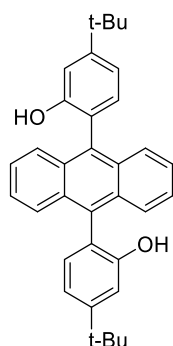
9,10-bis(4-(tert-butyl)-2-methoxyphenyl)-9,10-dihydroanthracene-9,10-diol (40):



39 (1.17g, 4.8 mmol) was weighed into a round bottom flask which was flushed with nitrogen. Dry Et_2O was added to the flask and it was cooled to -84 °C. Once cool $n\text{-BuLi}$ (3.0 ml, 4.8 mmol) was added and the flask was allowed to stir at r.t. for 0.25 h. A suspension of anthraquinone (0.25 g, 1.2 mmol) in Et_2O was added slowly and the reaction was left to stir for 18.5 h. The reaction was quenched with 1 M HCl, diluted with water, and extracted with DCM (3 x 40 ml). The crude was dried over MgSO_4 and concentrated *in vacuo*. The desired product was purified by trituration with hexane and yielded 0.50 g (0.9 mmol, 77 %) as white powder which was an isotropic mixture. **M.p.:** could not be measured as decomposition occurred above 160 °C; **$^1\text{H NMR}$** (400 MHz, CDCl_3) δ 8.22 (d, J = 8.1 Hz, 2H), 7.23 (dd, J = 5.9, 3.4 Hz, 4H), 7.19 (dd, J = 8.2, 1.7 Hz, 2H), 7.16 – 7.10 (m, 4H), 6.75 (d, J = 1.5 Hz, 2H), 3.11 (s, 6H), 2.98 (s, 2H), 1.32 (s, 18H); **$^{13}\text{C NMR}$** (75 MHz, CDCl_3) δ 155.2, 151.9, 139.8, 134.2, 127.4, 127.3, 125.7, 117.8, 111.9, 71.6, 56.4, 34.7, 31.5, 31.4. **HRMS** (ES m/z): calc. for $\text{C}_{36}\text{H}_{40}\text{O}_4^{23}\text{Na}$: 559.2824, found: 559.2830; **IR v** (cm^{-1}): 2960.73, 2902.87, 2866.22, 2357.01, 2341.58, 2330.01, 1610.56, 1573.91, 1558.48, 1539.20, 1506.41, 1456.26, 1446.61, 1409.96, 1286.52, 265.30, 1251.80, 1226.73, 1193.94, 1033.85, 989.48, 923.90, 893.04, 858.32, 821.68, 771.53, 682.80, 655.80, 588.29.

9,10-bis(4-(tert-butyl)-2-methoxyphenyl)anthracene (41):

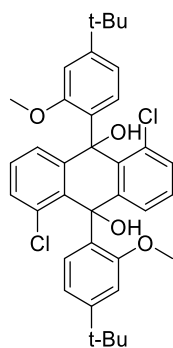
40 (490 mg, 0.919 mmol) was weighed into a round bottom flask, C₄H₈O was added, followed by the addition of a saturated solution of SnCl₂ in concentrated HCl (5 ml). The reaction was stirred at r.t. for 1 h after which it was diluted with water. The white precipitate formed was filtered off and washed with water then 1 M HCl. This gave 420 mg (0.835 mmol, 91 %) of desired product as a white powder without further purification. **M.p.:** >250 °C; **¹H NMR** (400 MHz, CDCl₃) δ 7.66 (m, 4H), 7.32 – 7.24 (m, 6H), 7.18 (m, 4H), 3.65 (s, 6H), 1.49 (s, 18H); **¹³C NMR** (75 MHz, CDCl₃) δ 157.8, 157.8, 152.6, 133.9, 133.7, 132.5, 132.5, 130.4, 130.3, 127.1, 124.8, 124.6, 124.6, 117.7, 108.8, 55.8, 55.8, 35.11, 31.6; **HRMS** (ES m/z): [M + H]⁺ calc. for C₃₆H₃₉O₂: 503.2950, found: 503.2952; **IR v** (cm⁻¹): 2960.73, 2931.80, 2900.94, 2864.29, 2357.01, 1504.48, 1462.04, 1406.11, 1386.82, 284.59, 1265.30, 1228.66, 1033.85, 945.12, 856.39, 815.89, 767.67, 669.30, 655.80.

6,6'-(anthracene-9,10-diyl)bis(3-(tert-butyl)phenol) (35):

To an oven-dried round bottom flask **41** (160 mg, 0.31 mmol) was added. After flushing with argon the flask was cooled to -78 °C and DCM (3.0 ml) added. BBr₃ (1.2 ml, 1.2 mmol) was added slowly and the reaction was allowed to warm to r.t. for 3 h. The reaction was quenched by dropwise addition of water after which the organic components were extracted using DCM (3 x 25 ml). The organic layers were combined and washed with saturated NaHCO₃ solution (10 ml), then dried over MgSO₄ and concentrated *in vacuo*. The desired

product was obtained as 96 mg (0.20 mmol, 65 %) of an off-white powder after purification by trituration with MeOH. **M.p.:** 126 – 128 °C; **¹H NMR** (400 MHz, CDCl₃) δ 7.78 (dd, *J* = 6.8, 3.2 Hz, 4H), 7.43 (dd, *J* = 6.8, 3.2 Hz, 4H), 7.30 – 7.14 (m, 8H) integral inaccurate as solvent peak overlaps, 4.55 (bs, 2H), 1.47 (s, 18H); **¹³C NMR** (75 MHz, CDCl₃) δ 153.7, 153.4, 131.8, 131.8, 130.9, 126.7, 126.2, 121.0, 118.0, 113.0, 34.9, 31.5; **HRMS** (ES m/z): [M + H]⁺ calc. for C₃₂H₃₅O₂: 475.2637, found: 475.2637; **IR v** (cm⁻¹): 3325.28, 2954.95, 2916.37, 2846.93, 2358.94, 2341.58, 1608.63, 1558.48, 1506.41, 1456.26, 1288.45, 1263.37, 1199.72, 1186.22, 1124.50, 1087.85, 1022.27, 952.84, 860.25, 815.89, 767.67, 723.31, 650.01, 607.58, 518.85.

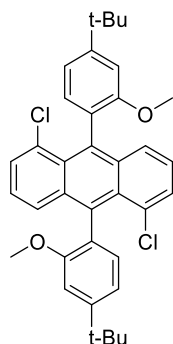
9,10-bis(4-(tert-butyl)-2-methoxyphenyl)-1,5-dichloro-9,10-dihydroanthracene-9,10-diol (46):



39 (700 mg, 2.88 mmol) was weighed into a round bottom flask. The system was then put under a nitrogen atmosphere and dry C₄H₈O was added. The flask was cooled to -78 °C and *n*-BuLi (1.9 ml, 3.04 mmol) was added, after which the reaction was stirred at r.t. for 0.5 h. A suspension of 1,5-dichloroanthraquinone (200 mg, 0.72 mmol) in C₄H₈O was added and the mixture was left to stir at r.t. for 24 h. The reaction was quenched with 1 M HCl and diluted with water. The crude was extracted with DCM (3 x 40 ml), dried over MgSO₄, and concentrated *in vacuo*. Purification by trituration with MeOH gave 300 mg (0.49 mmol, 68 %) of white powder as the desired product. **M.p.:** >250 °C; **¹H NMR** (400 MHz, CDCl₃) δ 8.00 (s, 2H), 7.41 (dd, *J* = 7.2, 2.0 Hz, 2H), 7.15 – 7.01 (m, 6H), 6.70 (s, 2H), 3.24 (s, 6H), 1.28 (s, 18H), OH proton peak not seen; **¹³C NMR** (101 MHz, CDCl₃) δ 154.7, 151.9, 135.4, 133.0, 131.3, 130.0, 128.0, 128.0, 127.6, 117.5, 111.1, 56.1, 34.7, 31.4; **HRMS** (ES m/z): calc. for C₃₆H₃₈O₄²³NaCl₂: 627.2045, found: 627.2046; **IR v** (cm⁻¹): 3589.53, 3560.59, 3076.46, 2960.73, 2902.87, 2864.29, 1608.63, 1573.91, 1566.20, 1496.76, 1456.26, 1433.11, 1406.11, 1361.74, 1340.53, 1286.52, 1265.30, 1226.73, 1188.15, 1143.79,

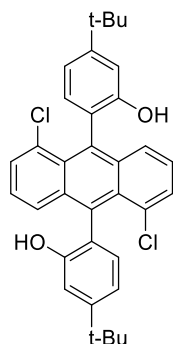
1031.92, 1004.91, 970.19, 923.90, 893.04, 856.39, 817.82, 796.60, 759.95, 736.81, 704.02, 686.66, 653.87.

9,10-bis(4-(tert-butyl)-2-methoxyphenyl)-1,5-dichloroanthracene (45):



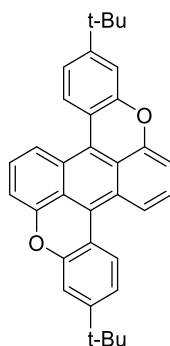
46 (110 mg, 0.18 mmol) was weighed into a round bottom flask, C₄H₈O was then added and the system was stirred until (PRECURSOR NUMBER) had dissolved. A saturated solution of SnCl₂ in concentrated HCl (3.0 ml) was added and the reaction was stirred at r.t for 3 h. The reaction was diluted with water and the precipitate formed was filtered off. The precipitate was washed with water followed by 1 M HCl. This reaction yielded 100 mg (0.17 mmol, 97 %) of the desired product as a yellow powder. NMR showed the product to be a mixture of two atropoisomers. **M.p.:** >250 °C **¹H NMR** (400 MHz, CDCl₃) δ 7.61 (dd, *J* = 8.5, 4.7 Hz, 1H), 7.45 (d, *J* = 7.0 Hz, 1H), 7.16 – 7.03 (m, 4H), 6.97 (d, *J* = 7.9 Hz, 1H), 3.74 (s, 1H), 3.70 (s, 2H), 1.45 (d, *J* = 10.1 Hz, 9H); **¹³C NMR** (101 MHz, CDCl₃) δ 157.9, 153.1, 134.0, 133.8, 132.1, 131.3, 129.2, 127.6, 127.3, 127.1, 124.3, 117.3, 108.1, 77.3, 77.0, 76.7, 55.8, 35.1, 31.7. **HRMS** (ES m/z): [M + H]⁺ calc. for C₃₆H₃₇O₂³⁵Cl₂: 571.2171, found: 571.2167; **IR v** (cm⁻¹): 3014.74, 2970.38, 2858.51, 2360.87, 2341.58, 1737.86, 1683.86, 1608.63, 1558.48, 1506.41, 1456.26, 1436.97, 1406.11, 1286.52, 1228.66, 1217.08, 1126.43, 1097.50, 1035.77, 981.77, 914.26, 854.47, 821.68, 786.96, 731.02, 692.44, 67.37, 526.57.

6,6'-{(1,5-dichloroanthracene-9,10-diyl)bis(3-(tert-butyl)phenol)} (44):

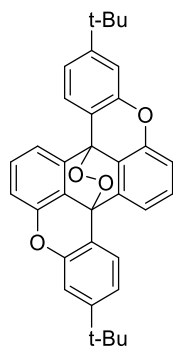


45 (140 mg, 0.24 mmol) was weighed into a two-necked round bottom flask which was put under a nitrogen atmosphere. Dry DCM was added and the flask was cooled to -78 °C, after which BBr₃ (0.73 ml, 0.73 mmol) was added and the reaction was warmed to r.t. overnight. The reaction was quenched with dropwise addition of water and the crude was extracted using DCM (3 x 35 ml). The organic layers were combined, dried over MgSO₄, and concentrated *in vacuo*. Purification by column chromatography (SiO₂; eluent: Hex/DCM 8:2 to DCM) yielded 80 mg (0.14 mmol, 61 %) of bright yellow powder. **M.p.:** >250 °C (decomp.); **¹H NMR** (400 MHz, CDCl₃) δ 7.73 (d, *J* = 8.9 Hz, 2H), 7.57 (d, *J* = 6.8 Hz, 2H), 7.30 – 7.23 (m, 4H) integral inaccurate due to overlapping with solvent peak, 7.15 – 7.04 (m, 6H), 4.46 (s, 2H), 1.44 (s, 18H) **HRMS** (ES m/z): [M + H]⁺ calc. for C₃₄H₃₃Cl₂O₂: 543.1858, found: 543.1861; **IR v** (cm⁻¹): 3535.52, 3495.01, 2960.73, 2899.01, 2866.22, 2360.87, 2341.58, 2331.94, 1614.42, 1570.06, 1558.48, 1541.12, 1516.05, 1506.41, 1489.05, 1471.69, 1456.26, 1436.97, 1411.89, 1392.61, 1373.32, 1361.74, 1336.67, 1290.38, 1236.37, 1188.15, 1147.65, 1118.71, 1080.14, 1024.20, 977.91, 929.69, 894.97, 860.25, 815.89, 786.96, 748.38, 729.09, 690.52, 665.44, 648.08.

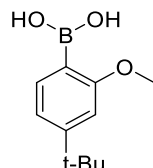
2,10-di-tert-butylbenzo[1,2,3-kl:4,5,6-k'l']dixanthene (43):



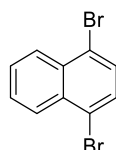
44 (43 mg, 0.08 mmol), K₂CO₃ (43 mg, 0.31 mmol) were weighed into a round bottom flask. The flask was flushed with nitrogen, DMSO added, and the reaction heated to 140 °C for 2 h. The mixture was cooled, diluted with water, extracted with DCM (2 x 50 ml), dried over MgSO₄, and concentrated *in vacuo*. The crude was purified by filtration over alumina (eluent: Hex) and yielded 11 mg (0.02 mmol, 29 %) of red solid. As the product degraded in air quickly only ¹H NMR could be performed; **¹H NMR** (300 MHz, CDCl₃) δ 8.05 (d, *J* = 8.3 Hz, 2H), 7.24 (dd, *J* = 8.6, 7.7 Hz, 2H), 7.14 (d, *J* = 1.9 Hz, 2H), 7.10 (dd, *J* = 8.4, 2.0 Hz, 2H), 6.95 – 6.71 (bs, 1H) integral inaccurate as reaction into endoperoxide occurs during measurement, 1.31 (s, 18H).

2,10-di-tert-butyl-4b,12b-epidioxybenzo[1,2,3-kl:4,5,6-k'l']dixanthene (47):

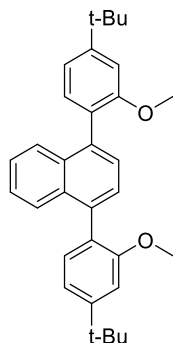
43 is left in CDCl_3 under ambient conditions for 24 h. TLC shows complete conversion to a new product. **M.p.** > 250 °C **$^1\text{H NMR}$** (400 MHz, CDCl_3) δ 7.75 (d, J = 8.7 Hz, 1H), 7.36 (d, J = 6.2 Hz, 2H), 7.30 – 7.23 (m, 3H), 7.09 (d, J = 8.4 Hz, 1H), 6.99 (d, J = 7.3 Hz, 1H); **$^{13}\text{C NMR}$** not performed due to insolubility **MS** (ES m/z): found: 502.23, required: 502.21.

(4-(*tert*-butyl)-2-methoxyphenyl)boronic acid (62):

1-bromo-4-(*tert*-butyl)-2-methoxybenzene (510 mg, 2.1 mmol) was weighed into an oven-dried round bottom flask which was put under a nitrogen atmosphere. Dry $\text{C}_4\text{H}_8\text{O}$ (5 ml) was added and the system was cooled to -78 °C, after which *n*-BuLi (1.4 ml, 2.2 mmol) was added. $\text{B}(\text{OMe})_3$ (370 mg, 3.6 mmol) was added and the reaction mixture was warmed to r.t. for 23 h. The reaction was quenched with 1 M HCl then diluted with water and the organic components extracted using EtOAc (3 x 30 ml). The organic layers were combined, dried over MgSO_4 , and concentrated *in vacuo*. Purification by column chromatography (SiO_2 ; eluent: Hex/Et₂O 8:2) yielded 360 mg (1.75 mmol, 84%) of the desired product as a white solid. **M.p.:** 105 – 108 °C; **$^1\text{H NMR}$** (400 MHz, CDCl_3) δ 7.78 (d, J = 7.7 Hz, 1H), 7.09 (dd, J = 7.7, 1.4 Hz, 1H), 6.95 (d, 1H), 5.68 (s, 2H), 3.96 (s, 3H), 1.36 (s, 9H); **$^{13}\text{C NMR}$** (101 MHz, CDCl_3) δ 164.6, 156.8, 136.5, 118.4, 107.2, 55.4, 35.2, 31.2; **MS** (EI, m/z) found: **IR** ν (cm⁻¹): 3535.52, 3419.79, 3213.41, 3010.88, 2953.02, 866.22, 2841.15, 1610.56, 1558.48, 1506.41, 1471.69, 1450.47, 1408.04, 1363.67, 1325.10, 1280.73, 1263.37, 1217.08, 1199.72, 1178.51, 1159.22, 1120.64, 1049.28, 997.20, 904.61, 850.61, 821.68, 750.31, 717.52, 667.37, 653.87, 634.58, 615.29, 567.07, 538.14.

1,4-dibromonaphthalene (61):¹⁰⁶

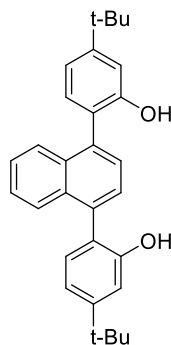
Naphthalene (210 mg, 1.6 mmol) was weighed into a round bottom flask, dry DCM was added and the flask was cooled to -35 °C in the dark. Br₂ (740 mg, 4.7 mmol) was added slowly and the reaction was left in the cooling bath overnight. The temperature had risen to 10 °C overnight so the reaction was quenched by addition of sat. aq. Na₂S₂O₃. It was diluted with water and the crude extracted with DCM (3 x 30 ml). The organic layers were combined and washed with water, sat. aq. Na₂S₂O₃, and 0.1 M aq. NaOH. The crude was dried over MgSO₄, concentrated *in vacuo*, and purified by column chromatography (SiO₂; eluent: Hexane). This yielded 280 mg (0.98 mmol, 61 %) of the desired product as white crystals. **M.p.:** 77 – 79 °C; **¹H NMR** (400 MHz, CDCl₃) δ 8.29 (dd, *J* = 6.4, 3.3 Hz, 2H), 7.74 – 7.63 (m, 2H), 7.28 (s, 2H); **¹³C NMR** (101 MHz, CDCl₃) δ 133.0, 130.1, 128.2, 127.8, 122.6; **MS** (EI, m/z) found: 285.88, required: 285.88; characterisation in accordance with literature.¹⁰⁶

1,4-bis(4-(tert-butyl)-2-methoxyphenyl)naphthalene (58):

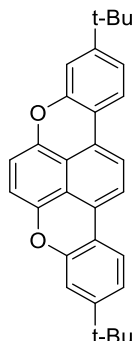
1,4-dibromonaphthalene (63 mg, 0.2 mmol), **62** (136 mg, 0.7 mmol), and K₂CO₃ (122 mg, 0.9 mmol) were weighed into a round bottom flask which was flushed with nitrogen. A degassed mixture of dioxane and water (4:1) was added followed by [Pd(PPh₃)₄] (13 mg, 0.01 mmol) under a flow of nitrogen. The reaction mixture was heated to 85 °C for 6.5 h. The reaction mixture was cooled to r.t. then diluted with water and the crude was extracted with DCM (3 x 25 ml). The crude was dried over MgSO₄, concentrated *in vacuo*, and purified by column chromatography (SiO₂; eluent: Hex/DCM 9:1 to Hex/DCM 8:2). This yielded 93 mg (0.2 mmol, 93 %) of the desired product as a white crystalline material. **M.p.:** 201-204 °C; **¹H NMR** (400 MHz, CDCl₃) δ 7.70 – 7.60 (m, 2H), 7.44 (d, *J* = 1.9 Hz, 2H), 7.38 – 7.31

(m, 2H), 7.29 (d, $J = 7.8$ Hz, 2H), 7.25 (d, $J = 9.0$ Hz, 2H), 7.15 – 7.05 (m, 4H), 3.74 (d, $J = 1.9$ Hz, 6H), 1.43 (s, 18H); **^{13}C NMR** (101 MHz, CDCl_3) δ 157.0, 157.0, 152.3, 136.4, 136.3, 132.3, 131.7, 127.0, 127.0, 126.9, 126.8, 125.1, 117.6, 117.5, 108.6, 108.5, 55.7, 55.6, 35.0, 31.5; **HRMS** (ES m/z): [M + H]⁺ calc. for $\text{C}_{32}\text{H}_{37}\text{O}_2$: 453.2794, found: 453.2797 **IR v** (cm^{-1}): 2951.09, 2927.94, 2899.01, 2862.36, 2831.50, 2362.80, 1608.63, 1558.48, 1498.69, 1456.26, 1402.25, 1381.03, 1361.74, 1280.73, 1261.45, 1228.66, 1145.72, 1116.78, 1091.71, 1035.77, 974.05, 904.61, 852.54, 842.89, 817.82, 767.67, 655.80.

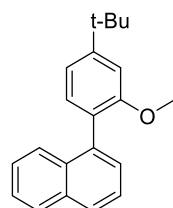
6,6'-(naphthalene-1,4-diyl)bis(3-(tert-butyl)phenol) (57):



58 (119 mg, 0.2 mmol) was weighed into a flask then put under a nitrogen atmosphere. Dry DCM was added and the system was stirred until all solids had dissolved. The flask was covered with aluminium foil and cooled to -78 °C. BBr_3 (1.3 ml, 1.3 mmol) was added carefully and the reaction was then allowed to stir at r.t. overnight. The reaction was quenched with careful addition of sat. aq. NaHCO_3 solution and diluted further with water. The crude was extracted using DCM (3 x 20 ml), dried over MgSO_4 , and concentration *in vacuo*. Purification by column chromatography (SiO_2 ; eluent: DCM) yielded 87 mg (0.2 mmol, 78 %) of an isomeric mixture of the desired product as a white solid. **M.p.:** 124–126 °C; **^1H NMR** (400 MHz, CDCl_3) δ 7.87 – 7.78 (m, 2H), 7.60 (d, $J = 1.5$ Hz, 2H), 7.55 – 7.49 (m, 2H), 7.30 – 7.23 (m, 2H), 7.18 – 7.10 (m, 2H), 4.89 (s, 1H), 4.84 (s, 1H), 1.44 (s, 18H); **^{13}C NMR** (101 MHz, CDCl_3) δ 153.4, 152.8, 152.7, 135.0, 134.9, 132.5, 132.5, 130.9, 130.7, 128.2, 127.0, 127.0, 126.5, 126.4, 123.1, 117.9, 117.8, 112.9, 112.9, 34.8, 31.4; **HRMS** (ES m/z): [M + H]⁺ calc. for $\text{C}_{30}\text{H}_{33}\text{O}_2$: 424.2481, found: 424.2477; **IR v** (cm^{-1}): 3566.38, 3425.58, 3215.34, 2954.95, 2902.87, 2866.22, 614.42, 1558.48, 508.33, 1500.62, 481.33, 1456.26, 1404.18, 1386.82, 1361.74, 1311.59, 294.24, 1263.37, 1211.30, 1141.86, 1130.29, 1114.86, 1080.14, 1026.13, 977.91, 939.33, 923.90, 71.82, 48.68, 12.03, 794.67, 765.74, 744.52, 702.09, 648.08.

3,10-di-tert-butylbenzo[3,4]isochromeno[7,8,1-mna]xanthene (56):

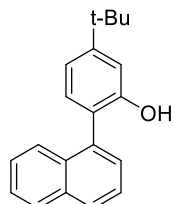
57 (76 mg, 0.18 mmol) was weighed into a round bottom flask, along with CuO (140 mg, 1.76 mmol). Nitrobenzene was added, and the reaction mixture was heated to 220 °C overnight. The nitrobenzene was distilled off, the crude dissolved in DCM and filtered over celite, and product purified by precipitation from DCM/EtOH to give 28 mg (0.07 mmol, 37 %) of orange solid. Orange crystals were obtained by recrystallization from DCM. **M.p.:** >250 °C; **¹H NMR** (300 MHz, C₆D₆) δ 7.39 (d, *J* = 8.3 Hz, 2H), 7.10 (s, 2H), 7.02 (d, *J* = 1.9 Hz, 2H), 6.92 (dd, *J* = 8.3, 1.9 Hz, 2H), 6.66 (s, 2H), 1.18 (s, 18H); **¹³C NMR** could not be measured due to insolubility; **HRMS** (ES, m/z): [M]⁺ calc. for C₃₀H₂₈O₂ 420.2089, found: 420.2086; **IR** ν (cm⁻¹): 2953.02, 2922.16, 2852.72, 2360.87, 2331.94, 1843.95, 1734.01, 1716.65, 1683.86, 1668.43, 1653.00, 1635.64, 1591.27, 570.06, 1506.41, 1463.97, 1423.47, 1369.46, 1303.88, 1274.95, 1255.66, 1234.44, 1201.65, 1159.22, 1138.00, 1093.64, 1041.56, 1020.34, 948.98, 921.97, 875.68, 864.11, 821.68, 806.25, 783.10, 702.09, 671.23, 632.65, 584.43, 555.50, 536.21; **UV**: $\lambda_{\text{max}}(\text{Hex})/\text{nm}$: 478 ($\epsilon/\text{dm}^3\text{mol}^{-1}\text{cm}^{-1}$: 34 700), 446 (39 100), 421 (28 300), 397 (20 500), 377 (11 000), 283 (46 100), 261 (36 400).

1-(4-(tert-butyl)-2-methoxyphenyl)naphthalene (67):

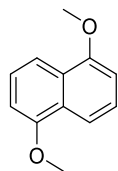
1-bromonaphthalene (74 mg, 0.36 mmol), **62** (109 mg, 0.52 mmol), and K₂CO₃ (104 mg, 0.75 mmol) were weighed into a two-necked round bottom flask which was put under a nitrogen atmosphere. A degassed mixture of dioxane/water (3.6:1) was added followed by [Pd(PPh₃)₄] under a flow of nitrogen. The flask was heated to 85 °C overnight, reaction was cooled to r.t. and diluted with water. The crude was extracted using DCM (3 x 30 ml), dried

over MgSO₄, and concentrated *in vacuo*. Purification by column chromatography (SiO₂; eluent: Hex to Hex/DCM 9:1), followed by trituration with MeOH yielded 73 mg (0.25 mmol, 70 %) of the desired product as white crystals. **M.p.**: decomposition above 169 °C; **¹H NMR** (400 MHz, CDCl₃) δ 7.88 (dd, *J* = 12.9, 8.1 Hz, 2H), 7.65 (d, *J* = 8.4 Hz, 1H), 7.54 (t, *J* = 7.6 Hz, 1H), 7.51 – 7.36 (m, 4H), 7.24 (d, *J* = 7.9 Hz, 1H), 7.16 – 7.06 (m, 2H), 3.72 (s, 1H), 1.45 (s, 9H); **¹³C NMR** (75 MHz, CDCl₃) δ 156.9, 152.4, 137.1, 133.5, 132.3, 131.4, 128.1, 127.5, 127.4, 126.7, 125.5, 125.4, 125.3, 117.6, 108.6, 55.6, 35.0, 31.5; **HRMS** (EI m/z): [M]⁺ calc. for C₂₁H₂₂O, 290.1671 found: 290.1664; **IR v** (cm⁻¹): 2956.87, 2924.09, 2854.65, 2358.94, 2330.01, 1608.63, 1562.34, 1498.69, 1456.26, 1406.11, 1392.61, 1361.74, 1280.73, 1232.51, 1178.51, 1141.86, 1097.50, 1035.77, 962.48, 904.61, 862.18, 821.68, 800.46, 775.38, 661.58, 572.86.

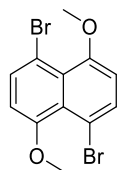
5-(tert-butyl)-2-(naphthalen-1-yl)phenol (66):



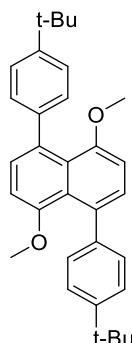
67 (62 mg, 0.21 mmol) was added to a round bottom flask which was put under a nitrogen atmosphere, and dry DCM was added. The flask was cooled to -78 °C 1 M BBr₃ (1.8 ml, 1.80 mmol) was added. The reaction was warmed to r.t. for 3 h, then quenched by the dropwise addition of water. The crude was extracted with DCM (3 x 15 ml), the organic layers combined, dried over MgSO₄, and concentrated *in vacuo*. This reaction yielded 52 mg (0.19 mmol, 88 %) of the desired product as white crystals without further purification. **¹H NMR** (300 MHz, CDCl₃) δ 7.97 – 7.89 (m, 2H), 7.72 (m, 1H), 7.61 – 7.43 (m, 4H), 7.24 – 7.19 (dd, *J* = 7.9, 0.4 Hz, 1H), 7.12 (dd, *J* = 1.5, 0.4 Hz, 1H), 7.09 (dd, *J* = 7.8, 1.9 Hz, 1H), 4.79 (s, 2H), 1.41 (s, 9H); **¹³C NMR** (75 MHz, CDCl₃) δ 153.2, 152.7, 134.2, 134.0, 132.0, 130.8, 128.7, 128.5, 128.3, 126.7, 126.4, 125.9, 125.8, 123.2, 117.7, 112.7, 34.8, 31.4; **HRMS** (EI m/z): [M]⁺ calc. for C₂₀H₂₀O, 276.1514 found: 276.1513; **IR v** (cm⁻¹): 3431.36, 2964.59, 2864.29, 1618.28, 1573.91, 1506.41, 1460.11, 1409.96, 1392.61, 1359.82, 1338.60, 1294.24, 1246.02, 1207.44, 1182.36, 1134.14, 1089.78, 1018.41, 966.34, 923.90, 862.18, 831.32, 821.68, 800.46, 779.24, 740.67, 707.88, 651.94, 567.07, 520.78, 511.14, 480.28, 420.48.

1,5-dimethoxynaphthalene (73):¹¹⁸

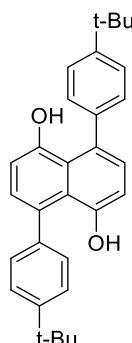
1,5-dihydroxynaphthalene (100 mg, 0.62 mmol) and K_2CO_3 (517 mg, 3.74 mmol) were weighed into an oven-dried round bottom flask which was put under a nitrogen atmosphere. Dry DMF (20 ml) was added followed by MeI (0.16 ml, 2.57 mmol) in dry DMF (5.0 ml) and the flask was heated to 55 °C for 20 h. The reaction mixture was cooled to r.t. and excess MeI quenched using 0.5 M NaOH then diluted further using water. Extraction of the organic components was performed using DCM (3 x 20 ml). The organic layers were combined, washed with water (2 x 30 ml), 0.5 M NaOH (1 x 30 ml), and brine (1 x 30 ml) then dried over MgSO_4 and concentrated *in vacuo*. Purification by hot filtration using hexane as the solvent yielded 92 mg (0.49 mmol, 78 %) of the desired product as yellow crystals. **M.p.:** 181 - 183 °C; **¹H NMR** (400 MHz, CDCl_3) δ 7.86 (d, J = 8.4 Hz, 2H), 7.40 (t, J = 8.1 Hz, 2H), 6.88 (d, J = 7.6 Hz, 2H), 4.02 (s, 6H); **¹³C NMR** (100 MHz, CDCl_3) δ 155.2, 126.6, 125.2, 114.2, 104.5, 55.5; **MS** (EI, m/z) found: 188.08, required 188.08; characterisation in accordance with literature.¹¹⁸

1,5-dibromo-4,8-dimethoxynaphthalene (72):¹⁰⁹

1,5-dimethoxynaphthalene (217 mg, 1.16 mmol) was weighed into a round bottom flask along with N-bromosuccinimide (454 mg, 2.55 mmol) and placed under a nitrogen atmosphere. MeCN (5 ml) was added and the suspension formed was stirred at r.t. for 24 h. The precipitate was filtered off and washed with MeCN. This yielded 211 mg (0.61 mmol, 53 %) of the desired product as a green solid. **M.p.:** decomposition above 166 °C; **¹H NMR** (400 MHz, CDCl_3) δ 7.73 (d, J = 8.4 Hz, 2H), 6.76 (d, J = 8.4 Hz, 2H), 3.95 (s, 6H); **¹³C NMR** (75 MHz, CDCl_3) δ 155.2, 133.7, 126.2, 108.4, 107.1, 55.7; **MS** (EI m/z) found: 345.92, requires 345.90; NMR spectra are in accordance with literature.¹⁰⁹

1,5-bis(4-(tert-butyl)phenyl)-4,8-dimethoxynaphthalene (71):

66 (179 mg, 0.52 mmol) was weighed into a round bottom flask, along with 4-(*tert*-butyl)phenylboronic acid (255 mg, 1.43 mmol), and K_2CO_3 (287 mg, 2.08 mmol). The flask was put under a nitrogen atmosphere, then a degassed mixture of 3:1 $\text{C}_4\text{H}_8\text{O}/\text{H}_2\text{O}$ was added, followed by $[\text{Pd}(\text{PPh}_3)_4]$ (21 mg, 0.02 mmol) under a flow of nitrogen. The reaction was heated to 70 °C for 16 h before being cooled to r.t. and diluted with water. The crude was extracted using DCM (3 x 40 ml), dried over Na_2SO_4 , and concentrated *in vacuo*. Purification by precipitation from DCM/MeOH gave 114 mg (0.25 mmol, 49 %) of the desired product as silver crystals. **M.p.:** > 250 °C; **$^1\text{H NMR}$** (300 MHz, CDCl_3) δ 7.39 – 7.36 (m, 4H), 7.27 – 7.24 (m, 6H), 6.82 (d, J = 8.0 Hz, 2H), 3.45 (s, 6H), 1.40 (s, 18H); **$^{13}\text{C NMR}$** (75 MHz, CDCl_3) δ 156.0, 148.0, 143.1, 131.7, 129.1, 128.3, 125.5, 123.5, 106.4, 55.5, 34.5, 31.6; **HRMS** (EC m/z): $[\text{M} + \text{H}]^+$ calc. for $\text{C}_{32}\text{H}_{37}\text{O}_2$, 453.2794, found: 453.2791; **IR v** (cm^{-1}): 2995.45, 2954.95, 2899.01, 2866.22, 2837.29, 2360.87, 2331.94, 1587.42, 1521.84, 1458.18, 1361.74, 1311.59, 1234.44, 1112.93, 1082.07, 1055.06, 1014.56, 835.18, 812.03, 748.38, 659.66, 646.15, 563.21, 532.35.

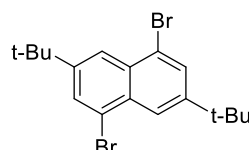
4,8-bis(4-(tert-butyl)phenyl)naphthalene-1,5-diol (70):

65 (120 mg, 0.27 mmol) was weighed into an oven-dried round bottom flask which was put under a nitrogen atmosphere and dry DCM (6.0 ml) was added. The flask was covered using aluminium foil and the solution cooled to -78 °C. 1.5 ml of 1M BBr_3 (1.5 mmol) was added

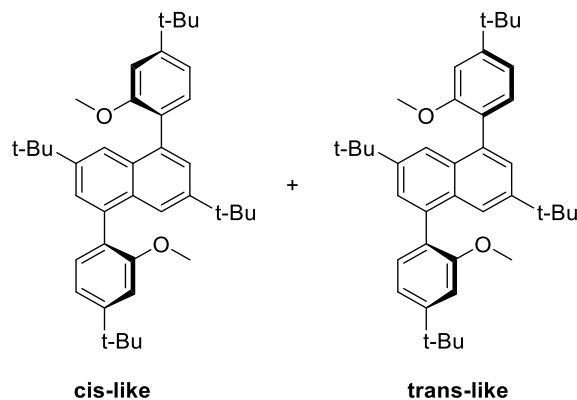
and the reaction was warmed to r.t. for 4 hours before being quenched by the careful addition of water. The crude was extracted using DCM (3 x 20 ml), washed with sat. aq. Na₂S₂O₃ (1 x 25 ml), dried over Na₂SO₄ and concentrated *in vacuo*. Purification by trituration in petroleum ether yielded 50 mg (0.12 mmol, 45 %) of the desired product as white crystals.

M.p.: **¹H NMR** (300 MHz, CDCl₃) δ 7.56 – 7.51 (m, 4H), 7.46 (m, 4H), 7.15 (d, *J* = 7.9 Hz, 2H), 6.90 (d, *J* = 7.9 Hz, 2H), 5.78 (s, 2H), 1.40 (s, 18H); **¹³C NMR** (75 MHz, CDCl₃) δ 153.4, 151.6, 138.0, 129.8, 129.6, 128.5, 126.0, 123.1, 111.0, 76.6, 34.8, 31.4; **HRMS** (EC m/z): [M + H]⁺ calc. for C₃₀H₃₃O₂, 425.2477, found: 425.2481; **IR v** (cm⁻¹): 3466.08, 3030.17, 2970.38, 2868.15, 2358.94, 2341.58, 1739.79, 1716.65, 1683.86, 1598.99, 1558.48, 1541.12, 1521.84, 1506.41, 1471.69, 1456.26, 1417.68, 1398.39, 1363.67, 1228.66, 1217.08, 1111.00, 1064.71, 1014.56, 27.76, 844.82, 33.25, 758.02, 732.95, 669.30, 624.9.

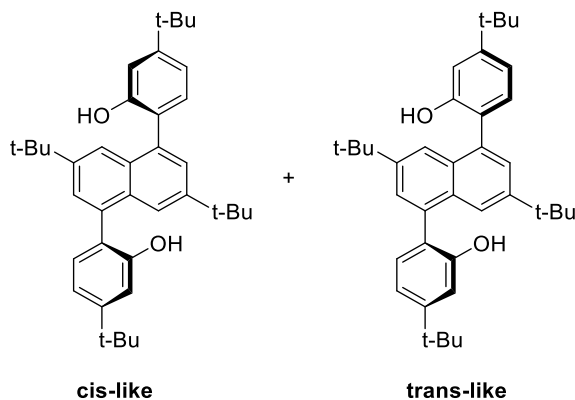
1,5-dibromo-3,7-di-*tert*-butylnaphthalene (77):¹¹⁰



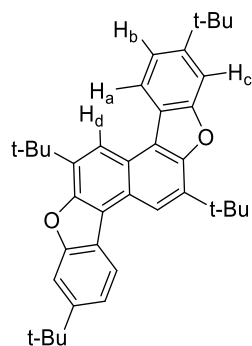
2,6-di-*tert*-butylnaphthalene (1.00 g, 4.16 mmol) and AlCl₃ (3 mg, 0.02 mmol) were dissolved in DCM (6 ml) under an inert atmosphere. To this, a solution of Br₂ (0.45 ml, 8.79 mmol) in DCM (6 ml) was added and the reaction was left to stir at room temperature for 24 h. After quenching with sat. aq. Na₂S₂O₃ solution the organic layer was diluted with DCM (75 ml), washed with sat. aq. Na₂S₂O₃ (2 x 100 ml), water (2 x 100 ml), and brine (1 x 100 ml). The product was then dried over Na₂SO₄ and concentrated *in vacuo*. This yielded 1.463 g (3.67 mmol, 88 %) of the desired product as a white solid. **M.p.** 202-204 °C; **¹H NMR** (300 MHz, CDCl₃) δ 8.12 (m, 2H), 7.89 (m, 2H), 1.42 (s, 18H); **¹³C NMR** (75 MHz, CDCl₃) δ 150.1, 131.0, 129.9, 123.1, 122.3, 35.2, 31.2; **MS** (EI m/z): found: 298.00, required: 298.01.

3,7-di-tert-butyl-1,5-bis(4-(tert-butyl)-2-methoxyphenyl)naphthalene (76):

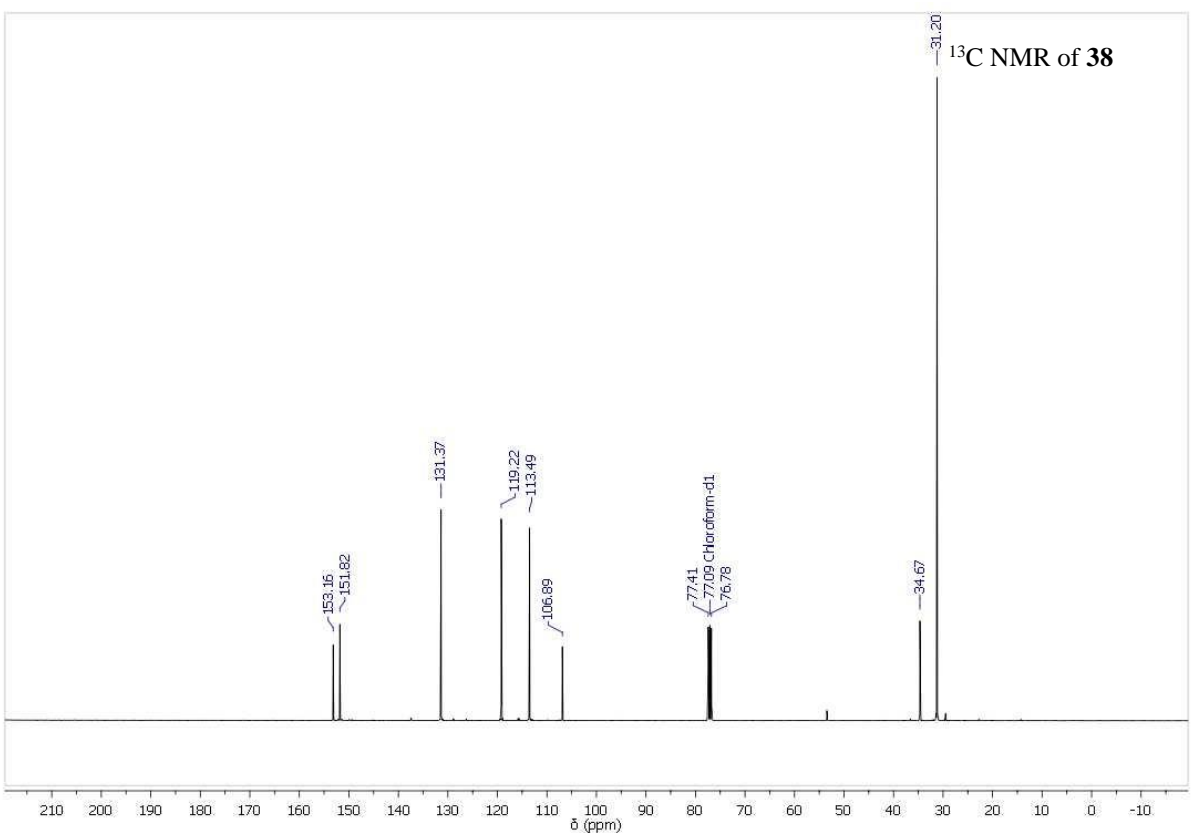
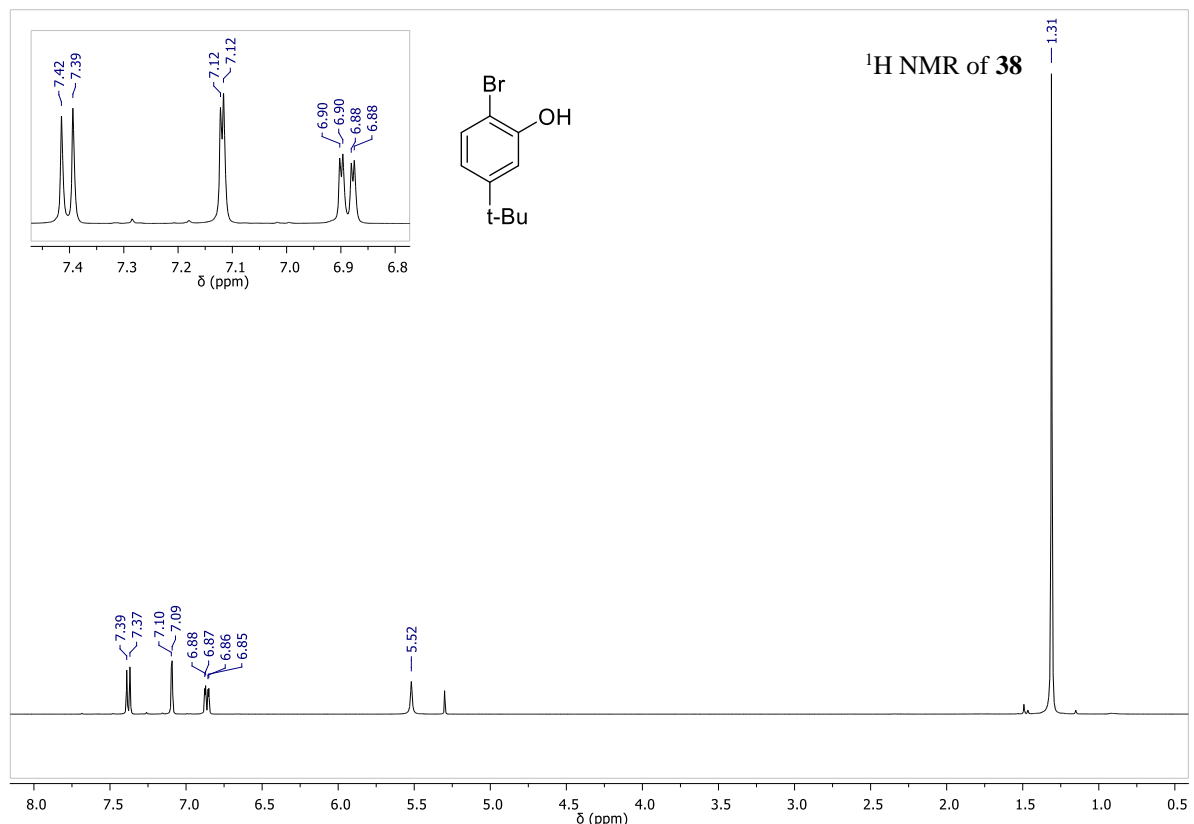
71 (273 mg, 0.69 mmol), **62** (485 mg, 2.32 mmol), and K₂CO₃ (438 mg, 3.17 mmol) were dissolved in a degassed mixture of dioxane and H₂O (15 ml:3 ml). [Pd(PPh₃)₄] (31 mg, 0.03 mmol) was added and the reaction heated to 85 °C for 20 h before being cooled and diluted with water. The crude product was extracted with DCM (3 x 50 ml), dried over Na₂SO₄, concentrated *in vacuo*, and purified by column chromatography (SiO₂; eluent: Pet Et to Pet Et/DCM 8:2). This yielded 281 mg (0.39 mmol, 56 %) of the desired product as a white solid. Characterisation Pending. **M.p.** 227-228 °C; **¹H NMR** (300 MHz, CDCl₃) δ 7.63 – 7.57 (m, 2H), 7.51 (dd, J = 3.2, 2.3 Hz, 2H), 7.36 (d, J = 7.8 Hz, 1H), 7.32 (d, J = 7.7 Hz, 1H), 7.20 – 7.10 (m, 4H), 3.81 (d, J = 3.6 Hz, 6H), 1.49 (s, 18H), 1.35 (s, 18H); **¹³C NMR** (75 MHz, CDCl₃) δ 156.9, 156.9, 152.0, 146.4, 146.4, 136.4, 131.9, 130.1, 129.9, 127.8, 126.4, 121.2, 121.0, 117.5, 117.4, 108.4, 108.2, 55.5, 35.0, 34.8, 31.6, 31.3; **HRMS** (ES m/z) [M + H]⁺ calc. for C₄₀H₅₃O₂, 565.4046 found: 565.4036; **IR v** (cm⁻¹): 2953.02, 2900.94, 2864.29, 1606.70, 1560.41, 1521.84, 1506.41, 1489.05, 1473.62, 1458.18, 1396.46, 1361.74, 1284.59, 1267.23, 1228.66, 1201.65, 1180.44, 1155.36, 1134.14, 1124.50, 1085.92, 1037.70, 1004.91, 950.91, 912.33, 885.33, 848.68, 823.60, 812.03, 783.10, 731.02, 704.02, 684.73, 659.66, 576.72, 549.71, 503.42, 470.63, 462.92.

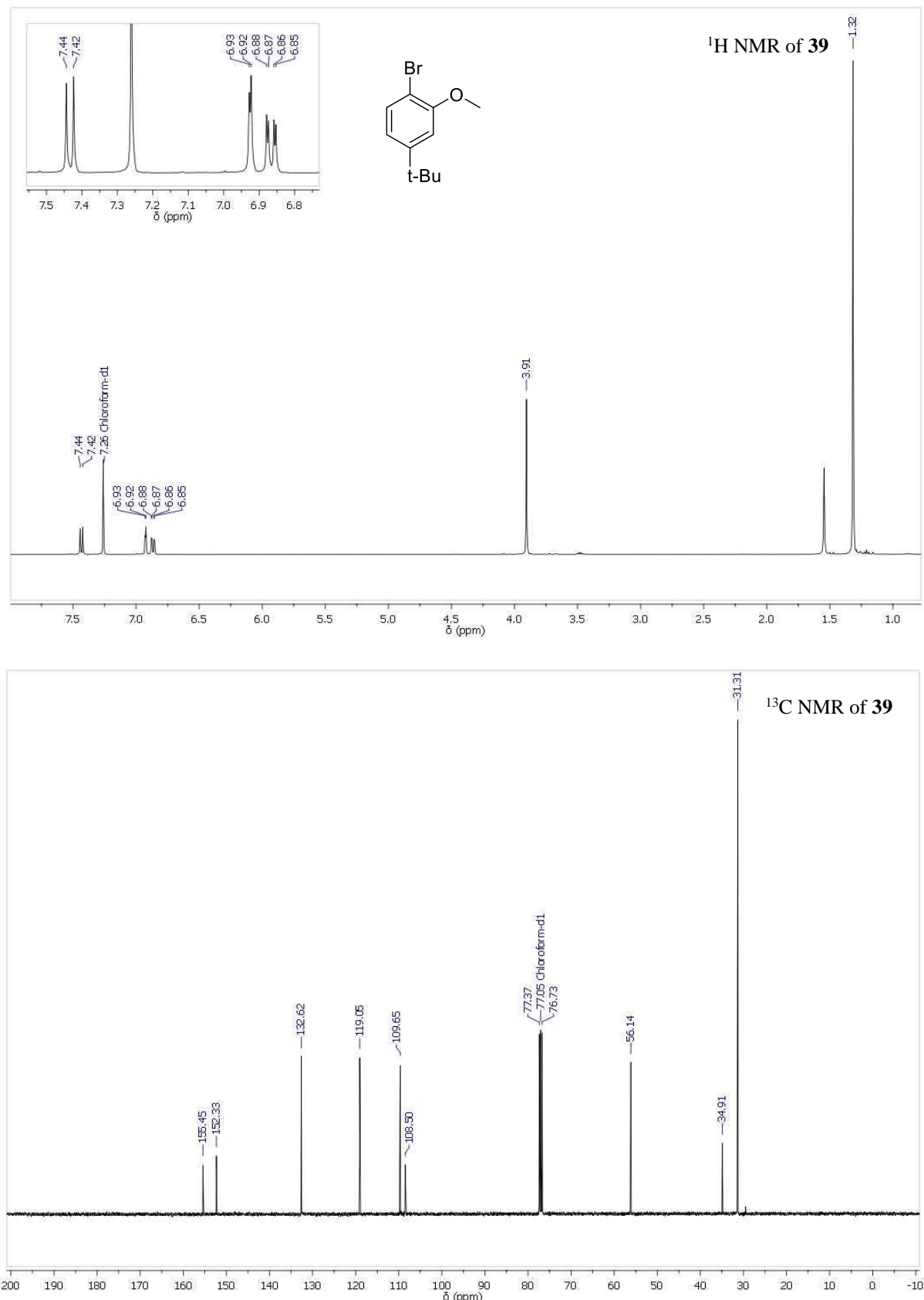
6,6'-(3,7-di-tert-butylnaphthalene-1,5-diyl)bis(3-(tert-butyl)phenol) (75):

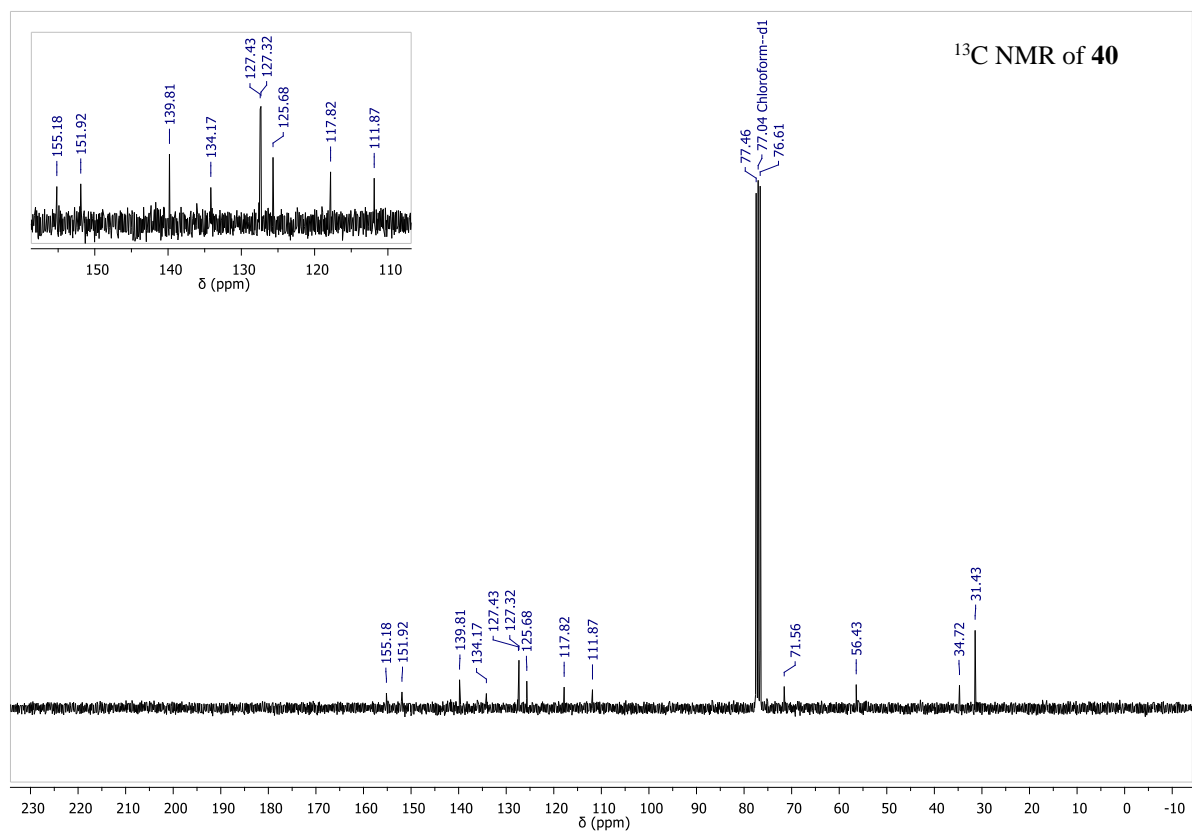
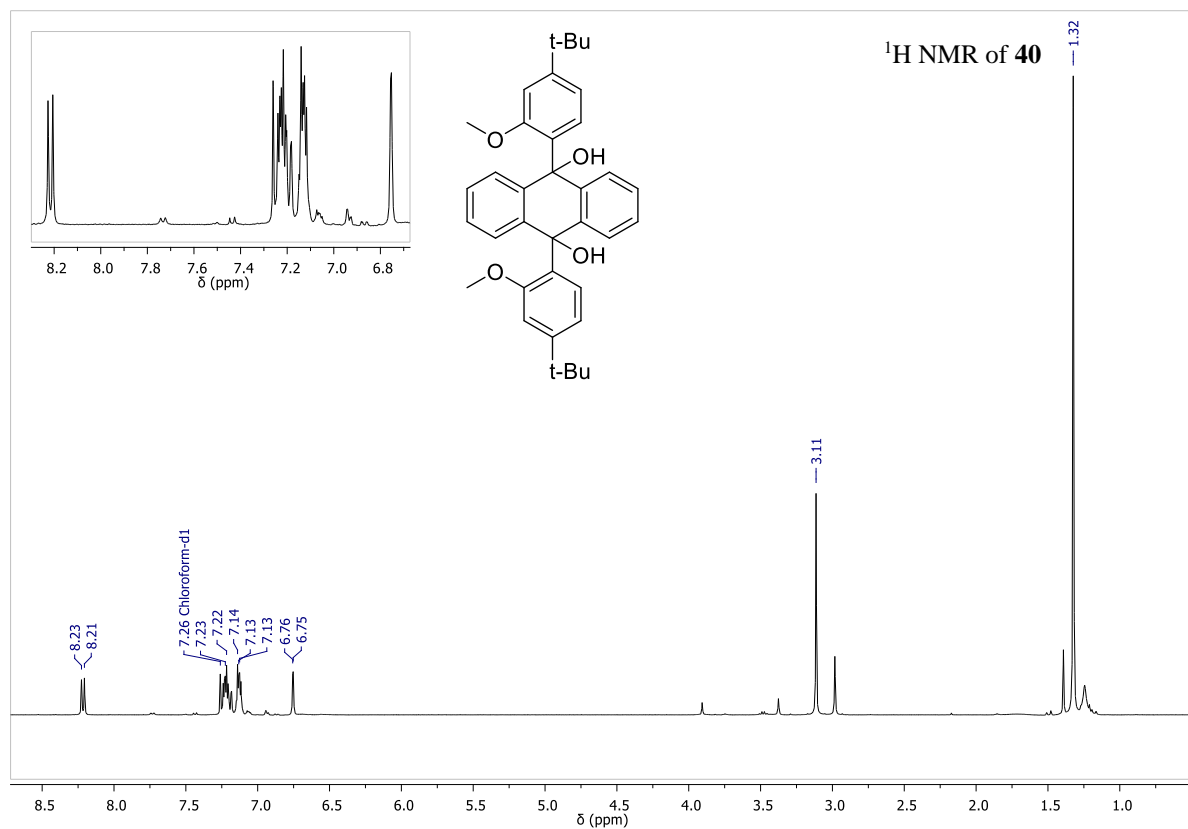
70 (260 mg, 0.46 mmol) was weighed into an oven-dried round bottom flask and put under a nitrogen atmosphere. The flask was covered to minimise the exposure to light and the system cooled to -78 °C. BBr₃ (1.8 ml, 1.80 mmol) was added and the reaction warmed to room temperature for 4 h before being quenched by the dropwise addition of water. The crude was extracted with DCM (3 x 30 ml), dried over Na₂SO₄, concentrated *in vacuo*, and purified by column chromatography (SiO₂; eluent: Pet Et/DCM 7:3 to Pet Et/DCM 3:7). This yielded 118 mg (0.22 mmol, 48 %) of the desired product as a white solid. Characterisation pending. **M.p.** >250 °C; **¹H NMR** (300 MHz, CDCl₃) δ 7.68 (dd, J = 2.1, 1.6 Hz, 2H), 7.59 (d, J = 1.8 Hz, 2H), 7.27 (m, 3H due to solvent peak overlap), 7.17 – 7.09 (m, 4H), 4.92 (s, 1H), 4.87 (s, 1H), 1.42 (s, 18H), 1.31 (s, 18H) NMR suggests a mixture of isomers present; **¹³C NMR** (75 MHz, CDCl₃) δ 153.2, 152.8, 148.8, 134.3, 134.3, 130.8, 130.8, 130.5, 127.8, 123.8, 121.1, 117.7, 112.7, 35.0, 34.8, 31.4, 31.2; **HRMS** (ES m/z) [M]⁺ calc. for C₃₈H₄₈O₂, 536.3654 found: 536.3658; **IR v** (cm⁻¹): 3547.09, 3523.95, 3439.08, 2960.73, 1772.58, 1624.06, 1598.99, 1560.41, 1508.33, 1473.62, 1458.18, 400.32, 1361.74, 1305.81, 1267.23, 1249.87, 1188.15, 1153.43, 1130.29, 1116.78, 097.50, 1076.28, 1022.27, 937.40, 920.05, 891.11, 875.68, 783.10, 705.95, 688.59, 661.58, 599.86, 549.71, 518.85, 472.56, 418.55.

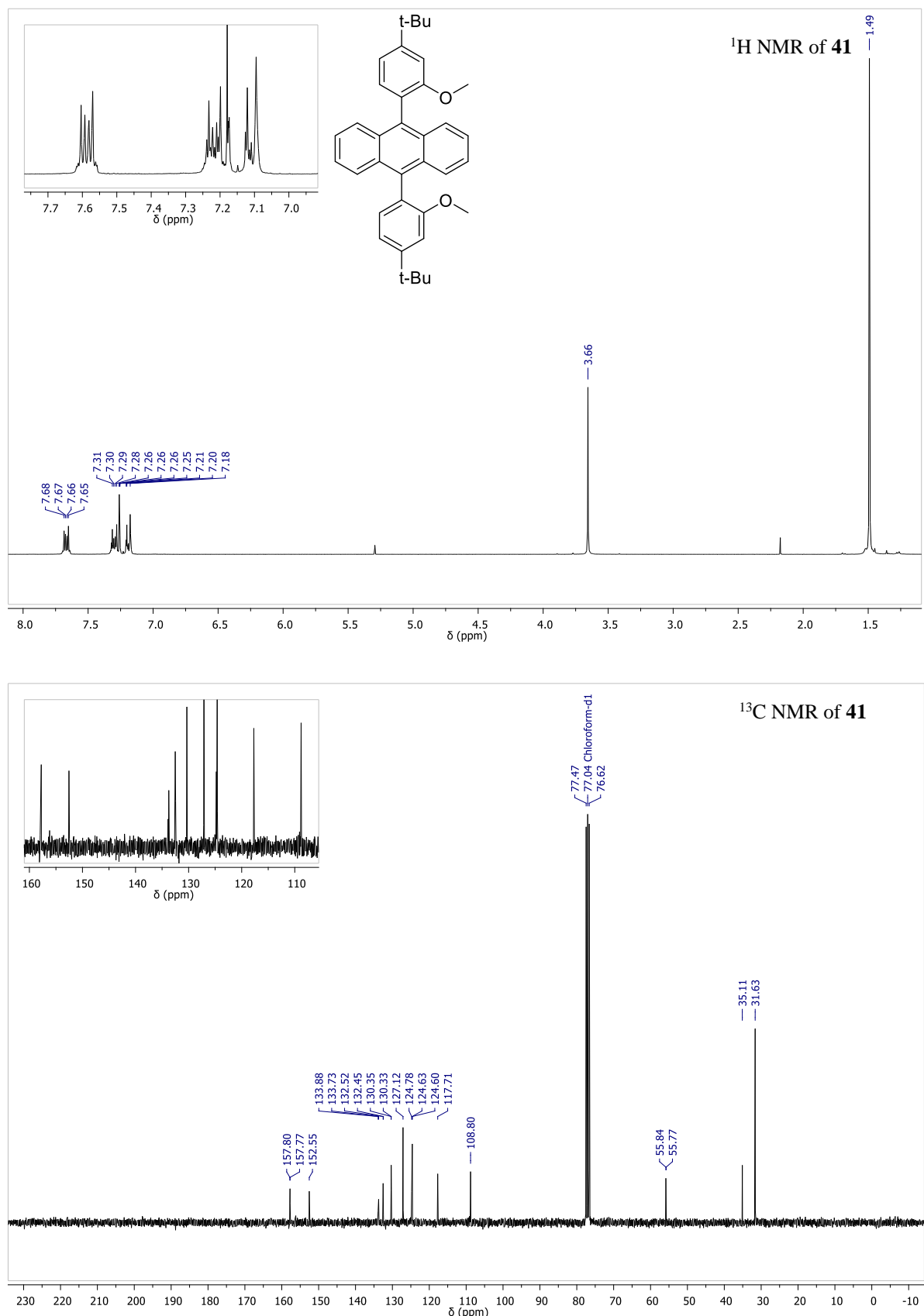
2,6,9,13-tetra-*tert*-butylnaphtho[2,1-b:6,5-b']bisbenzofuran (78):

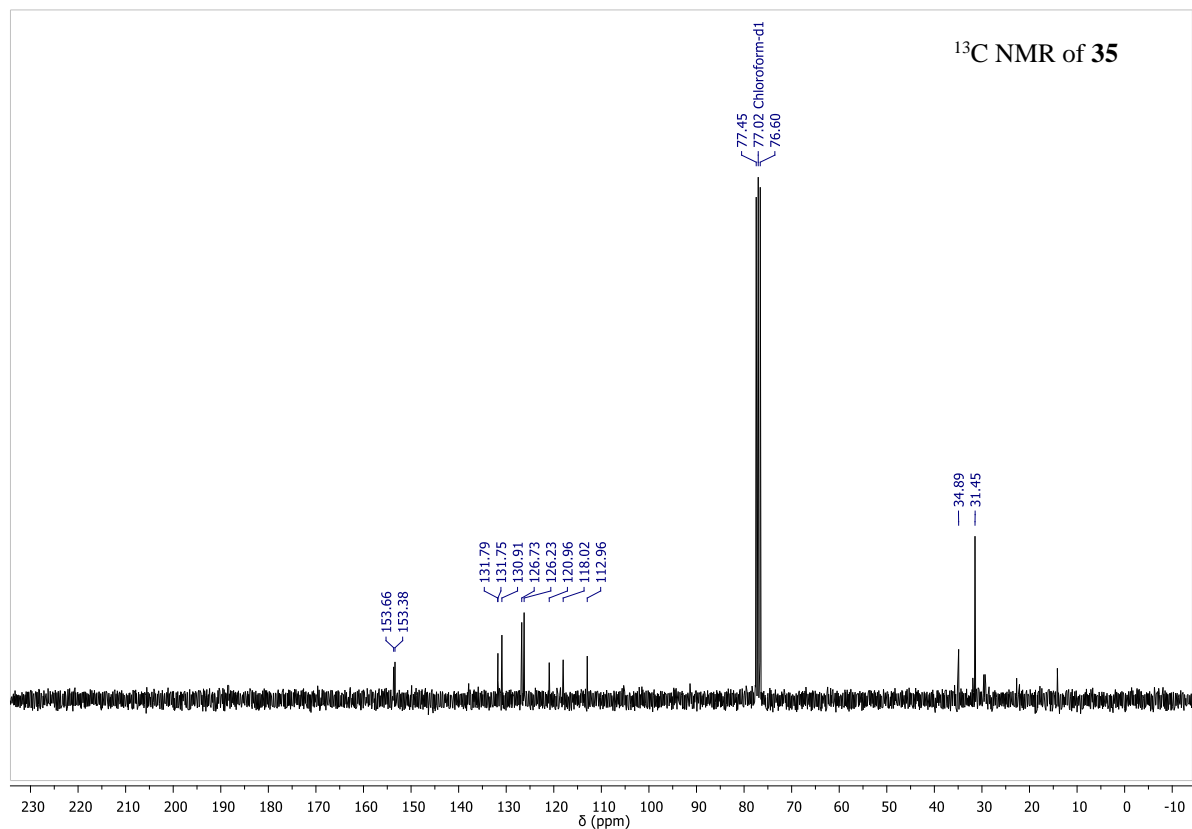
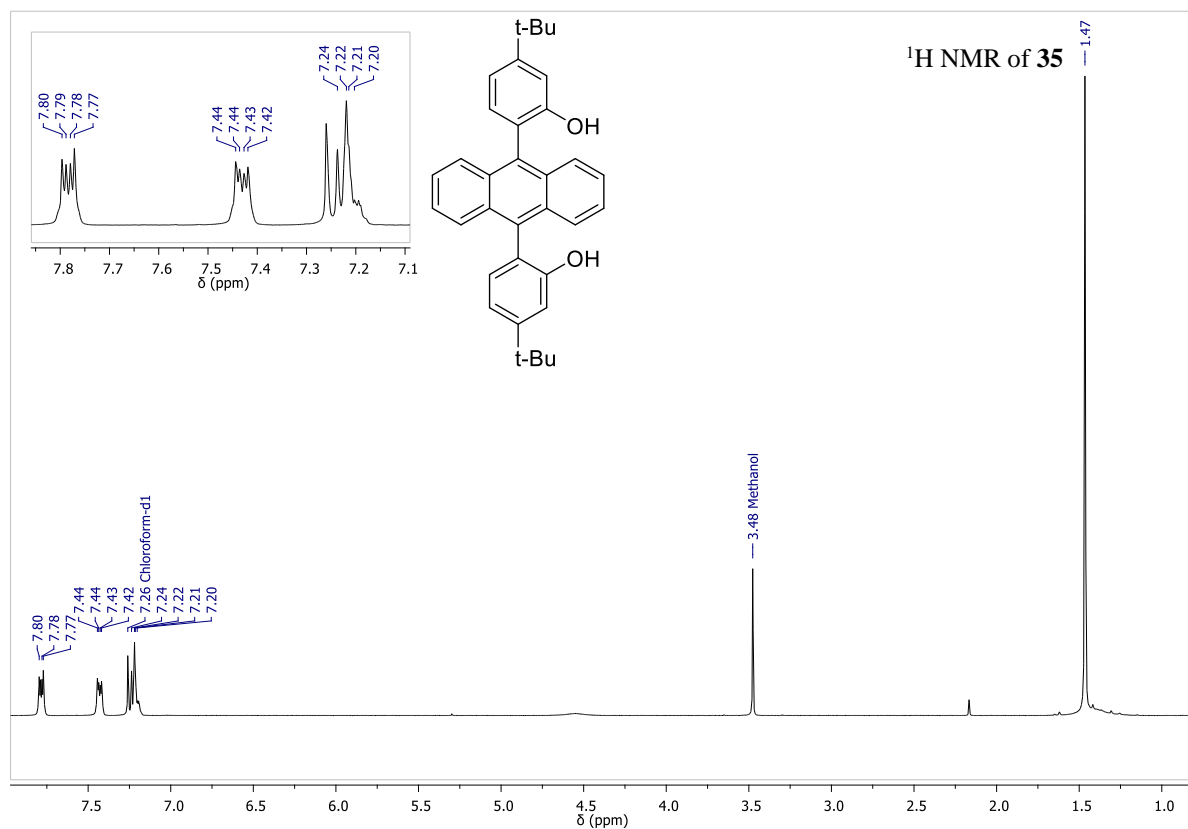
69 (65 mg, 0.12 mmol) and CuO (186 mg, 2.26 mol) were suspended in PHNO₂. The mixture was heated to reflux for 23.5 h before the solvent was distilled off under reduced pressure. The crude was dissolved in DCM and filtered over celite®. Precipitation from (C₂H₅)COOCH₃/CH₃OH gave 8 mg (0.02 mmol, 17 %) of the desired product as a yellow powder. **M.p.** **¹H NMR** (300 MHz, CDCl₃) δ 8.49 (s, 2H, H_d), 8.29 (d, J = 8.3 Hz, 2H, H_a), 7.71 (d, J = 1.6 Hz, 2H, H_c), 7.51 (dd, J = 8.3, 1.7 Hz, 2H), 1.69 (s, 18H), 1.41 (s, 18H). **¹³C NMR** (75 MHz, CDCl₃) δ 155.9, 152.7, 149.9, 135.8, 124.7, 122.2, 121.3, 120.8, 119.0, 118.4, 108.6, 77.5, 77.2, 77.0, 76.6, 35.2, 35.1, 31.7, 30.0. **HRMS** (ES m/z): [M]⁺ calc. for C₃₈H₄₄O₂, 523.3341 found: 523.3340; **IR** ν (cm⁻¹): 2954.95, 2902.87, 2866.22, 1728.22, 1627.92, 1618.28, 1570.06, 1517.98, 1462.04, 1425.40, 1392.61, 1361.74, 1307.74, 1261.45, 1236.37, 1226.73, 1207.44, 1166.93, 1120.64, 1083.99, 1062.78, 1026.13, 925.83, 66.04, 808.17, 763.81, 736.81, 675.09, 657.73, 601.79, 547.78, 505.35, 459.06, 414.70.

NMR Spectra of Synthesised Compounds:**2-bromo-5-(*tert*-butyl)phenol (**38**)**

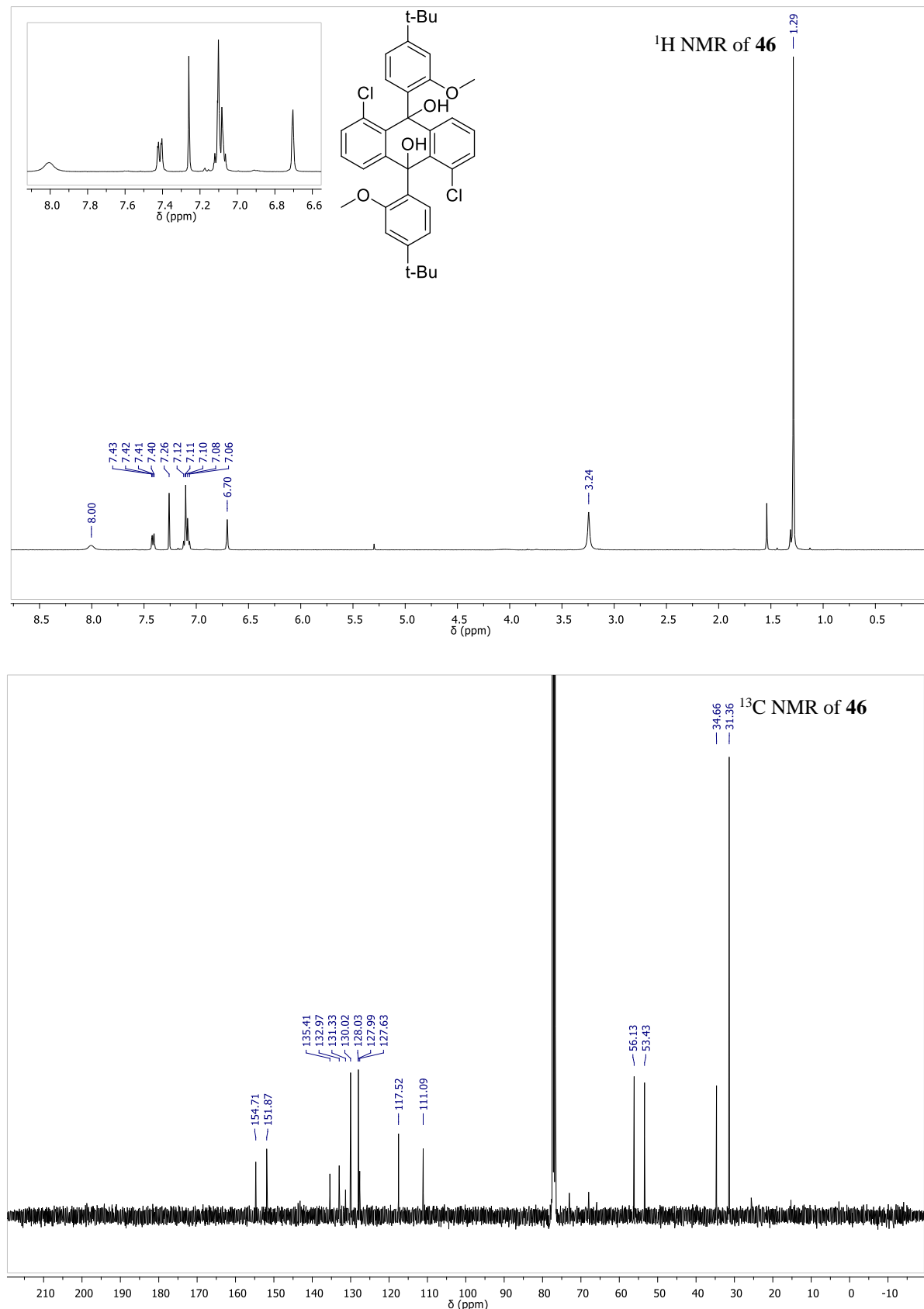
1-bromo-4-(*tert*-butyl)-2-methoxybenzene (39**)**

9,10-bis(4-(tert-butyl)-2-methoxyphenyl)-9,10-dihydroanthracene-9,10-diol (40**)**

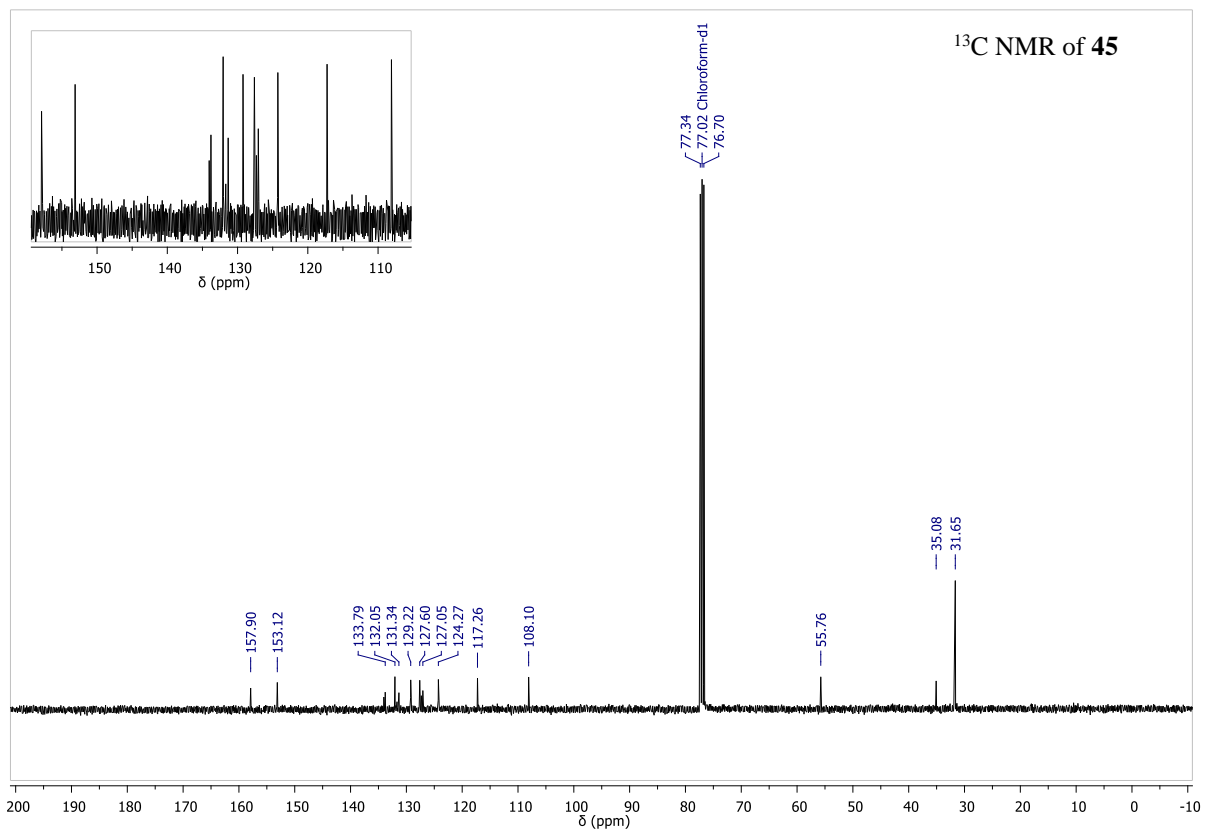
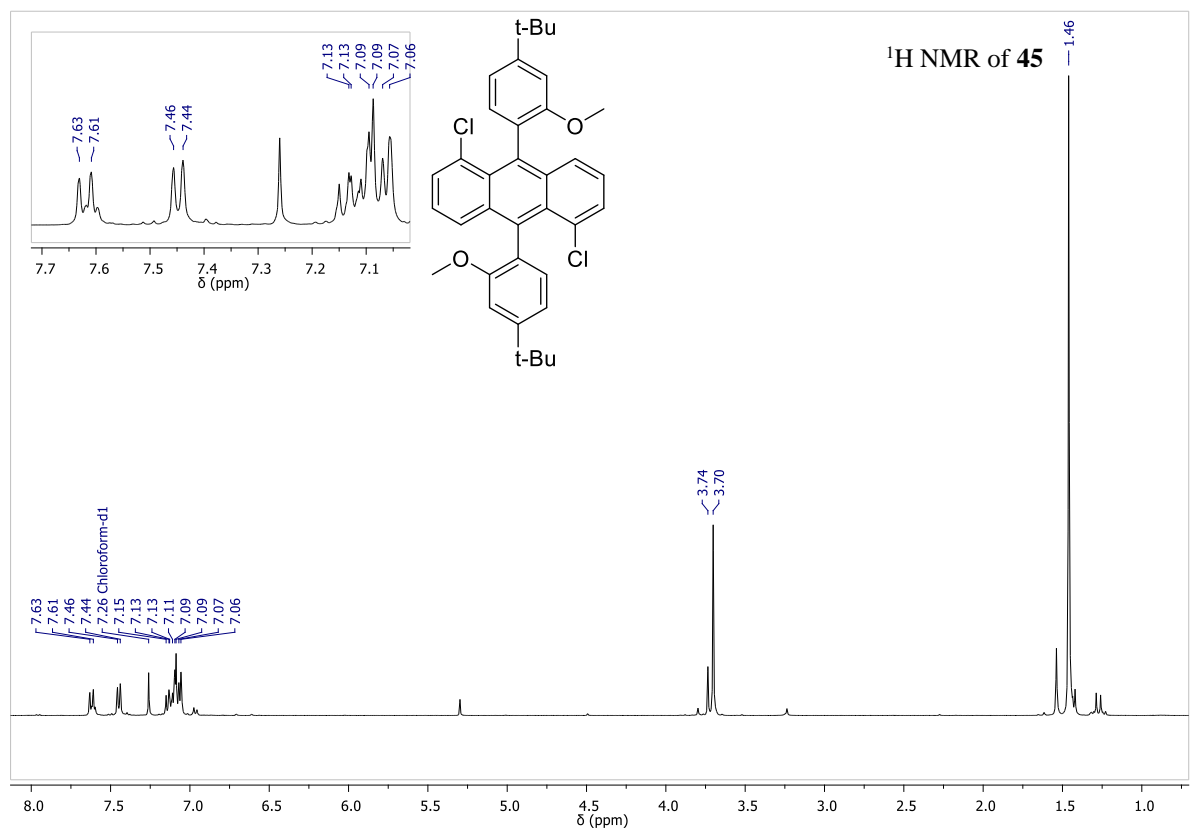
9,10-bis(4-(tert-butyl)-2-methoxyphenyl)anthracene (41**)**

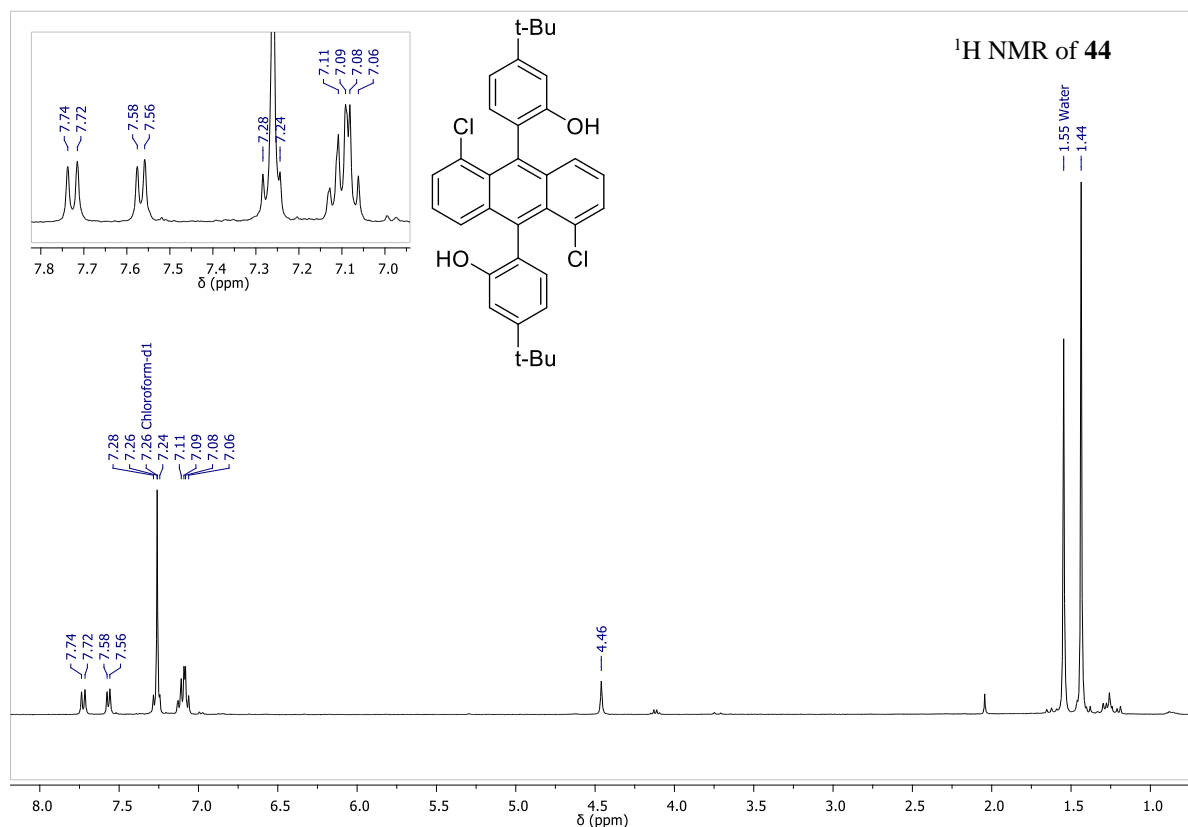
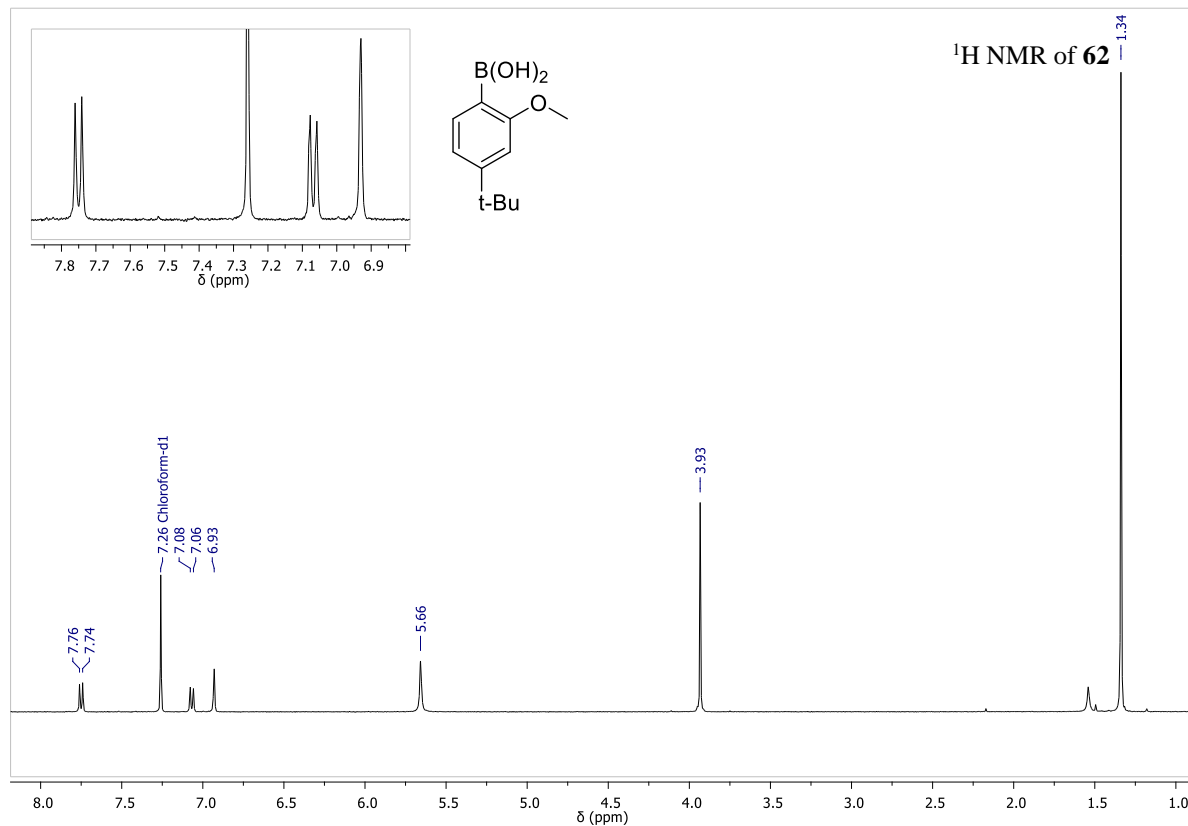
6,6'-(anthracene-9,10-diyl)bis(3-(tert-butyl)phenol) (35)

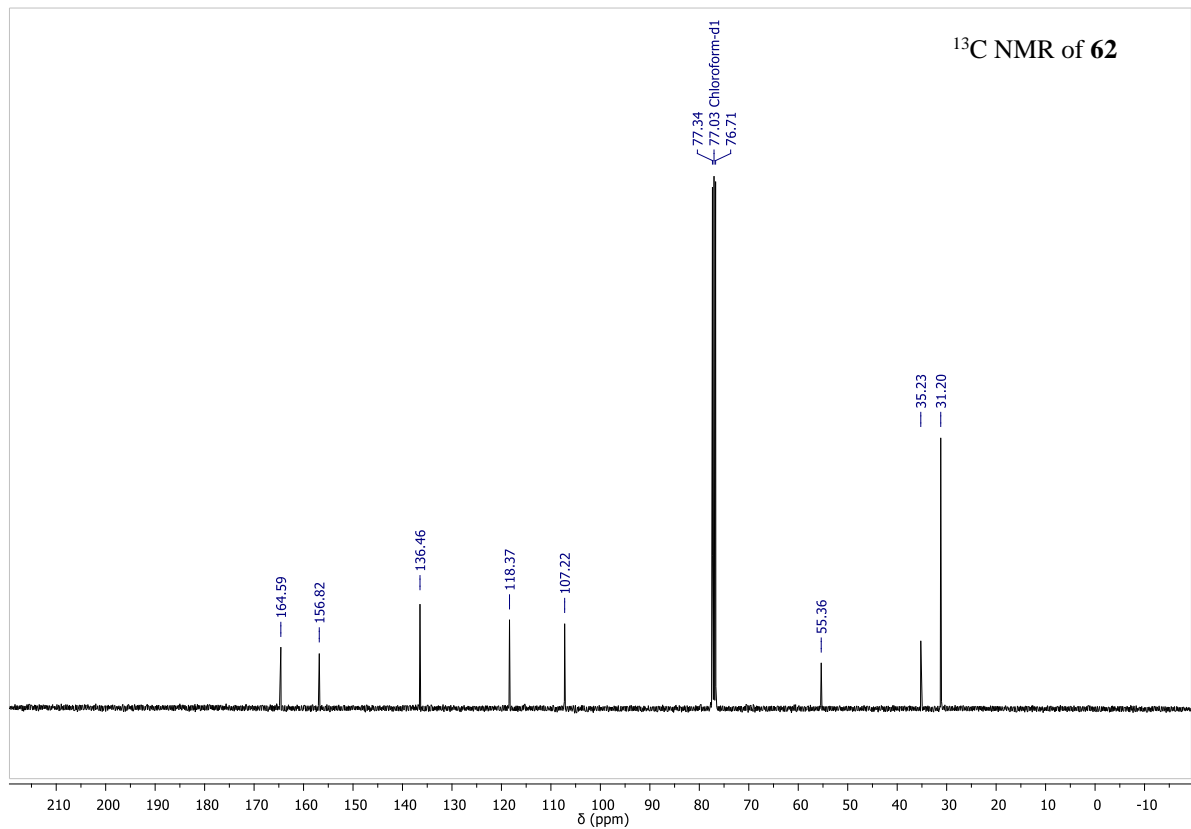
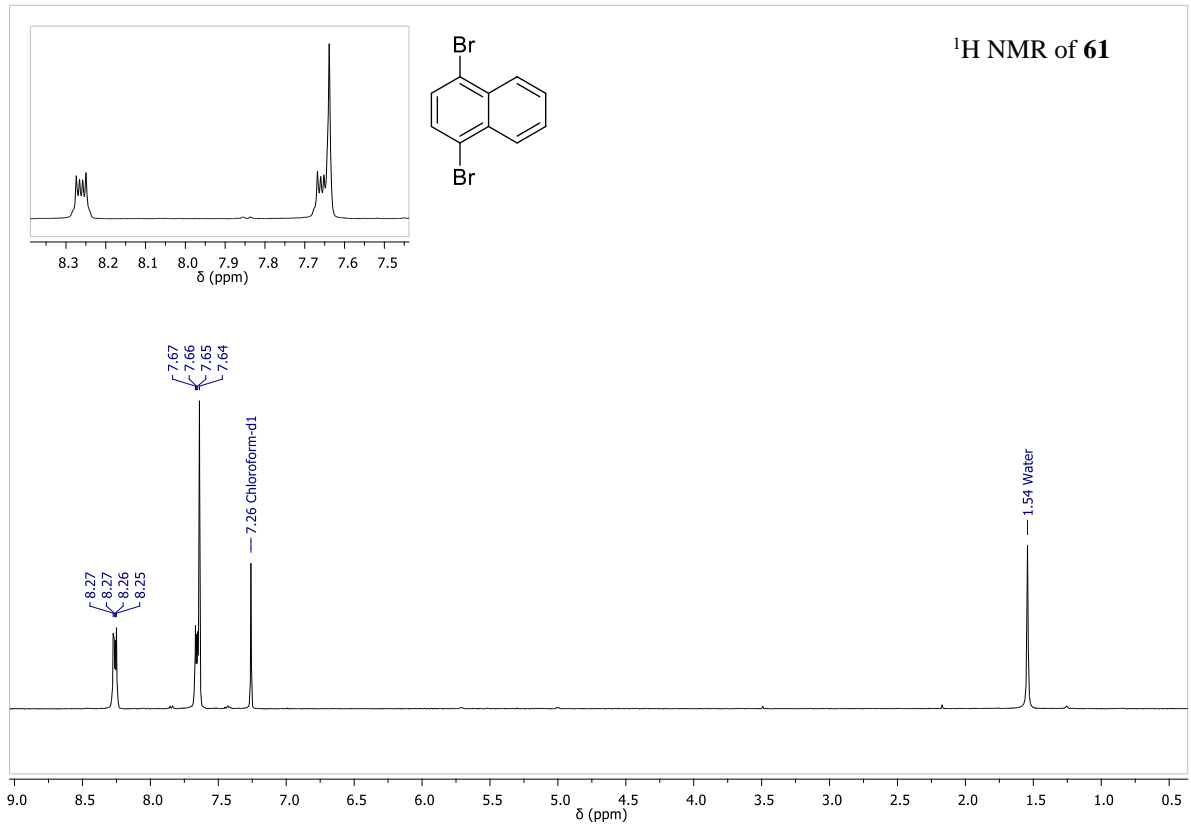
9,10-bis(4-(tert-butyl)-2-methoxyphenyl)-1,5-dichloro-9,10-dihydroanthracene-9,10-diol (46**)**

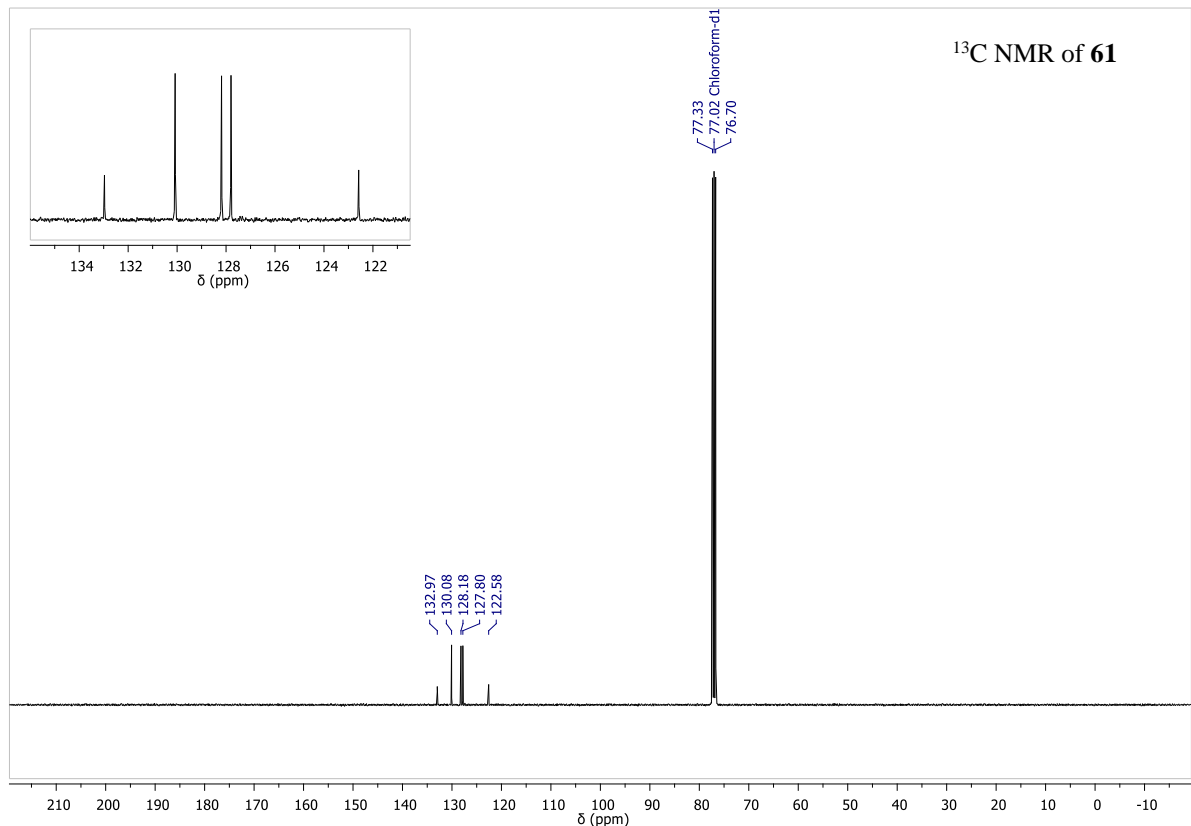


9,10-bis(4-(tert-butyl)-2-methoxyphenyl)-1,5-dichloroanthracene (45)

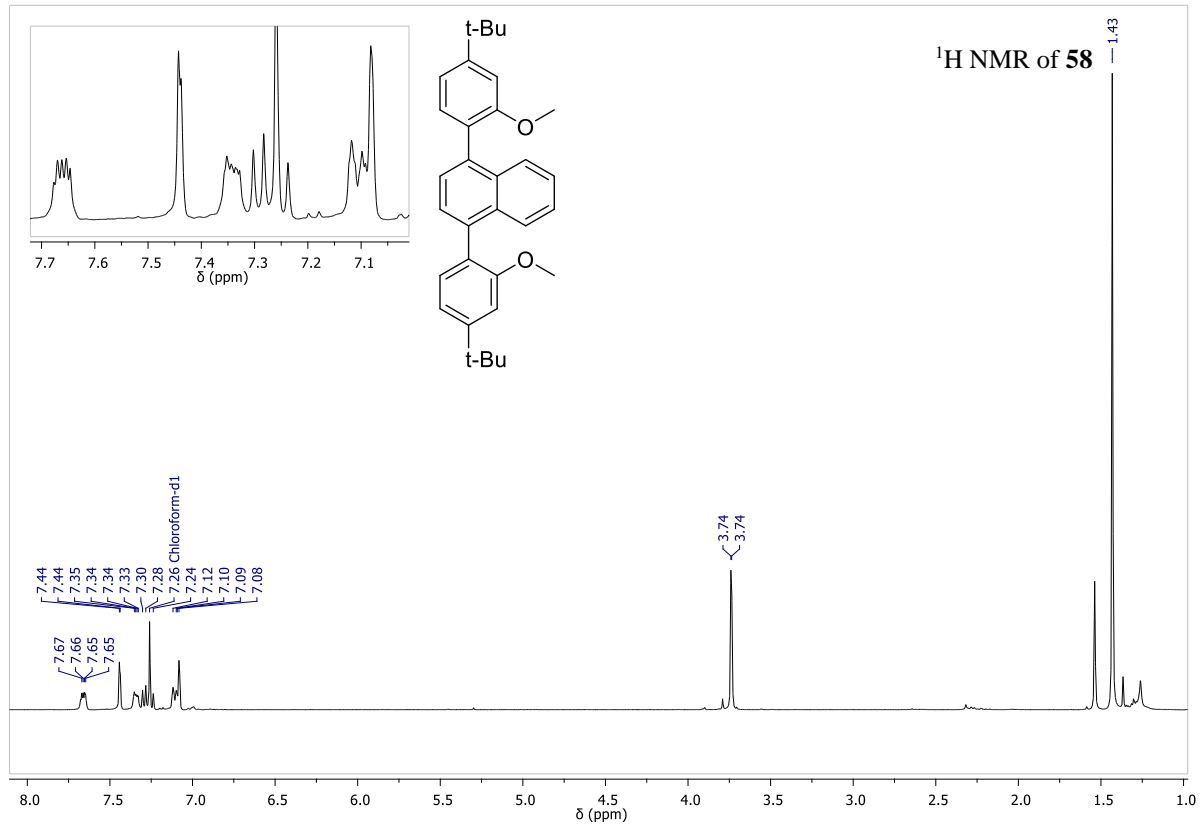


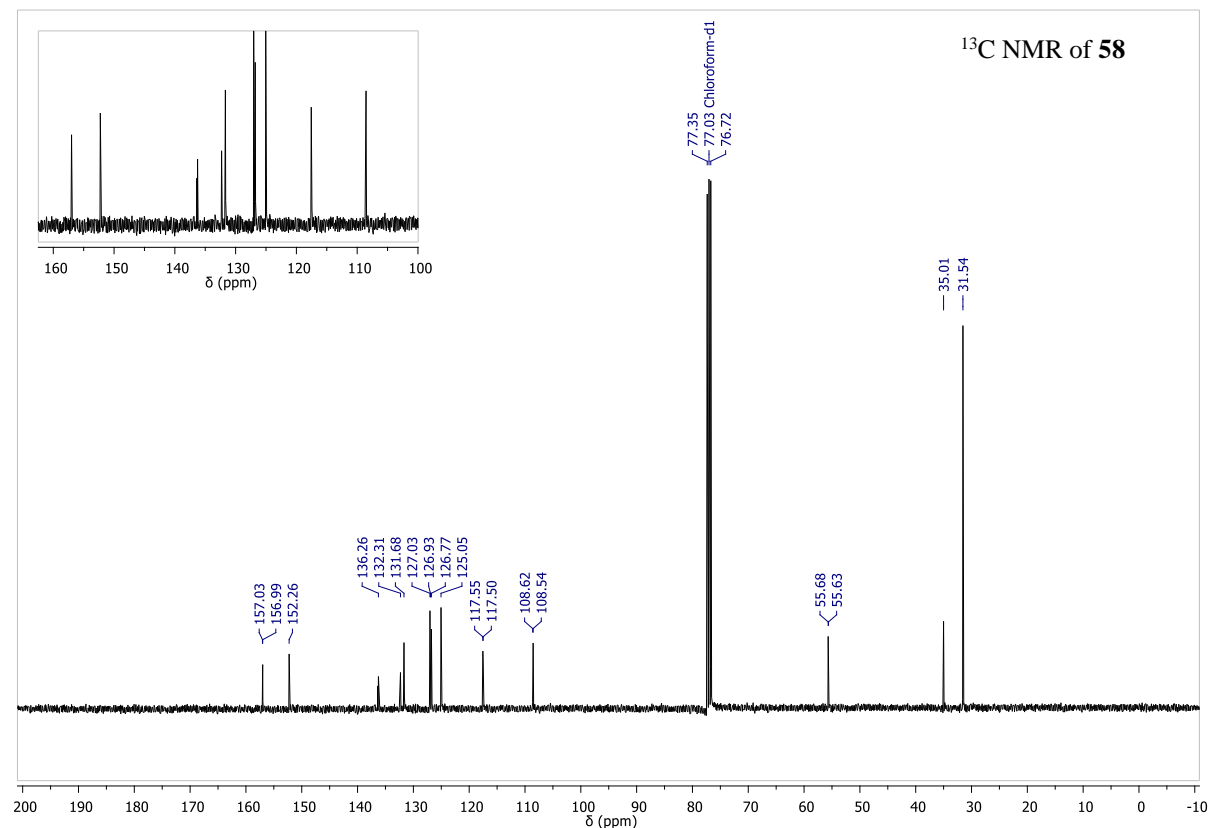
6,6'-(1,5-dichloroanthracene-9,10-diyl)bis(3-(tert-butyl)phenol) (44)**(4-(tert-butyl)-2-methoxyphenyl)boronic acid (62)**

**1,4-dibromonaphthalene (61)**

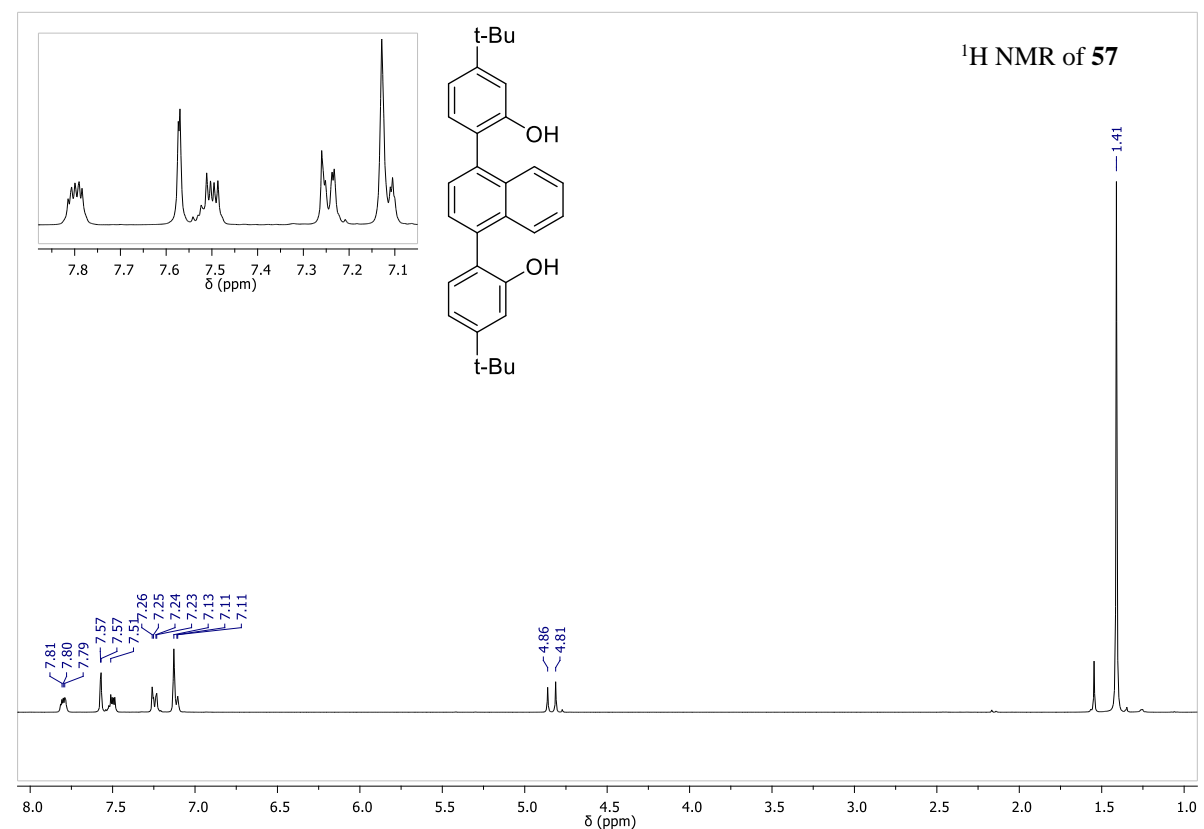


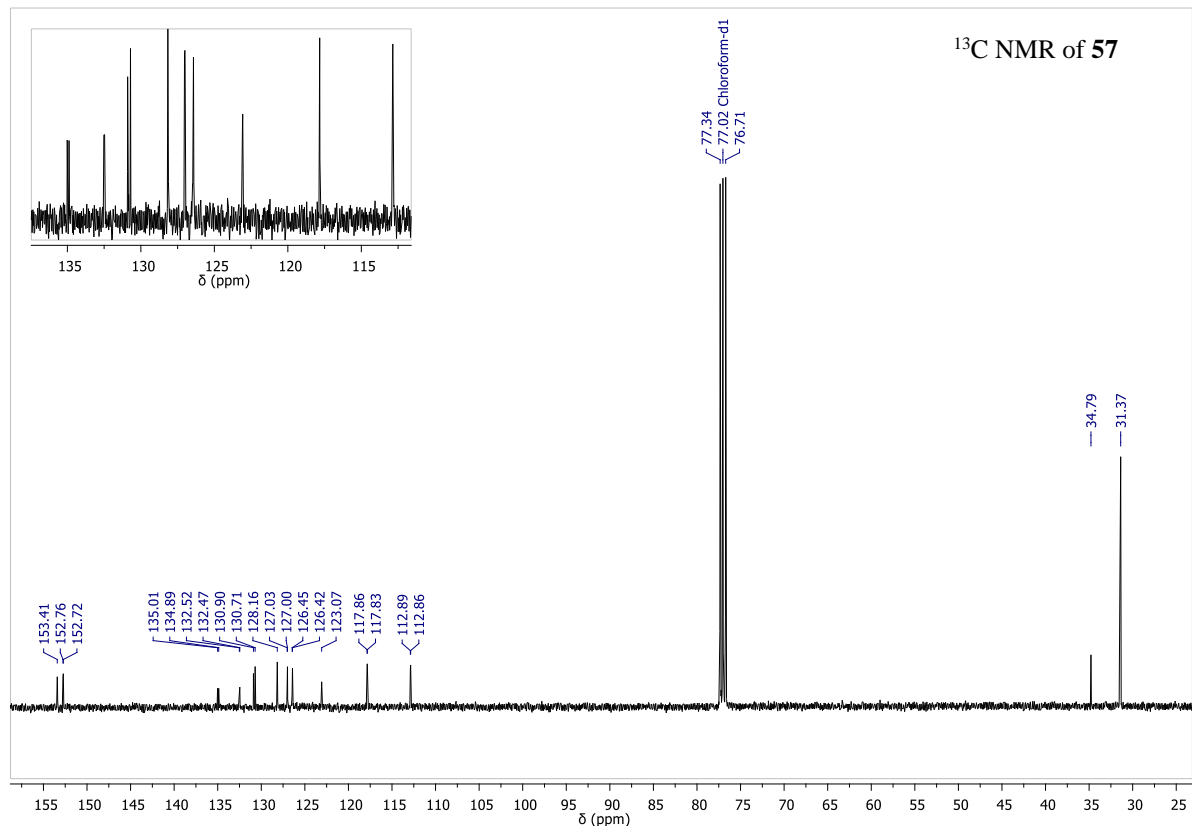
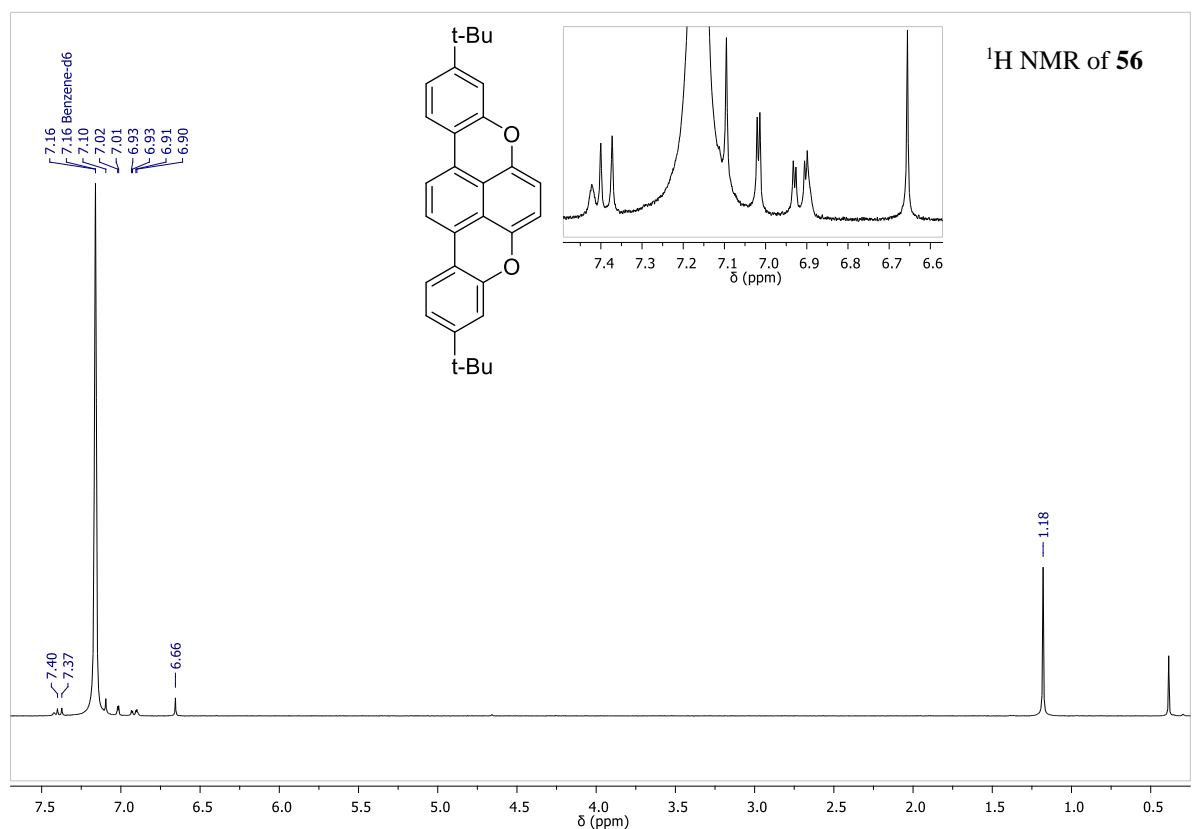
1,4-bis(4-(tert-butyl)-2-methoxyphenyl)naphthalene (**58**)

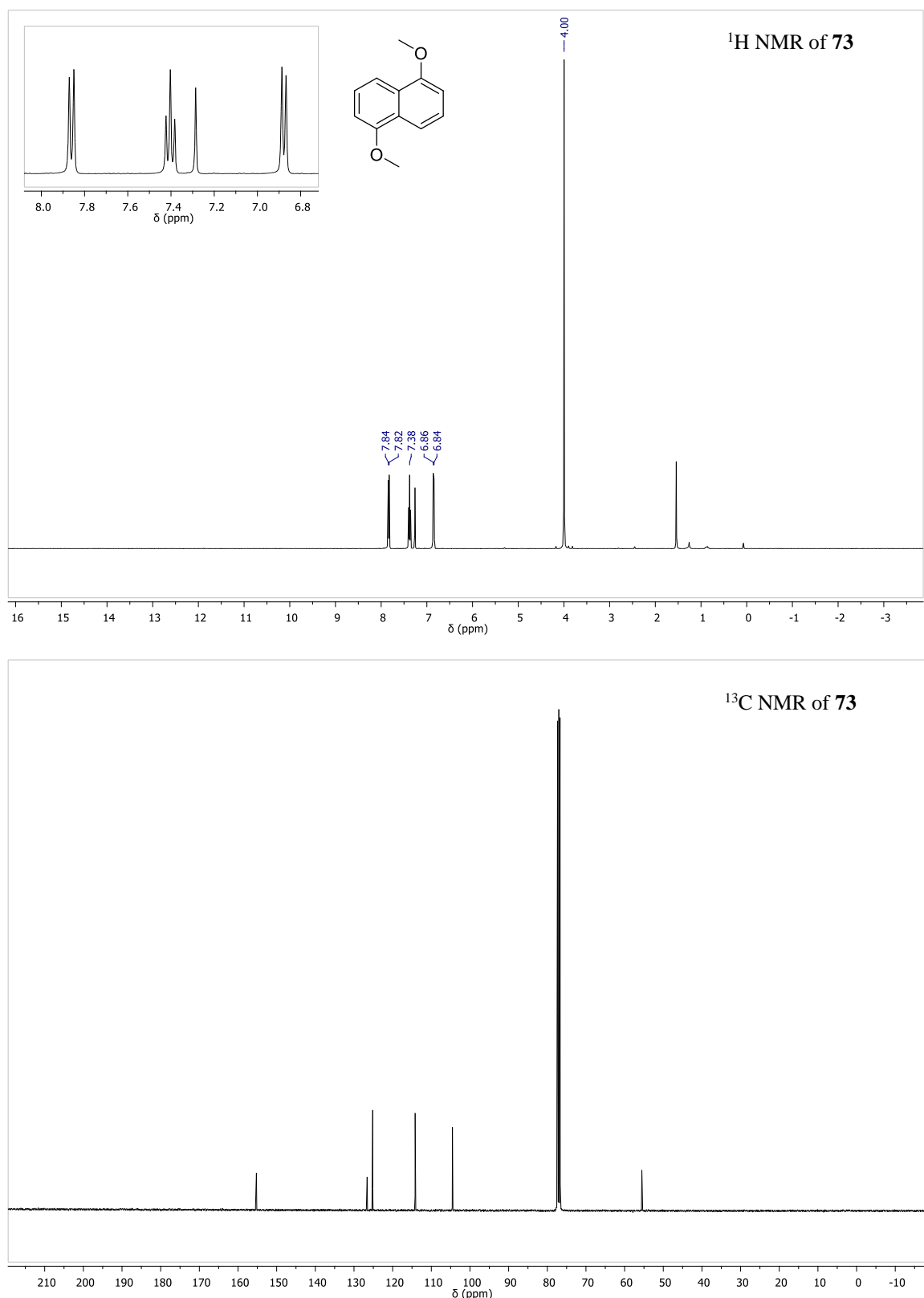


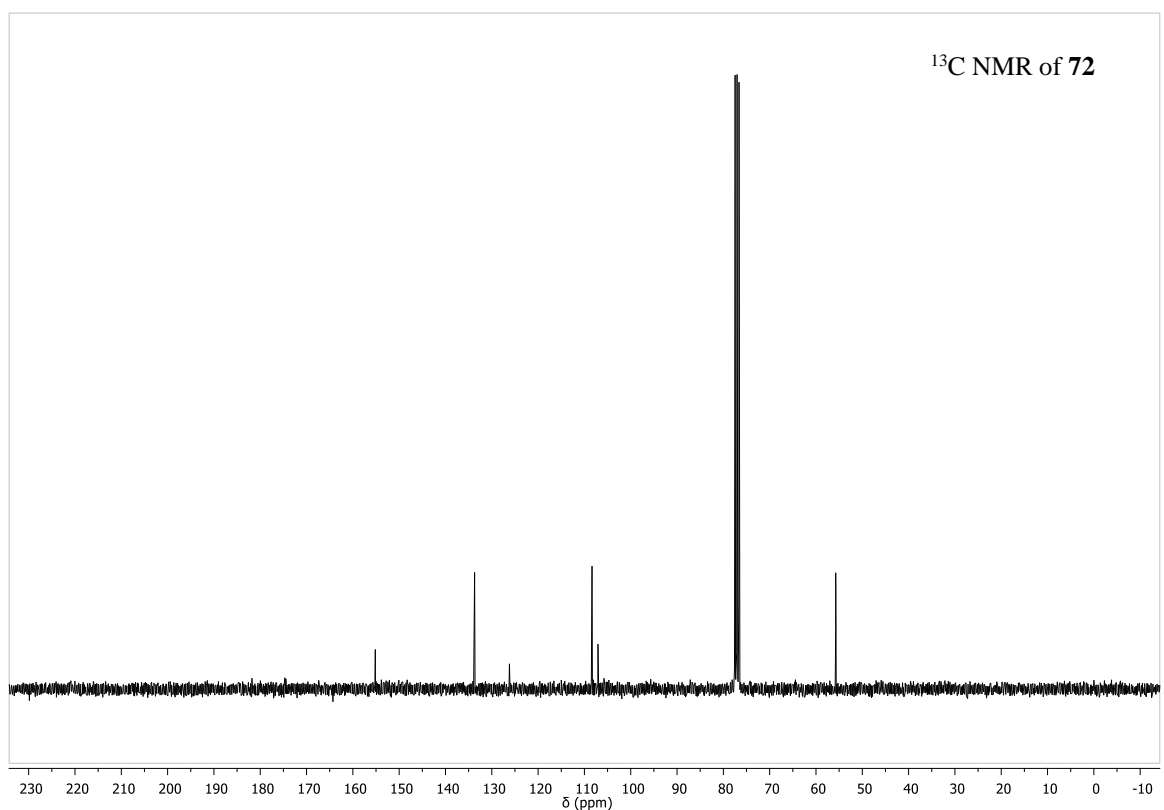
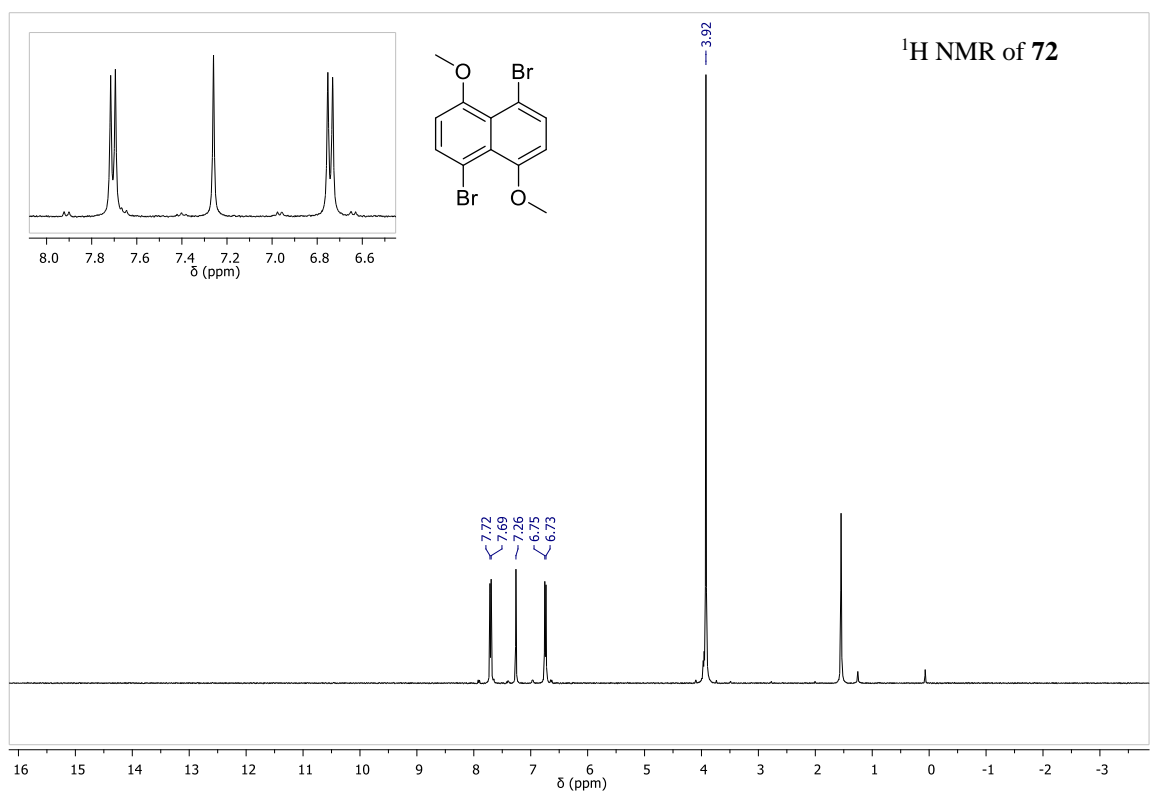


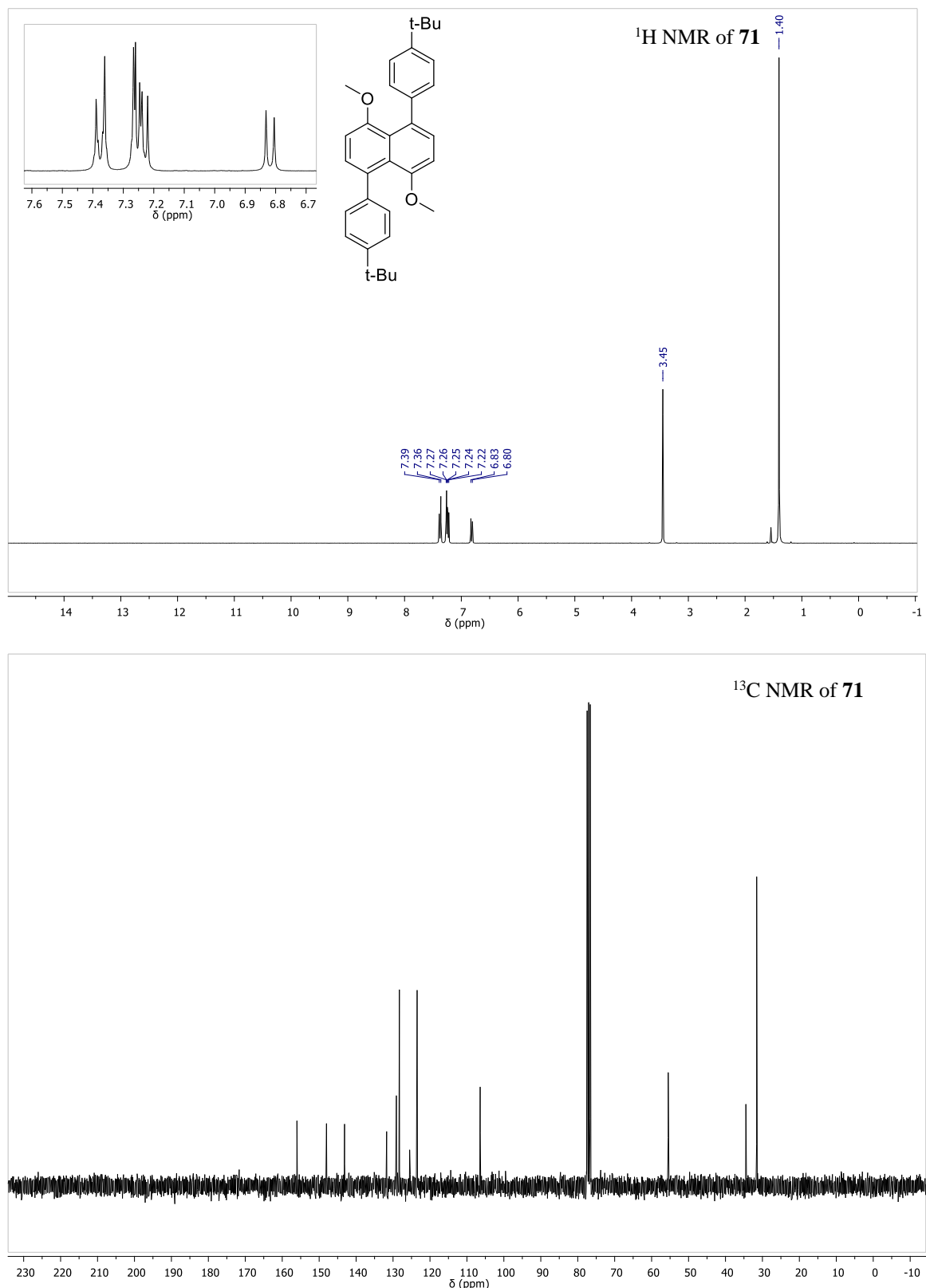
6,6'-(naphthalene-1,4-diyl)bis(3-(tert-butyl)phenol) (**57**)

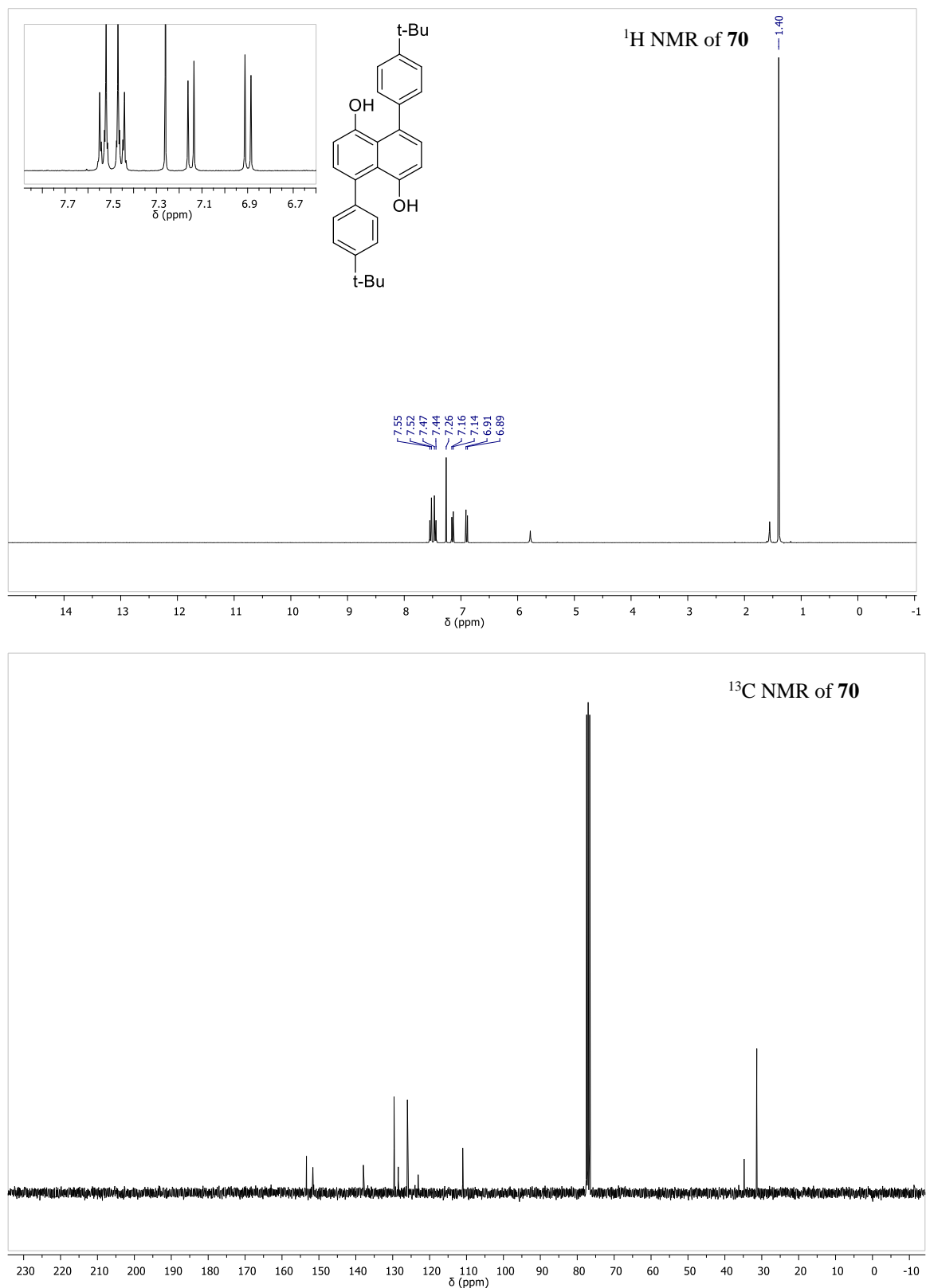


**3,10-di-tert-butylbenzo[3,4]isochromeno[7,8,1-mna]xanthene (56)**

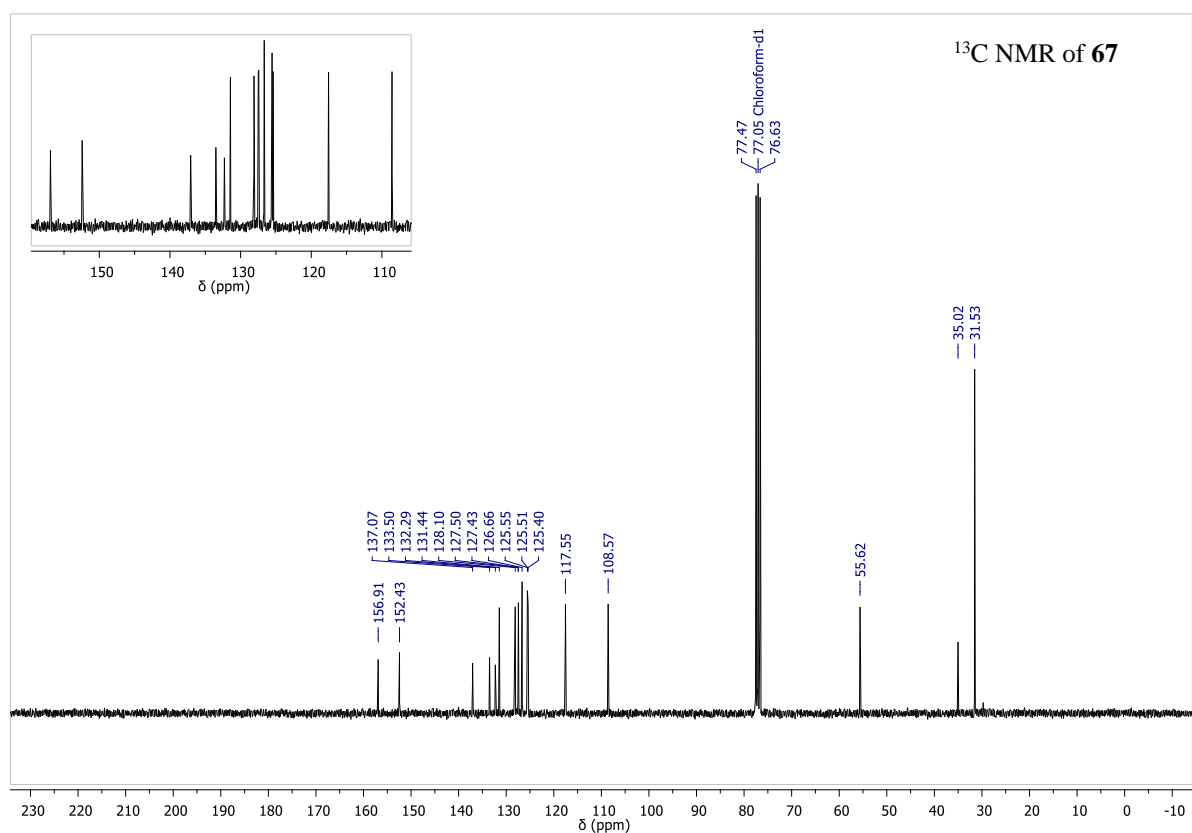
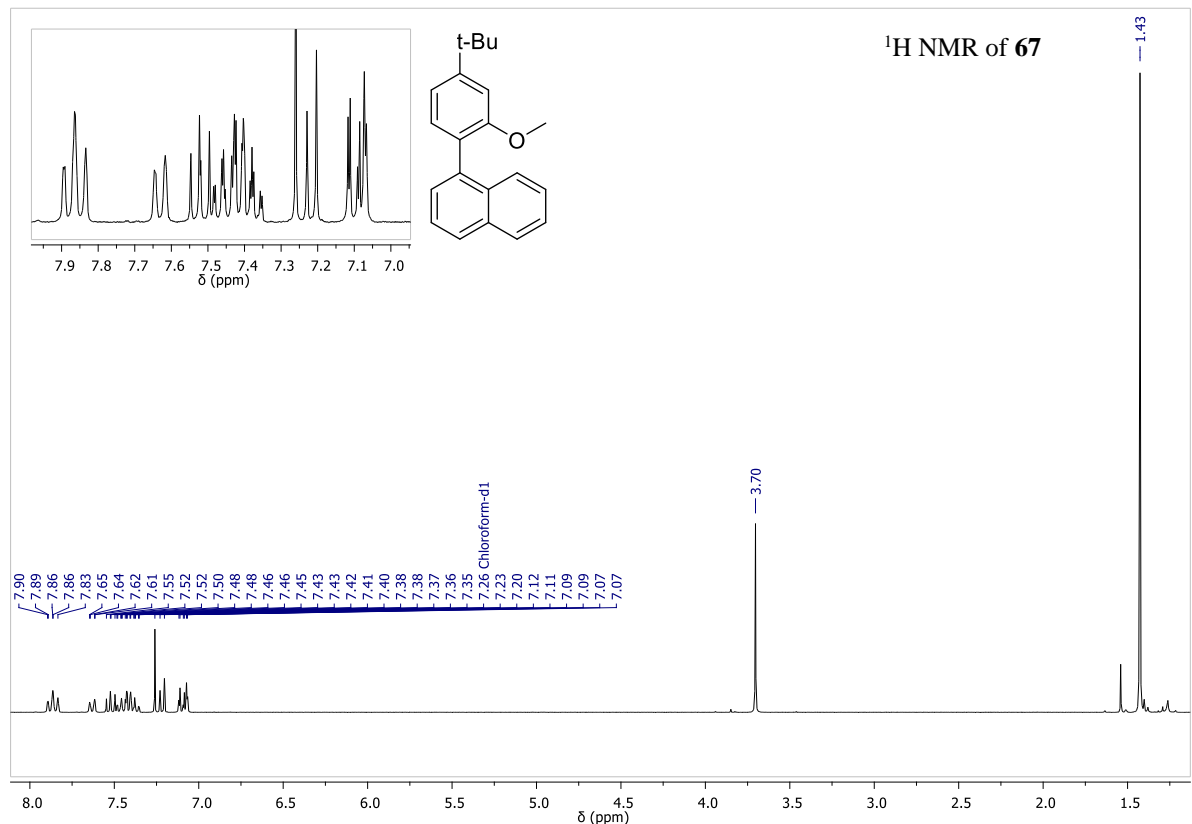
1,5-dimethoxynaphthalene (73)

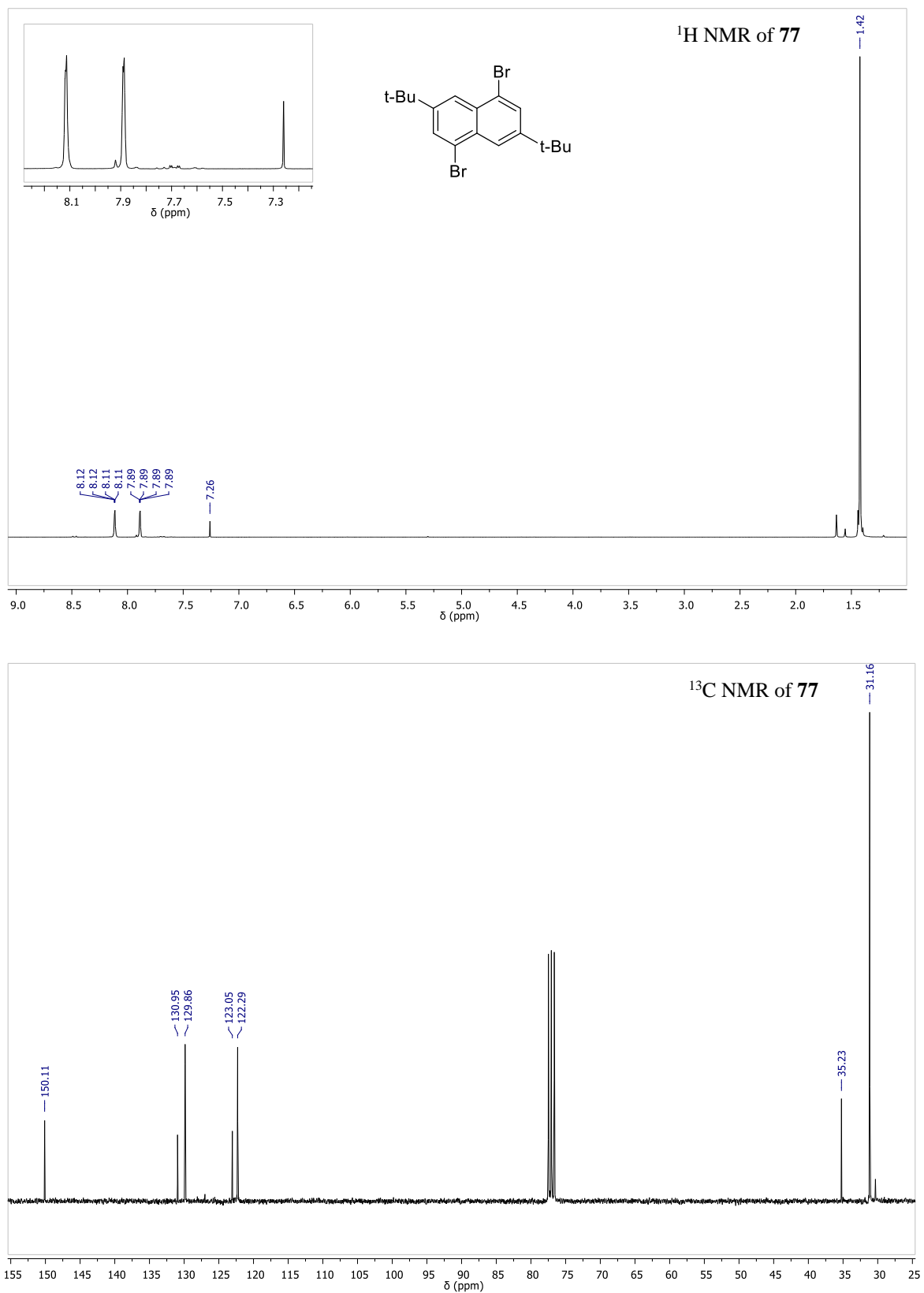
1,5-dibromo-4,8-dimethoxynaphthalene (72)

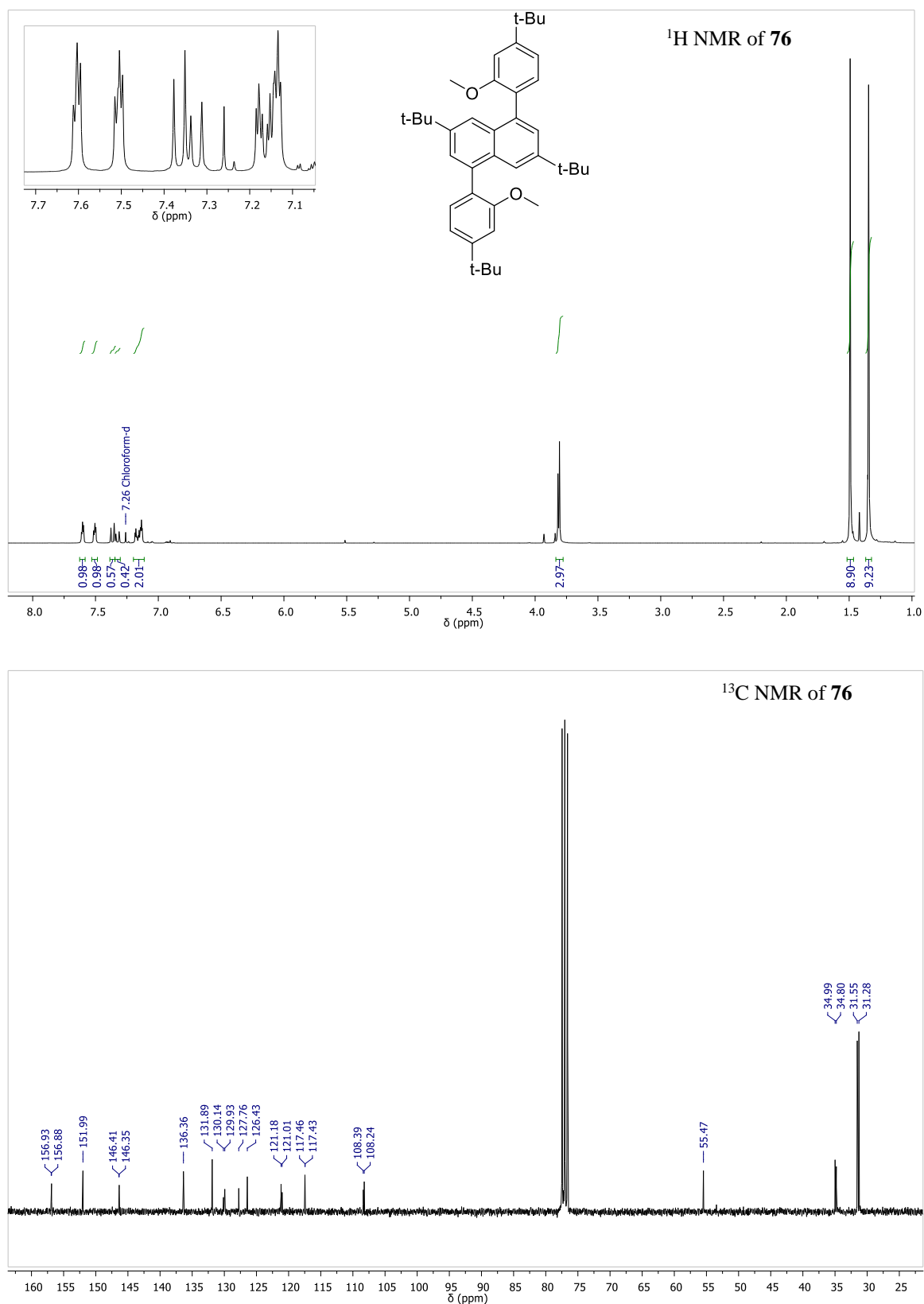
1,5-bis(4-(tert-butyl)phenyl)-4,8-dimethoxynaphthalene (71)

4,8-bis(4-(tert-butyl)phenyl)naphthalene-1,5-diol (70**)**

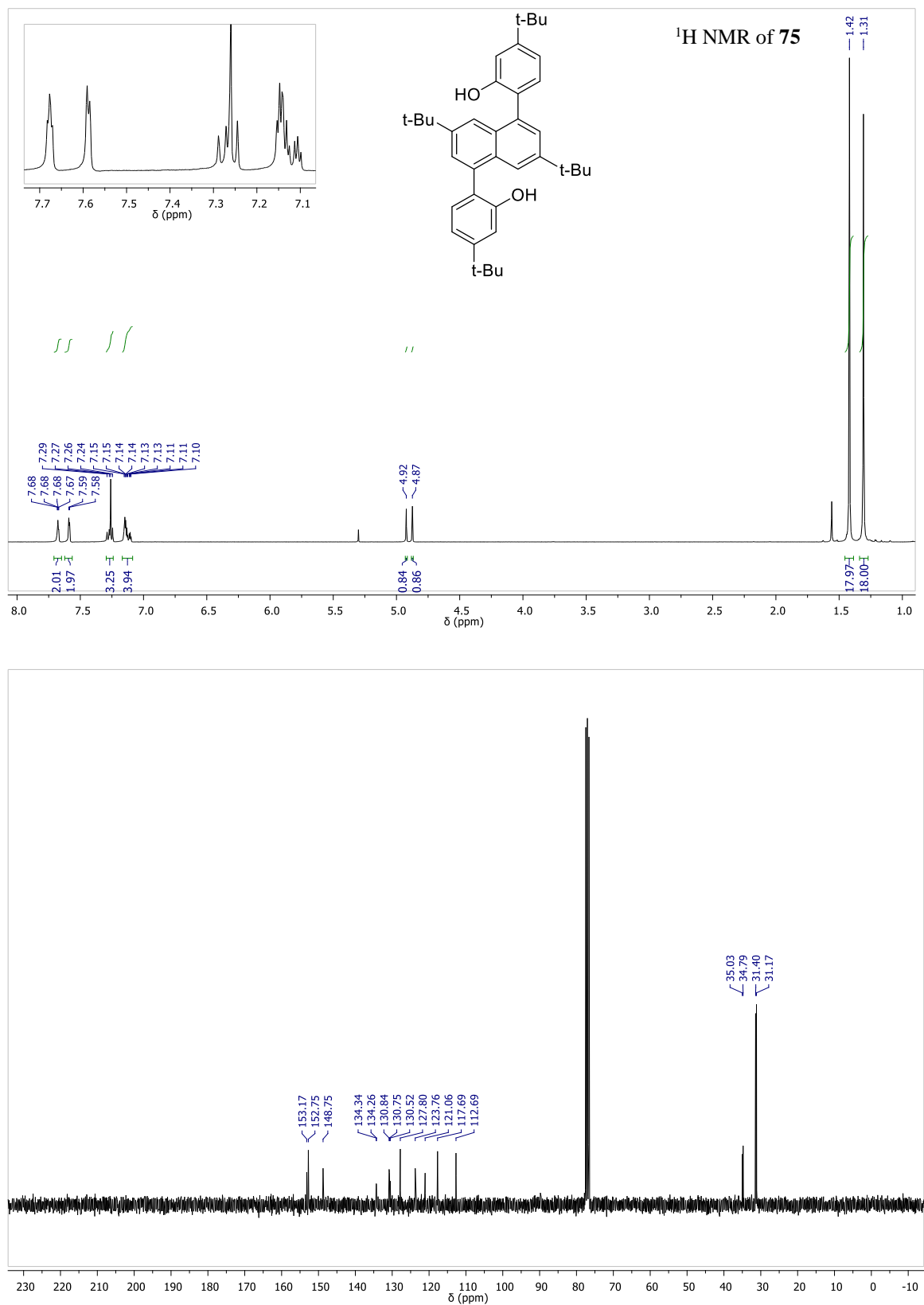
1-(4-(tert-butyl)-2-methoxyphenyl)naphthalene (67)



1,5-dibromo-3,7-di-tert-butylnaphthalene (77)

3,7-di-tert-butyl-1,5-bis(4-(tert-butyl)-2-methoxyphenyl)naphthalene (76)

6,6'-(3,7-di-tert-butylnaphthalene-1,5-diyl)bis(3-(tert-butyl)phenol) (75)



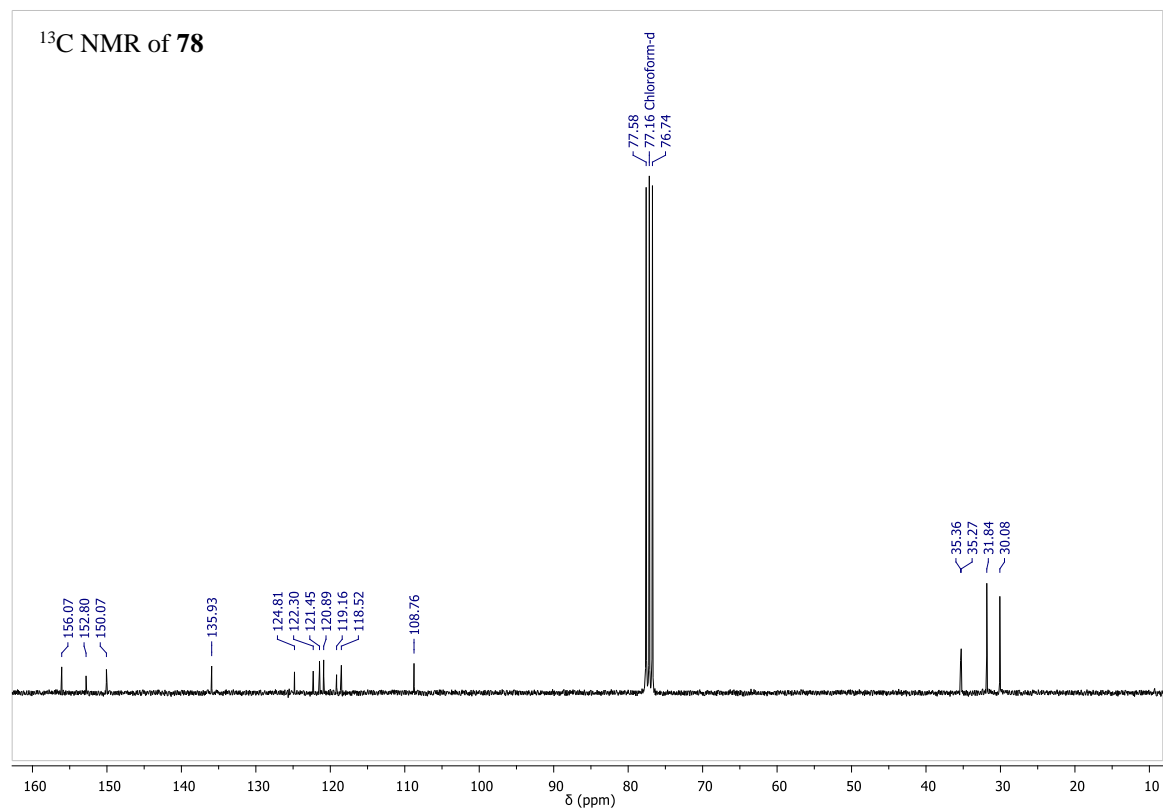
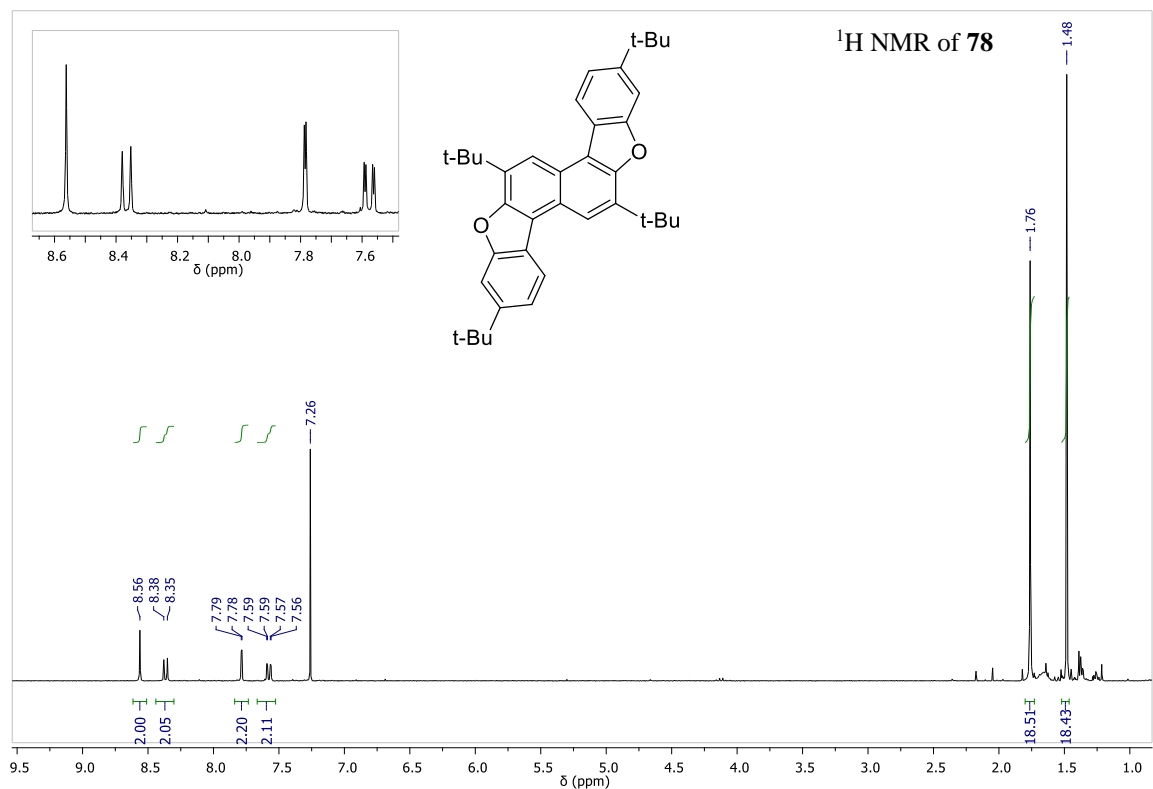
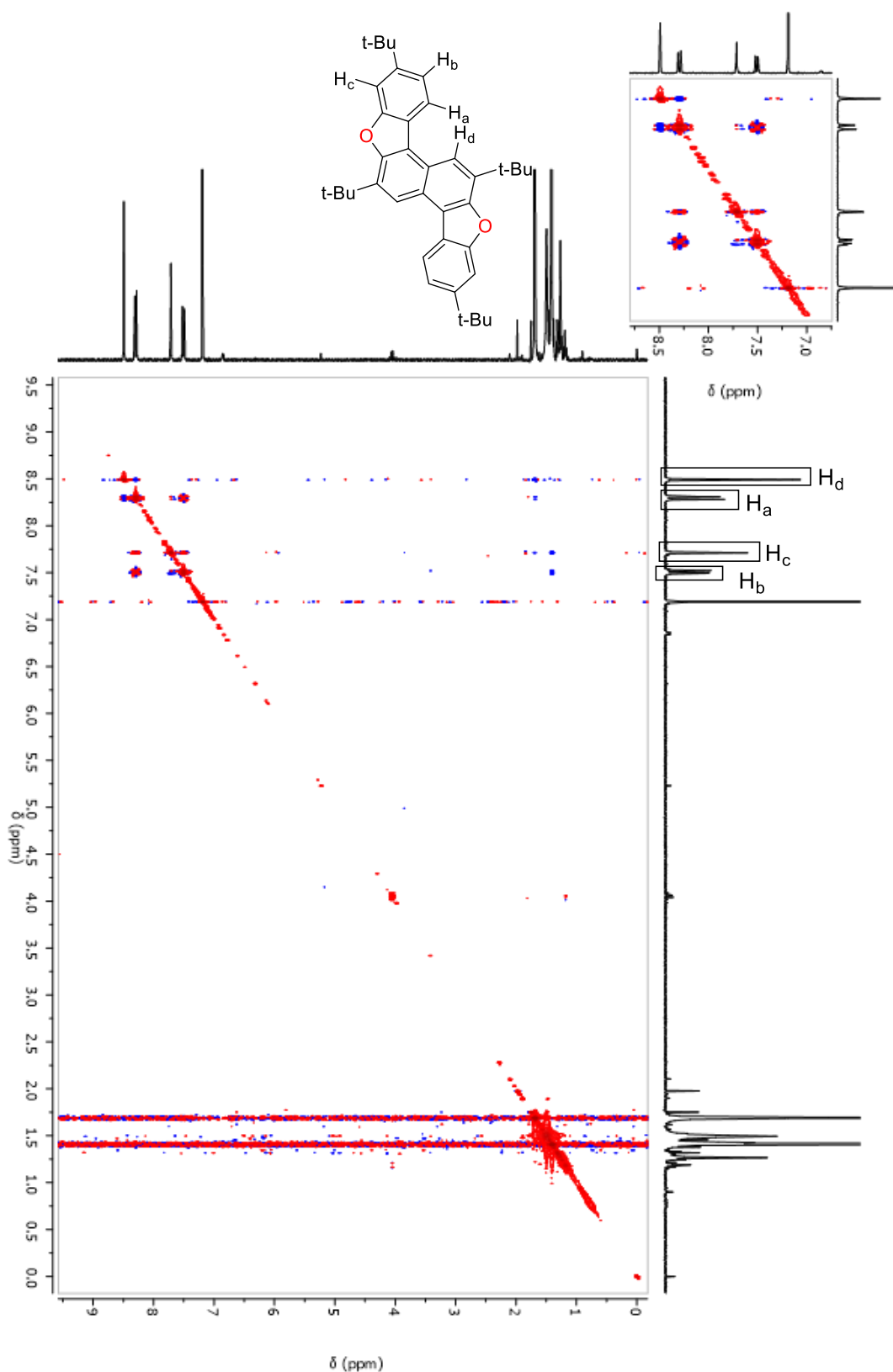
2,6,9,13-tetra-*tert*-butylnaphtho[2,1-b:6,5-b']bisbenzofuran (78)

Figure 38: 2D NOESY ^1H NMR of 78.

X-Ray Crystallography**Crystal Data and structure refinement for 1,4-cyclised naphthalene (56)****Crystal data:**

Empirical formula	C30 H28 O2
Formula weight	420.52
Crystal system	Triclinic
Space group	P -1
Unit cell dimensions	a = 5.7772(4) Å a = 95.418(6)°. b = 17.4971(14) Å b = 90.510(5)°. c = 21.8096(13) Å g = 96.593(6)°.
Volume	2179.8(3) Å ³
Z	4
Density (calculated)	1.281 Mg/m3
Absorption coefficient	0.078 mm-1
F(000)	896
Crystal size	0.217 x 0.111 x 0.036 mm3

Data collection:

Temperature	200(2) K
Wavelength	0.71073 Å
Theta range for data collection	3.493 to 29.497°.
Index ranges	-7<=h<=7, -19<=k<=23, -29<=l<=24
Reflections collected	17082
Independent reflections	10135 [R(int) = 0.0507]
Completeness to theta =	25.242° 99.8 %

Refinement:

Refinement method	Full-matrix least-squares on F2
Data / restraints / parameters	10135 / 0 / 577
Goodness-of-fit on F ²	1.022
Final R indices [I>2sigma(I)]	R1 = 0.0969, wR2 = 0.2325
R indices (all data)	R1 = 0.1933, wR2 = 0.2997

Extinction coefficient	n/a
Largest diff. peak and hole	0.439 and -0.325 e.Å ⁻³

Crystal data and structure refinement for 3,6-cyclised naphthalene (78)

Crystal data:

Empirical formula	C38 H44 O2
Formula weight	532.73
Crystal system	Monoclinic
Space group	P 21/c
Unit cell dimensions	a = 12.8794(14) Å a= 90°. b = 10.3656(7) Å b= 97.786(9)°. c = 11.6096(9) Å g = 90°.
Volume	1535.6(2) Å ³
Z	2
Density (calculated)	1.152 Mg/m ³
Absorption coefficient	0.528 mm ⁻¹
F(000)	576
Crystal size	0.205 x 0.101 x 0.056 mm ³

Data Collection:

Temperature	200(2) K
Wavelength	1.54184 Å
Theta range for data collection	3.464 to 73.955°.
Index ranges	-15<=h<=13, -11<=k<=12, -14<=l<=14
Reflections collected	13878
Independent reflections	3065 [R(int) = 0.0950]
Completeness to theta =	67.684° 100.0 %

Refinement

Refinement method	Full-matrix least-squares on F ²
Data / restraints / parameters	3065 / 0 / 172
Goodness-of-fit on F ²	1.012

Final R indices [I>2sigma(I)]	R1 = 0.0664, wR2 = 0.1612
R indices (all data)	R1 = 0.1220, wR2 = 0.2004
Extinction coefficient	n/a
Largest diff. peak and hole	0.236 and -0.256 e. \AA -3

Quantum Yield Calculations

Quantum yield in solution was determined using the equation seen below. Curcumin was employed as a standard and the samples were tested in solution under ambient conditions.

$$\Phi_{sample} = \Phi_{standard} \left(\frac{I_{sample}}{A_{sample}} \times \frac{A_{standard}}{I_{standard}} \right) \left(\frac{\eta_{sample}^2}{\eta_{standard}^2} \right)$$

The solutions of Curcumin (in EtOH) and 1,4-cyclised naphthalene product (in C₆H₁₂) were diluted until they possessed absorption maxima less than 0.1. Each were then excited at 445 nm and the emission spectra measured. Insertion of the values for the integration of the respective spectra into the above equation yielded the emission quantum efficiency.

Electrochemical Analysis

Cyclic voltammetry experiments were performed at room temperature in dry nitrogen-purged DCM (dried over activated molecular sieves prior to use) using an Autolab Pgstat12. Dry nitrogen was bubbled through the sample prior to, and during measurements. The working electrode used was a glassy carbon electrode (3 mm diameter), the counter electrode was a Pt wire, and an Ag/Ag⁺ reference electrode was used.

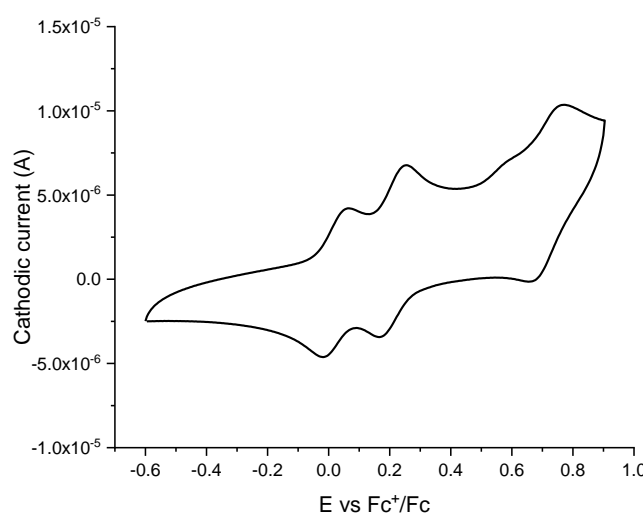


Figure 39: CV of **55** performed using ferrocene as a reference. Performed in 0.1M Bu₄NBF₄ solution at a scan rate of 100 mV/s

Prior to use the working electrode was polished on a felt pad using 1.0 µm or 0.3 µm alumina. Spectroelectrochemical characterisation was performed using a thin layer quartz cuvette (path length of 2 mm) equipped with an optically transparent platinum minigrid working electrode, platinum auxiliary wire counter electrode, and an Ag/Ag⁺ non-aqueous reference electrode.

Using the results of the CV experiment with ferrocene as an internal reference (Figure 39), the energy of the HOMO of **11** can be calculated. Using the equations below,^{119,120} the energy of the HOMO was found to be – 5.3 eV. This was done using the half-wave potentials which were calculated using the formula: $E_{1/2} = (E_{pa} + E_{pc}) / 2$ where E_{pa} is the peak anode potential and E_{pc} is the peak cathode potential.⁹⁴

$$E_{\text{HOMO}} = -(5.1 \text{ eV} + E^{\text{l}}_{\text{ox}} \text{ vs. Fc}^{+}/\text{Fc})$$

$$E_{\text{LUMO}} = -(5.1 \text{ eV} + E^{\text{l}}_{\text{red}} \text{ vs. Fc}^{+}/\text{Fc})$$

The energy of the LUMO could not be calculated using this method as a reduction peak was not observed even when the CV sweep was extended to -1.5 V.

Electrochromic Device Building

Fabrication of a liquid electrolyte device:

The ECDs were realised by depositing a drop of compound dissolved in a DCM (approximately 1 mg in 1 ml) on to a substrate covered with an electroactive layer (PET/ITO or glass/FTO). An adhesive square template was then used to encapsulate the deposited electrochrome and the substrate was trimmed to size, when possible. Electrolyte was then deposited evenly within the template, and a second substrate layer with more deposited electrochrome was used to close the device, making sure the coloured areas of the device did not overlap. Copper tape was then attached to each of the substrate layers, forming two electrodes. A potential was then applied across the device using an Autolab Pgstat12 potentiostat.

Fabrication of a cured electrolyte device:

An adhesive square template was attached to a substrate coated with an electroactive layer. Electrolyte was deposited within this template and then cured with UV radiation ($\lambda = 346$ nm) for 15 minutes. Two smaller sheets of substrate with deposited electrochrome were then used to close the device (Figure 36). Copper tape was attached to the two substrates

possessing electrochromic materials, forming the two electrodes. A potential was then applied across the device using an Autolab Pgstat12 potentiostat.

References

- 1 C. G. Granqvist, E. Avendaño and A. Azens, *Thin Solid Films*, 2003, **442**, 201–211.
- 2 R. J. Mortimer, *Annu. Rev. Mater. Res.*, 2011, **41**, 241–268.
- 3 C.-G. Granqvist, *Nat. Mater.*, 2006, **5**, 89–90.
- 4 R. J. Mortimer, *Electrochimica Acta*, 1999, **44**, 2971–2981.
- 5 R. J. Mortimer, A. L. Dyer and J. R. Reynolds, *Displays*, 2006, **27**, 2–18.
- 6 C.-G. Granqvist, in *Electrochromic Materials and Devices*, Wiley-VCH, 2015, pp. 3–39.
- 7 L. Shao, X. Zhuo and J. Wang, *Adv. Mater.*, 2018, **30**, 1704338.
- 8 D. R. Rosseinsky and R. J. Mortimer, *Adv. Mater.*, 2001, **13**, 783–793.
- 9 S. K. Deb, *Appl. Opt.*, 1969, **8**, 192–195.
- 10 ynvisible - things alive, <http://www.ynvisible.com/technology>, (accessed 17 June 2018).
- 11 K. H. Lee, Y. K. Fang, W. J. Lee, J. J. Ho, K. H. Chen and K. C. Liao, *Sens. Actuators B*, 2000, **69**, 96–99.
- 12 C.-C. Liao, F.-R. Chen and J.-J. Kai, *Sol. Energy Mater. Sol. Cells*, 2006, **90**, 1147–1155.
- 13 E. B. Franke, C. L. Trimble, J. S. Hale, M. Schubert and J. A. Woollam, *J. Appl. Phys.*, 2000, **88**, 5777–5784.
- 14 M. Deepa, M. Kar and S. A. Agnihotry, *Thin Solid Films*, 2004, **468**, 32–42.
- 15 D. Gogova, A. Iossifova, T. Ivanova, Z. Dimitrova and K. Gesheva, *J. Cryst. Growth*, 1999, **198–199**, 1230–1234.
- 16 H.-S. Shim, J. W. Kim, Y.-E. Sung and W. B. Kim, *Sol. Energy Mater. Sol. Cells*, 2009, **93**, 2062–2068.
- 17 Y.-M. Lu and C.-P. Hu, *J. Alloys Compd.*, 2008, **449**, 389–392.
- 18 E. Ozkan, S.-H. Lee, P. Liu, C. E. Tracy, F. Z. Tepehan, J. R. Pitts and S. K. Deb, *Solid State Ionics*, 2002, **149**, 139–146.
- 19 A. Subrahmanyam and A. Karuppasamy, *Sol. Energy Mater. Sol. Cells*, 2007, **91**, 266–274.
- 20 M. K. Carpenter, R. S. Conell and D. A. Corrigan, *Sol. Energy Mater.*, 1987, **16**, 333–346.
- 21 W. Estrada, A. M. Andersson and C. G. Granqvist, *J. Appl. Phys.*, 1988, **64**, 3678–3683.
- 22 J. L. Garcia-Miquel, Q. Zhang, S. J. Allen, A. Rougier, A. Blyr, H. O. Davies, A. C. Jones, T. J. Leedham, P. A. Williams and S. A. Impey, *Thin Solid Films*, 2003, **424**, 165–170.
- 23 C. M. Lampert, T. R. Omstead and P. C. Yu, *Sol. Energy Mater.*, 1986, **14**, 161–174.
- 24 A. ŠUrca, B. Orel and B. Pihlar, *J. Sol-Gel Sci. Technol.*, 1997, **8**, 743–749.
- 25 K. Nakaoka, J. Ueyama and K. Ogura, *J. Electroanal. Chem.*, 2004, **571**, 93–99.
- 26 S. F. Cogan, N. M. Nguyen, S. J. Perrotti and R. D. Rauh, *J. Appl. Phys.*, 1989, **66**, 1333–1337.
- 27 M. Mousavi, Gh. H. Khorrami, A. Kompany and Sh. T. Yazdi, *Appl. Phys. A*, 2017, **123**, 755.
- 28 R. M. J. Lemos, J. C. B. Alcázar, N. L. V. Carreño, J. Andrade, A. Pawlicka, J. Kanicki, A. Gundel, C. F. Azevedo and C. O. Avellaneda, *Mol. Cryst. Liq. Cryst.*, 2017, **655**, 40–50.
- 29 T. Maruyama and T. Kanagawa, *J. Electrochem. Soc.*, 1995, **142**, 1644–1647.
- 30 E. Avendaño, A. Azens, G. A. Niklasson and C. G. Granqvist, *Sol. Energy Mater. Sol. Cells*, 2004, **84**, 337–350.
- 31 P. M. Beaujuge and J. R. Reynolds, *Chem. Rev.*, 2010, **110**, 268–320.

- 32 G. Sonmez, C. K. F. Shen, Y. Rubin and F. Wudl, *Angew. Chem.*, 2004, **116**, 1524–1528.
- 33 M. Aizawa, S. Watanabe, H. Shinohara and H. Shirakawa, *J. Chem. Soc. Chem. Commun.*, 1985, **0**, 264–265.
- 34 C. L. Gaupp, K. Zong, P. Schottland, B. C. Thompson, C. A. Thomas and J. R. Reynolds, *Macromolecules*, 2000, **33**, 1132–1133.
- 35 M. Mastragostino, C. Arbizzani, A. Bongini, G. Barbarella and M. Zambianchi, *Electrochimica Acta*, 1993, **38**, 135–140.
- 36 A. L. Dyer, M. R. Craig, J. E. Babiarz, K. Kiyak and J. R. Reynolds, *Macromolecules*, 2010, **43**, 4460–4467.
- 37 A. Kumar and J. R. Reynolds, *Macromolecules*, 1996, **29**, 7629–7630.
- 38 K. H. Skorenko, A. C. Faucett, J. Liu, N. A. Ravvin, W. E. Bernier, J. M. Mativetsky and W. E. Jones, *Synth. Met.*, 2015, **209**, 297–303.
- 39 P. Camurlu, *RSC Adv.*, 2014, **4**, 55832–55845.
- 40 A. F. Diaz, J. Castillo, K. K. Kanazawa, J. A. Logan, M. Salmon and O. Fajardo, *J. Electroanal. Chem. Interfacial Electrochem.*, 1982, **133**, 233–239.
- 41 Y. Murakami and T. Yamamoto, *Polym. J.*, 1999, **31**, 476–478.
- 42 E. C. S. Coelho, V. B. Nascimento, A. S. Ribeiro and M. Navarro, *Electrochim. Acta*, 2014, **123**, 441–449.
- 43 A. K. A. Almeida, J. M. M. Dias, A. J. C. Silva, D. P. Santos, M. Navarro, J. Tonholo, M. O. F. Goulart and A. S. Ribeiro, *Electrochim. Acta*, 2014, **122**, 50–56.
- 44 W. Choi, H. C. Ko, B. Moon and H. Lee, *J. Electrochem. Soc.*, 2004, **151**, E80–E83.
- 45 C. Chevrot, E. Ngbilo, K. Kham and S. Sadki, *Synth. Met.*, 1996, **81**, 201–204.
- 46 M. M. Verghese, M. K. Ram, H. Vardhan, S. M. Ashraf and B. D. Malhotra, *Adv. Mater. Opt. Electron.*, 1996, **6**, 399–402.
- 47 M. M. Verghese, M. K. Ram, H. Vardhan, B. D. Malhotra and S. M. Ashraf, *Polymer*, 1997, **38**, 1625–1629.
- 48 F. Tran-Van, T. Henri and C. Chevrot, *Electrochim. Acta*, 2002, **47**, 2927–2936.
- 49 F. Baycan Koyuncu, S. Koyuncu and E. Ozdemir, *Org. Electron.*, 2011, **12**, 1701–1710.
- 50 S.-H. Hsiao and S.-W. Lin, *Polym. Chem.*, 2016, **7**, 198–211.
- 51 S. Tirkeş and A. M. Önal, *J. Appl. Polym. Sci.*, 2007, **103**, 871–876.
- 52 J. R. Reynolds, A. D. Child, J. P. Ruiz, S. Y. Hong and D. S. Marynick, *Macromolecules*, 1993, **26**, 2095–2103.
- 53 T. Kobayashi, H. Yoneyama and H. Tamura, *J. Electroanal. Chem. Interfacial Electrochem.*, 1984, **161**, 419–423.
- 54 M. Leclerc, J. Guay and L. H. Dao, *Macromolecules*, 1989, **22**, 649–653.
- 55 J. W. Chevalier, J. Y. Bergeron and L. H. Dao, *Macromolecules*, 1992, **25**, 3325–3331.
- 56 G. D'Aprano, M. Leclerc, G. Zotti and G. Schiavon, *Chem. Mater.*, 1995, **7**, 33–42.
- 57 S. Xiong, S. Li, X. Zhang, R. Wang, R. Zhang, X. Wang, B. Wu, M. Gong and J. Chu, *J. Electron. Mater.*, 2018, **47**, 1167–1175.
- 58 G. J. Stec, A. Lauchner, Y. Cui, P. Nordlander and N. J. Halas, *ACS Nano*, 2017, **11**, 3254–3261.
- 59 S.-I. Park, Y.-J. Quan, S.-H. Kim, H. Kim, S. Kim, D.-M. Chun, C. S. Lee, M. Taya, W.-S. Chu and S.-H. Ahn, *Int. J. Precis. Eng. Manuf.-Green Technol.*, 2016, **3**, 397–421.
- 60 M. Layani, P. Darmawan, W. L. Foo, L. Liu, A. Kamyshny, D. Mandler, S. Magdassi and P. S. Lee, *Nanoscale*, 2014, **6**, 4572–4576.
- 61 E. O. Polat, O. Balci and C. Kocabas, *Sci. Rep.*, DOI:10.1038/srep06484.

- 62 Z. Ji, S. K. Doorn and M. Sykora, *ACS Nano*, 2015, **9**, 4043–4049.
- 63 J. D. Klein, A. Yen, R. D. Rauh and S. L. Clauson, *Appl. Phys. Lett.*, 1993, **63**, 599–601.
- 64 S. I. Cordoba de Torresi, R. M. Torresi, G. Ciampi and C. A. Luengo, *J. Electroanal. Chem.*, 1994, **337**, 283–285.
- 65 K. Lee, A.-Y. Kim and J. Kee Lee, *Sol. Energy Mater. Sol. Cells*, 2015, **139**, 44–50.
- 66 N. Alegret, A. Dominguez-Alfaro, M. Salsamendi, I. J. Gomez, J. Calvo, D. Mecerreyres and M. Prato, *Inorganica Chim. Acta*, 2017, **468**, 239–244.
- 67 Y. Ishigaki, Y. Hayashi, K. Sugawara, T. Shimajiri, W. Nojo, R. Katoono, T. Suzuki, Y. Ishigaki, Y. Hayashi, K. Sugawara, T. Shimajiri, W. Nojo, R. Katoono and T. Suzuki, *Molecules*, 2017, **22**, 1900.
- 68 G. A. Corrente, E. Fabiano, F. Manni, G. Chidichimo, G. Gigli, A. Beneduci and A.-L. Capodilupo, *Chem. Mater.*, 2018, **30**, 5610–5620.
- 69 R. Sydam, M. Deepa and A. G. Joshi, *Org. Electron.*, 2013, **14**, 1027–1036.
- 70 X. Zhang, E. L. Clennan and N. Arulسامي, *Org. Lett.*, 2014, **16**, 4610–4613.
- 71 M. Takase, V. Enkelmann, D. Sebastiani, M. Baumgarten and K. Müllen, *Angew. Chem.*, 2007, **119**, 5620–5623.
- 72 C. Romero-Nieto, M. Marcos, S. Merino, J. Barberá, T. Baumgartner and J. Rodríguez-López, *Adv. Funct. Mater.*, 2011, **21**, 4088–4099.
- 73 M. Stolar, J. Borau-Garcia, M. Toonen and T. Baumgartner, *J. Am. Chem. Soc.*, 2015, **137**, 3366–3371.
- 74 C. Reus, M. Stolar, J. Vanderkley, J. Nebauer and T. Baumgartner, *J. Am. Chem. Soc.*, 2015, **137**, 11710–11717.
- 75 T. Suzuki, S. Mikuni, Y. Ishigaki, H. Higuchi, H. Kawai and K. Fujiwara, *Chem. Lett.*, 2009, **38**, 748–749.
- 76 G. Li, L. Xu, W. Zhang, K. Zhou, Y. Ding, F. Liu, X. He and G. He, *Angew. Chem. Int. Ed.*, 2018, **57**, 4897–4901.
- 77 P. Pander, R. Motyka, P. Zassowski, M. Lapkowski, A. Swist and P. Data, *J. Phys. Chem. C*, 2017, **121**, 11027–11036.
- 78 A. Cihaner and F. Algı, *Adv. Funct. Mater.*, 2008, **18**, 3583–3589.
- 79 N. Kobayashi, M. Sasaki and K. Nomoto, *Chem. Mater.*, 2009, **21**, 552–556.
- 80 N. Lv, M. Xie, W. Gu, H. Ruan, S. Qiu, C. Zhou and Z. Cui, *Org. Lett.*, 2013, **15**, 2382–2385.
- 81 B. Yao, J. Zhang and X. Wan, in *Electrochromic Materials and Devices*, Wiley-VCH, 2015, pp. 211–240.
- 82 G. Shabir, A. Saeed and P. Ali Channar, A Review on the Recent Trends in Synthetic Strategies and Applications of Xanthene Dyes, <https://www.ingentaconnect.com/contentone/ben/mroc/2018/00000015/00000003/a0t00003#>, (accessed 31 October 2018).
- 83 A. Destine-Monvemay, P. C. Lacaze and A. Cherigui, *J. Electroanal. Chem.*, 1989, **260**, 75–90.
- 84 B. Yao, Y. Zhou, X. Ye, R. Wang, J. Zhang and X. Wan, *Org. Lett.*, 2017, **19**, 1990–1993.
- 85 T. H. Jozefiak, J. E. Almlöf, M. W. Feyereisen and L. L. Miller, *J. Am. Chem. Soc.*, 1989, **111**, 4105–4106.
- 86 T. H. Jozefiak and L. L. Miller, *J. Am. Chem. Soc.*, 1987, **109**, 6560–6561.
- 87 J. E. Almlöf, M. W. Feyereisen, T. H. Jozefiak and L. L. Miller, *J. Am. Chem. Soc.*, 1990, **112**, 1206–1214.
- 88 S. N. Keller, N. L. Veltri and T. C. Sutherland, *Org. Lett.*, 2013, **15**, 4798–4801.

- 89 O. Anamimoghadam, M. D. Symes, D.-L. Long, S. Sproules, L. Cronin and G. Bucher, *J. Am. Chem. Soc.*, 2015, **137**, 14944–14951.
- 90 O. Anamimoghadam, M. D. Symes, C. Busche, D.-L. Long, S. T. Caldwell, C. Flors, S. Nonell, L. Cronin and G. Bucher, *Org. Lett.*, 2013, **15**, 2970–2973.
- 91 A. Dettling, A. Rieker and B. Speiser, *Tetrahedron Lett.*, 1988, **29**, 4533–4534.
- 92 G. Frenking, A. Rieker, J. Salbeck and B. Speiser, *Z. Für Naturforschung B*, 1996, **51**, 377–380.
- 93 L. Đorđević, N. Demitri and D. Bonifazi, *Unpubl. Work.*
- 94 T. Miletic, A. Fermi, I. Orfanos, A. Avramopoulos, F. De Leo, N. Demitri, G. Bergamini, P. Ceroni, M. G. Papadopoulos, S. Couris and D. Bonifazi, *Chem. Eur. J.*, 2017, **23**, 2363–2378.
- 95 T. Miletic, *Unpubl. Work.*
- 96 R. Schmidt, W. Drews and H.-D. Brauer, *J. Photochem.*, 1982, **18**, 365–378.
- 97 J. Zhao, Y. Wang, Y. He, L. Liu and Q. Zhu, *Org. Lett.*, 2012, **14**, 1078–1081.
- 98 D. Stassen, N. Demitri and D. Bonifazi, *Angew. Chem. Int. Ed.*, 2016, **128**, 6051–6055.
- 99 L. Shu, P. Wang, W. Liu and C. Gu, *Org. Process Res. Dev.*, 2012, **16**, 1866–1869.
- 100 J. Ichikawa, H. Tanabe, S. Yoshida, T. Kawai, M. Shinjo and T. Fujita, *Chem. – Asian J.*, 2013, **8**, 2588–2591.
- 101 W. Gu and R. B. Silverman, *Org. Lett.*, 2003, **5**, 415–418.
- 102 Q. Miao, X. Chi, S. Xiao, R. Zeis, M. Lefenfeld, T. Siegrist, M. L. Steigerwald and C. Nuckolls, *J. Am. Chem. Soc.*, 2006, **128**, 1340–1345.
- 103 Y. Fujiwara, R. Ozawa, D. Onuma, K. Suzuki, K. Yoza and K. Kobayashi, *J. Org. Chem.*, 2013, **78**, 2206–2212.
- 104 Z. Yi, H. Okuda, Y. Koyama, R. Seto, S. Uchida, H. Sogawa, S. Kuwata and T. Takata, *Chem. Commun.*, 2015, **51**, 10423–10426.
- 105 J. A. Dodge and A. R. Chamberlin, *Tetrahedron Lett.*, 1988, **29**, 4827–4830.
- 106 W. Guo, E. Faggi, R. M. Sebastián, A. Vallribera, R. Pleixats and A. Shafir, *J. Org. Chem.*, 2013, **78**, 8169–8175.
- 107 J.-H. Ho, Y.-H. Chen, L.-T. Chou, P.-W. Lai and P.-S. Chen, *Tetrahedron Lett.*, 2014, **55**, 5727–5731.
- 108 T. Kamei, T. Takanori, N. Takenaka, JP. Pat., JP 2018-39777 A, 2018.
- 109 Y. Pan and Z. Peng, *Tetrahedron Lett.*, 2000, **41**, 4537–4540.
- 110 R. G. Harvey, J. Pataki, C. Cortez, P. Di Raddo and C. X. Yang, *J. Org. Chem.*, 1991, **56**, 1210–1217.
- 111 M. A. Christensen, C. R. Parker, T. J. Sørensen, S. de Graaf, T. J. Morsing, T. Brock-Nannestad, J. Bendix, M. M. Haley, P. Rapta, A. Danilov, S. Kubatkin, O. Hammerich and M. B. Nielsen, *J. Mater. Chem. C*, 2014, **2**, 10428–10438.
- 112 H. Chen, G. Cong and Y.-C. Lu, *J. Energy Chem.*, 2018, **27**, 1304–1325.
- 113 A. Stopin, *Unpubl. Work.*
- 114 S. Geiger, O. Kasian, A. M. Mingers, K. J. J. Mayrhofer and S. Cherevko, *Sci. Rep.*, 2017, **7**, 4595.
- 115 A. Dailey, J. Shin and C. Korzeniewski, *Electrochimica Acta*, 1998, **44**, 1147–1152.
- 116 A. Serov and C. Kwak, *Appl. Catal. B Environ.*, 2010, **97**, 1–12.
- 117 H. Konishi, K. Aritomi, T. Okano and J. Kiji, *Bull. Chem. Soc. Jpn.*, 1989, **62**, 591–593.
- 118 O. Cakmak, I. Demirtas and H. T. Balaydin, *Tetrahedron*, 2002, **58**, 5603–5609.
- 119 A. L. Spek, *Acta Crystallogr. Sect. D: Biol. Crystallogr.*, 2009, **65**, 148–155.
- 120 C. M. Cardona, W. Li, A. E. Kaifer, D. Stockdale and G. C. Bazan, *Adv. Mater.*, 2011, **23**, 2367–2371.